A new type of relaxation oscillation in a model with rate-and-state friction

K Uldall Kristiansen

Department of Applied Mathematics and Computer Science, Technical University of Denmark, 2800 Kgs. Lyngby, Denmark

E-mail: krkri@dtu.dk

Abstract

In this paper, we prove the existence of a new type of relaxation oscillation occurring in a one-block Burridge–Knopoff model with Ruina rate-and-state friction law. In the relevant parameter regime, the system is a slow-fast ordinary differential equation with two slow variables and one fast. The oscillation is special for several reasons: firstly, its singular limit is unbounded, the amplitude of the cycle growing like $\log \epsilon^{-1}$ as $\epsilon \to 0$. As this estimate reflects, the unboundedness of the cycle—for this non-polynomial system—cannot be captured by a simple ϵ-dependent scaling of the variables, in contrast to e.g. Gucwa and Szmolyan (2009 *Discrete Continuous Dyn. Syst.* S **2** 783–806). We therefore obtain its limit on the Poincaré sphere. Here we find that the singular limit consists of a slow part on an attracting critical manifold, and a fast part on the equator (i.e. at ∞) of the Poincaré sphere, which includes motion along a center manifold. The reduced flow on this center manifold runs out along the manifold's boundary, in a special way, leading to a complex return to the slow manifold. We prove the existence of the limit cycle by showing that a return map is a contraction. The main technical difficulty lies in the fact that the critical manifold loses hyperbolicity at an exponential rate at infinity. We therefore use the method in Kristiansen (2017 *Nonlinearity* **30** 2138–84), applying the standard blowup technique in an extended phase space. In this way, we identify a singular cycle, consisting of 12 pieces, all with desirable hyperbolicity properties, that enables the perturbation into an actual limit cycle for $0 < \epsilon \ll 1$. The result proves a conjecture in Bossolini *et al* (2017 *Nonlinearity* **30** 2805–34). The Bossolini *et al* (2017 *Nonlinearity* **30** 2805–34) also includes a preliminary analysis based on the approach in Kristiansen (2017 *Nonlinearity* **30** 2138–84) but several details were missing. We provide all the details in the present manuscript and lay out the geometry

of the problem, detailing all of the many blowup steps.

(Some figures may appear in colour only in the online journal)

Contents

1. Introduction

Relaxation oscillations are special periodic solutions of singularly perturbed ordinary differential equations. They consist of long periods of 'in-activity' interspersed with short periods of rapid transitions. Mathematically, they are classically defined for slow-fast systems

$$\epsilon \dot{x} = f(x, y, \epsilon),$$
$$\dot{y} = g(x, y, \epsilon), \tag{1.1}$$

as elements Γ_ϵ of a family of periodic orbits $\{\Gamma_\epsilon \mid \epsilon \in (0, \epsilon_0]\}$ whose $\epsilon \to 0$ limit (in the Hausdorff sense), Γ_0, is a closed loop consisting of a union of (a) *slow* orbits of the reduced problem:

$$0 = f(x, y, 0),$$
$$\dot{y} = g(x, y, 0),$$

and (b) fast orbits of the layer problem:

$$x' = f(x, y, 0),$$
$$y' = 0.$$

Here $()' = \frac{d}{d\tau}$ and $\dot{()} = \frac{d}{dt}$ are related for $\epsilon > 0$ by

$$\tau = \epsilon^{-1} t,$$

τ is called the fast time whereas t is called the slow time. Obviously, Γ_0 should allow for a consisting orientation of positive (slow and fast) time. Γ_0 is in this case called a singular cycle.

The prototypical system, where relaxation oscillations occur, is the van der Pol system, see e.g. [27]. Here the critical manifold $C = \{(x, y) \mid f(x, y, 0) = 0\}$ is N-shaped and relaxation oscillations Γ_ϵ occur, in generic situations, near a Γ_0 consisting of the leftmost and rightmost pieces of the N-shaped critical manifold C interspersed by two horizontal lines connecting these branches at the 'folds'. See figure 1(a).

But other types of relaxation oscillations also exist. The simplest examples appear in slow-fast systems in nonstandard form

$$\dot{z} = h(z, \epsilon), \tag{1.2}$$

where $C = \{z \mid h(z, 0) = 0\}$ is a critical manifold. Here relaxation oscillations may even be the union of one single fast orbit and a single slow orbit on S. These oscillations are also called two-stroke oscillations, see [18, 29] and figure 1(b). In [15], for example, a planar slow-fast system of the form (1.1) is considered. Here limit cycles Γ_ϵ exist which also have segments that follow the different time scales, t and τ. But Γ_ϵ grows unboundedly as $\epsilon \to 0^+$ and the limit Γ_0 is therefore not a cycle. However, in the polynomial model considered by [15] there exists an ϵ-dependent scaling of the variables that captures the unboundedness and in these scaled variables the system is transformed into a system of nonstandard form (1.2). For this system, Γ_0 becomes a closed cycle, albeit with some degeneracy along a critical manifold. Similar (generalised) relaxation oscillations also occur in systems close to piecewise smooth limits as $\epsilon \to 0$, see e.g. [19, 21, 25]. In these systems, where the notion of slow and fast orbits have to be generalised, (slow) segments of the relaxation oscillation appear close to the discontinuity set.

The relaxation oscillations described above can all be analyzed by geometric singular perturbation theory (GSPT). The terminology GSPT is frequently used as a reference to a collection of theories and methods for studying singularly perturbed ODEs using invariant
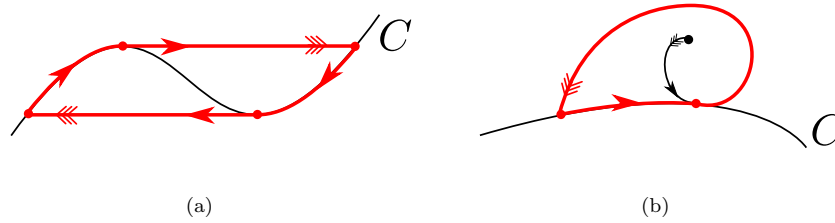
Figure 1. In (a): the prototypical example of a relaxation oscillation in a planar slow-fast system with a folded critical manifold. In (b): example of a relaxation oscillation in slow-fast system in nonstandard form.
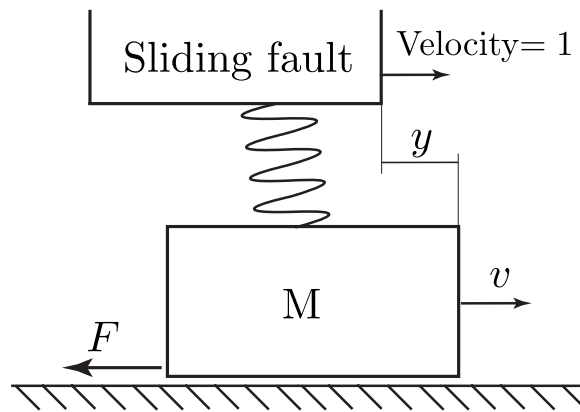
Figure 2. Illustration of model (1.4).

manifolds. This follows, first and foremost, Fenichel's original theory [12–14] for the perturbation of compact normally hyperbolic critical manifolds and their stable and unstable manifolds. Nowadays, following [26], see also [8], GSPT also consists of the blowup method as the key technical tool, allowing for an extension of Fenichel's geometric theory near non-hyperbolic points. (The GSPT framework also consists of the exchange lemma [20, 38] and entry-exit functions, [5, 16, 17], neither of which will be important in the present manuscript.)

In the present paper, we will consider the following slow-fast system

$$
\begin{aligned}
\dot{x} &= -e^z \left(x + (1 + \alpha)z \right), \\
\dot{y} &= e^z - 1, \\
\epsilon \dot{z} &= -e^{-z} \left(y + \frac{x + z}{\xi} \right),
\end{aligned}
\tag{1.3}
$$

with $\alpha > 0, \xi > 0$ and $0 < \epsilon \ll 1$. This is a caricature model of an earthquake fault, see section 1.1 below. Relaxation oscillations in this system therefore models the seismic cycle of earthquakes with years, decades even, of inactivity preceded by sudden dramatic shaking of the ground: the earthquake.

Similar to the case in [15], limit cycles of (1.3) also grow unboundedly as $\epsilon \to 0$. But in contrary to [15], the right hand side of (1.3) does not have polynomial growth, and as a result, the unboundedness of the solutions cannot be captured by a scaling of the variables. We will in this paper therefore have to work on the Poincaré sphere. Here we then prove the existence of limit cycles Γ_ϵ, whose limit Γ_0 as $\epsilon \to 0$ consists of a single slow orbit on
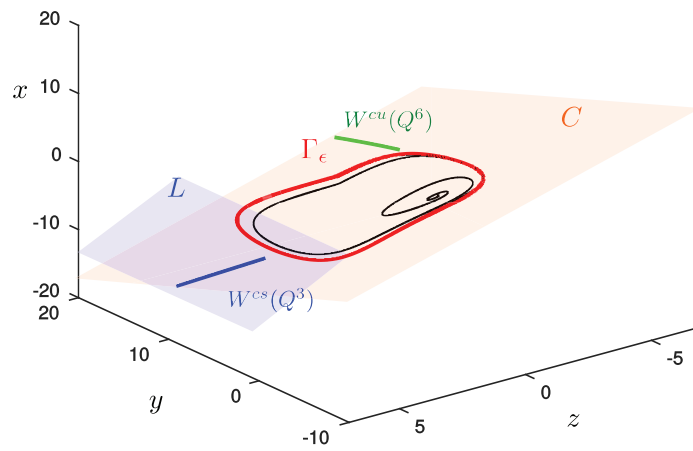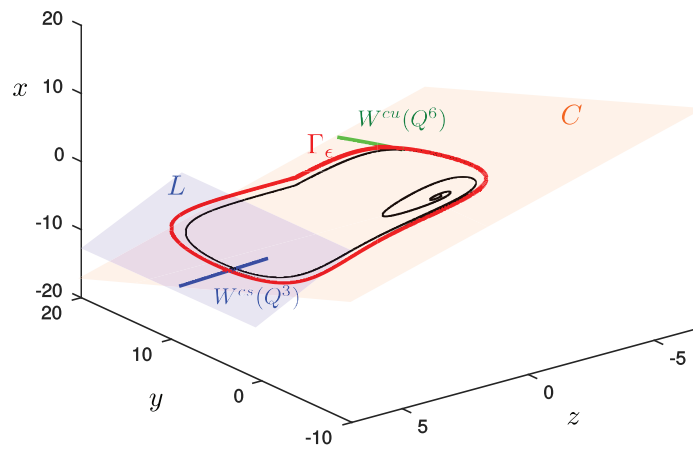
Figure 3. Limit cycles in red for $\alpha = 0.8$, $\xi = 0.5$. In (a): $\epsilon = 0.01$ and in (b): $\epsilon = 0.001$. The motion in the diagrams is clockwise. The black curves are transients showing the contraction towards the limit cycle. The orange hyperplane C is the critical manifold, see (1.6). The subset of the limit cycles, that is close to this plane, is accurately described by the reduced problem, see (1.8). However, away from C, we see that the limit cycles initially follow the blue plane L until they return to C again, being attracting to the center-like manifold $W^{cu}(Q^6)$ (green).
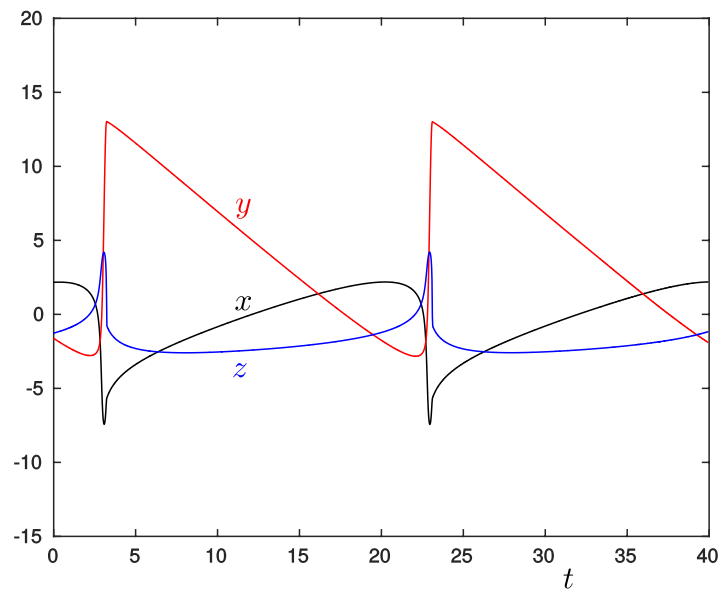
(a)
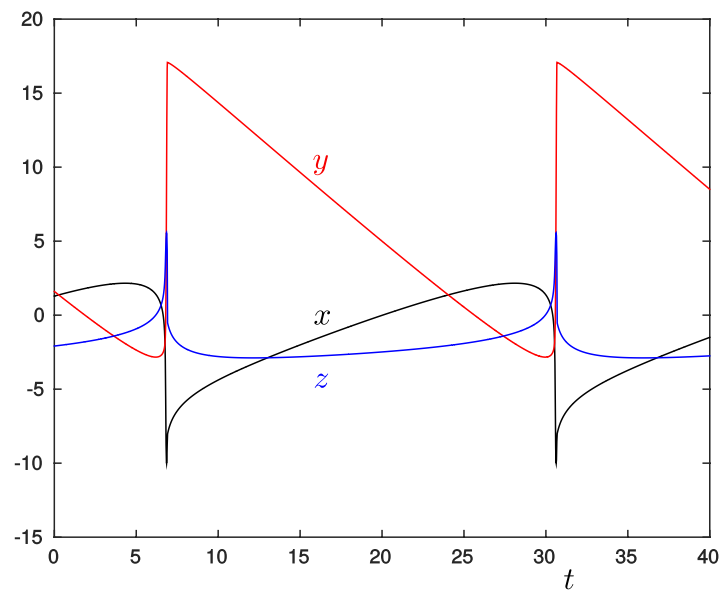
(b)

Figure 4. x, y and z (black, red and blue, respectively) in figure 3 as functions of t for $\xi = 0.5$ and $\alpha = 0.8$. In (a): $\epsilon = 0.01$. In (b): $\epsilon = 0.001$. Both solutions are of relaxation type (two-stroke) in the sense that long periods of moderate 'activity' are interspersed with rapid transitions. The effect of decreasing ϵ is seen to be two-fold: firstly, the transitions between the slow phases become sharper and, secondly, the amplitude grows (slightly). Notice also how the period of the periodic solution depends upon ϵ.
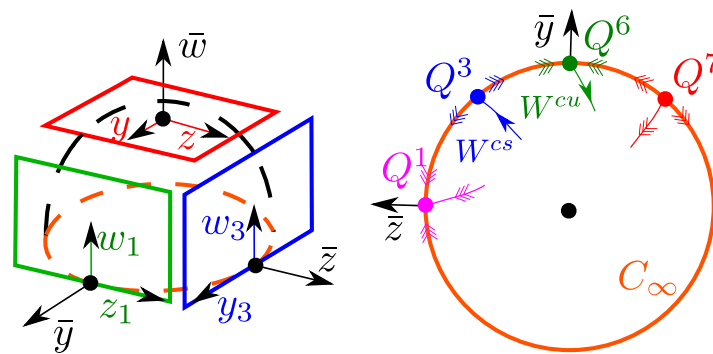
Figure 5. Poincaré compactification of the reduced problem. The point Q^6 is not a true equilibrium of $\widehat{X}$, instead it is an essential singularity $e^{`0/0`}$. However, subsequent 'blowup' of this point and further desingularization reveal, see [3], that Q^6 essentially acts like a (nonhyperbolic) saddle (as illustrated in the figure).

the two-dimensional (2D) attracting critical manifold $C = \{(x, y, z) \mid y + (x + z)/\xi = 0\}$. The 'fast' part of Γ_0 occurs at 'infinity' (i.e. the equator of the Poincaré sphere) and is non-trivial and perhaps even surprising. We uncover this structure by applying the method in [22] to gain hyperbolicity where this is lost due to exponential decay of eigenvalues. In particular, Γ_0 only has desirable hyperbolicity properties upon several blowup transformations. The main theorem, theorem 1.5, proves a conjecture in [3].

1.1. Mathematical modelling of earthquake faulting

The model we consider, described by the equation (1.3), consists of a single block dragged along a frictional surface by a spring, the end of which moves at a constant velocity. We set this velocity to 1, without loss of generality. The model is illustrated in figure 2. Here v is the velocity of the block and y is the relative position, measuring the deformation of the spring. If the moving spring models a sliding fault, then the system becomes a caricature model of an earthquake fault. It is therefore also the extreme case of a single-block version of the Burridge–Knopoff model, which idealizes the earthquake fault as a chain of spring-block systems of the type shown in figure 2. More importantly, the Burridge–Knopoff model has a continuum limit as the distance between the chain blocks vanishes and travelling wave solutions of the resulting PDE system, see [3, section 2.1], are basically solutions of the one-block system. See [35] for a different derivation.

The unknown in figure 2, and in earthquake modelling in general, is the friction force F. Within engineering, friction is frequently modelled using Coulomb-like laws, e.g. the stiction law or the Stribeck law [2, 11, 31]. However, these laws do not account for any of the microscopic processes that are known to occur when surfaces interact in relative motion. Consequently, such models cannot produce phenomena known to occur in earthquakes. To capture this, one can use *rate-and-state friction laws*. Such models attempt to account for additional physics, like the condition of the contacting asperities [39], by adding additional variables, called 'state variables', to the problem. The first models of this kind, the Dieterich law [6, 7] and the Ruina law [37], were obtained from experiments on rocks. In contrast to e.g. Coulomb's simple model, the friction force in these models depends logarithmically on the velocity. (It was only later realized that this decay actually agree with theory of Arrhenius

processes resulting from breaking bonds at the atomic level [36].) Recently, these friction laws have also been used to describe sea ice friction [30].

In this paper, we consider the Ruina friction law. This gives the following equations for the model in figure 2

$$
\begin{aligned}
\dot{x} &= -v\left(x + (1+\alpha)\log v\right), \\
\dot{y} &= v - 1, \\
\epsilon\dot{v} &= -y - \frac{x + \log v}{\xi},
\end{aligned}
\tag{1.4}
$$

in its nondimensionalised form. See [3, 10] for further details on the derivation. The variable x is a single 'state variable'. As in [3] we put $z = \log v$ and arrive at model (1.3), which we shall study in this manuscript as a singular perturbed problem with $0 < \epsilon \ll 1$.

Numerically, existence of relaxation-type oscillations for $\alpha > \xi$ and small values of $\epsilon > 0$ is a well-known fact [10, 35]. See also figure 3, computed in MATLAB using ode23s with tolerances 10^{-12}. Figure 4 shows x, y and z (black, red and blue, respectively) as functions of t. Notice the slow-fast, relaxation-type structure of the periodic solutions; y, describing the position of the block, for example, decreases moderately everywhere except for tiny time intervals where it increases very rapidly. In this paper, we are interested in a rigorous proof of the existence of these oscillations and en-route on how to apply classical methods of singular perturbation theory to (1.4), or equivalently (1.3), with non-polynomial growth of the right hand side.

1.2. Previous results on the singular limit of (1.3)

In the following we review some results from [3] on the singular limit of (1.3). Our notation will in some places slightly differ from that in [3].

In terms of the fast time $\tau = \epsilon^{-1}t$, the (slow) system (1.3) becomes the (fast) system

$$
\begin{aligned}
x' &= -\epsilon e^z\left(x + (1+\alpha)z\right), \\
y' &= \epsilon(e^z - 1), \\
z' &= -e^{-z}\left(y + \frac{x + z}{\xi}\right).
\end{aligned}
\tag{1.5}
$$

Setting $\epsilon = 0$ in (1.5) then gives the layer problem

$$
\begin{aligned}
x' &= 0, \\
y' &= 0, \\
z' &= -e^{-z}\left(y + \frac{x + z}{\xi}\right),
\end{aligned}
$$

for which the hyperplane

$$
C = \left\{ (x, y, z) \,\middle|\, y + \frac{x + z}{\xi} = 0 \right\}
\tag{1.6}
$$

is the critical manifold. This manifold is normally hyperbolic and attracting since the linearization about any point C gives

$$
-\xi^{-1}e^{-z},
\tag{1.7}
$$
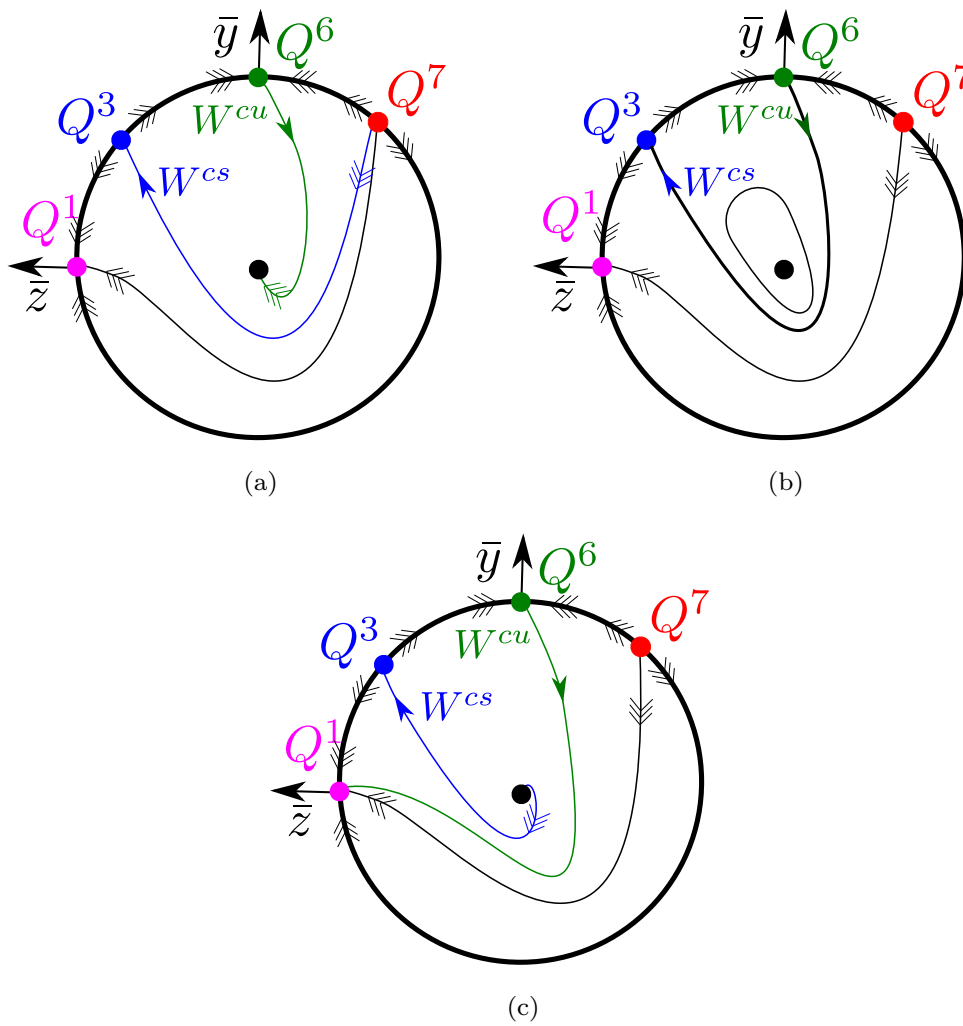
Figure 6. Phase portraits of the reduced problem on the Poinacaré sphere. In (a): $\alpha < \xi$, in (b): $\alpha = \xi$ (the Hamiltonian case) and finally in (c): $\alpha > \xi$. The point Q^6 is not a equilibrium of $\widehat{X}$. Instead it is an essential singularity due to $e^{`0/0'}$. But the analysis of [3] shows that it essentially acts like a nonhyperbolic saddle, having a unique unstable manifold $W^{cu}(Q^6)$ (see also lemma 7.6).

as a single nonzero eigenvalue. However, C is not compact. Fenichel's theory [14] therefore only guarantees the smooth perturbation S_ϵ of fixed compact sub-manifolds (with boundary) $S_0 \subset C$ for all $0 \leqslant \epsilon \ll 1$.

Setting $\epsilon = 0$ in (1.3), gives a reduced problem on C, which we write in terms of (the physical meaningful variables) (y, z) as follows

$$\begin{aligned} \dot{y} &= e^z - 1, \\ \dot{z} &= \xi + e^z \left(\alpha z - \xi y - \xi \right) \end{aligned} \tag{1.8}$$

with

$$x = m(y, z) := -\xi y - z, \tag{1.9}$$

using (1.6). Recall that x is a 'state' variable describing the friction—it models a combination of effects and is difficult to measure and observe in practice, see e.g. [39].

In [3] the authors show that (1.8) has a degenerate Hopf bifurcation at $\alpha = \xi$, where periodic orbits emerge at once due to a Hamiltonian structure:

$$\begin{pmatrix} \dot{y} \\ \dot{z} \end{pmatrix} = J(y, z) \nabla H(y, z), \tag{1.10}$$

where

$$J(y, z) = \begin{pmatrix} 0 & \xi^{-1} e^{\xi y + z} \\ -\xi^{-1} e^{\xi y + z} & 0 \end{pmatrix},$$

$$H(y, z) = -\xi e^{-\xi y}(y - z + 1 - e^{-z}) + 1 - e^{-\xi y}.$$

The authors of [3] then put the reduced problem (1.8) on the Poincaré sphere in the following way: consider $S^2 = \{(\bar{y}, \bar{z}, \bar{w}) \in \mathbb{R}^3 \,|\, \bar{y}^2 + \bar{z}^2 + \bar{w}^2 = 1\}$ and let $\phi : S^2 \cap \{\overline{w} > 0\} \to \mathbb{R}^2$ be defined by

$$(\bar{y}, \bar{z}, \bar{w}) \mapsto \begin{cases} y &=& \bar{w}^{-1}\bar{y}, \\ z &=& \bar{w}^{-1}\bar{z}. \end{cases} \tag{1.11}$$

By pull-back, the vector-field (1.8) gives a vector-field $\overline{X}$ on $(\bar{y}, \bar{z}, \bar{w}) \in S^2 \cap \{\overline{w} > 0\}$. (1.11) is then also a chart, obtained by central projection onto the hyperplane $\bar{w} = 1$, parameterizing $\bar{w} > 0$ of S^2. Let Q^6 be defined by $(\bar{y}, \bar{z}, \bar{w}) = (1, 0, 0)$. Then by appropriate re-parametrizations of time—essentially slowing (speeding) time down (up) for $\bar{z} > 0$ ($\bar{z} < 0$, respectively)—they obtain a well-defined vector-field:

$$\widehat{X} := r^{-1}\overline{X},$$

on $S^2 \cap \{\overline{w} \geqslant 0\} \backslash \{Q^6\}$, that leaves the 'equator', i.e. the subset defined by $\overline{w} = 0$, invariant. Here $r = r(\bar{y}, \bar{z}, \bar{w})$ is strictly positive for $\overline{w} > 0$, so that $\widehat{X}$ and $\overline{X}$ are equivalent on $\{\overline{w} > 0\}$. The point Q^6 is an essential singularity $e^{'0/0'}$ that—loosely speaking—divides the equator into points where e^z in (1.8) is 'exponentially small' from points were this quantity is 'exponentially large'. See [19] where similar essential singularities are studied using the same methods.

To describe S^2 near the equator $\overline{w} = 0$ the authors in [3] studied two separate directional charts:

$$\phi_1 : S^2 \cap \{\bar{y} > 0\} \to \mathbb{R}^2,$$
$$\phi_3 : S^2 \cap \{\bar{z} > 0\} \to \mathbb{R}^2,$$

defined by

$$(\bar{y}, \bar{z}, \bar{w}) \mapsto \begin{cases} z_1 &=& \bar{y}^{-1}\bar{z}, \\ w_1 &=& \bar{y}^{-1}\bar{w}, \end{cases} \tag{1.12}$$

$$(\bar{y}, \bar{z}, \bar{w}) \mapsto \begin{cases} y_3 &=& \bar{z}^{-1}\bar{y}, \\ w_3 &=& \bar{z}^{-1}\bar{w}, \end{cases} \tag{1.13}$$

respectively. These charts are obtained by central projections onto the hyperplanes tangent to S^2 at $\bar{y} = 1$ and $\bar{z} = 1$, respectively. See figure 5. The authors then found three equilibria of $\widehat{X}$ within $\overline{w} = 0$: Q^1 where $\bar{y} = 0$, $\bar{z} = 1$, Q^3 where $\bar{y}^{-1}\bar{z} = \alpha^{-1}\xi$, $\bar{y} > 0$, and Q^7 where

$\bar{y}^{-1}\bar{z} = -\xi$, $\bar{y} > 0$. Here Q^1 is an attracting hyperbolic node while Q^7 is a repelling hyperbolic node. The point Q^3, on the other hand, is a nonhyperbolic saddle, with a hyperbolic unstable manifold along the equator and a nonhyperbolic stable manifold (a unique center manifold), which we denote by $W^{cs}(Q^3)$. Finally, using a separate blowup approach, the singular point Q^6 was found to act like a saddle, with one 'stable manifold' along the equator of the sphere, and a unique center-like unstable manifold, which we shall denote $W^{cu}(Q^6)$. See also figure 5 (and lemma 7.6 below for details).

Remark 1.1.   As is standard, we use different arrows to separate center directions from hyperbolic ones. As demonstrated in figure 5, see e.g. the nonhyperbolic saddle Q^3, center directions are shown by single-headed arrows whereas triple-headed arrows represent hyperbolic directions.

Following [3], we describe the invariant manifolds of Q^3 and Q^6 using the original coordinates (y, z) of C as follows.

Lemma 1.2.   *Consider any $\alpha > 0, \xi > 0$. Then there exists two unique one-dimensional (1D) invariant manifolds $W^{cu}(Q^6)$ and $W^{cs}(Q^3)$ for the reduced flow on C with the following asymptotics:*

$$z = -\log(y)\left(1 + \frac{\alpha}{\xi y}\right), \tag{1.14}$$

$$z = \frac{\xi}{\alpha}y + \frac{(1+\alpha)\xi}{\alpha^2}, \tag{1.15}$$

as $y \to \infty$, respectively. Under the flow of $\widehat{X}$, the manifold $W^{cu}(Q^6)$ is the set of all trajectories with the asymptotics in (1.14) backwards in time (or simply, the 'unstable set' of Q^6) whereas $W^{cs}(Q^3)$ is the set of all trajectories with the asymptotics (1.15) forward in time (or simply, the stable set of Q^3). Moreover, for $\alpha = \xi$, $W^{cs}(Q^3)$ and $W^{cu}(Q^6)$ coincide, such that there exists a unique orbit on C with the asymptotics in $(1.14)_{\alpha=\xi}$ in backward time and $(1.15)_{\alpha=\xi}$ in forward time, respectively (i.e. a 'heteroclinic' orbit of $\widehat{X}$). The intersection is transverse in (y, z, α)-space:

(a) *For $\alpha > \xi$: $W^{cu}(Q^6)$ is contained within the stable set of Q^1, in such a way that $z(t) \to \infty$ and $z(t)^{-1}y(t) \to 0$ with $y(t) > 0$, in forward time, while $W^{cs}(Q^3)$ is contained within the unstable set of $(y, z) = (0, 0)$.*

(b) *For $\alpha < \xi$: $W^{cu}(Q^6)$ is contained within the stable set of $(y, z) = (0, 0)$, while $W^{cs}(Q^3)$ is contained within the unstable set of Q^7 with the asymptotics*

$$z = -\xi y,$$

for $y \to \infty$ in backward time.

Proof.   This is essentially [3, proposition 5.1]. Notice, in [3], however, the authors use Melnikov theory and only deduce (a) and (b) locally near $\alpha = \xi$. To show that these statements hold for any $\alpha > \xi$ and $\alpha < \xi$, respectively, we simply use that H is a Lyapunov function:

$$\frac{\mathrm{d}H}{\mathrm{d}t}(y, z) = -\xi e^{-\xi y}(e^z - 1)z(\alpha - \xi),$$
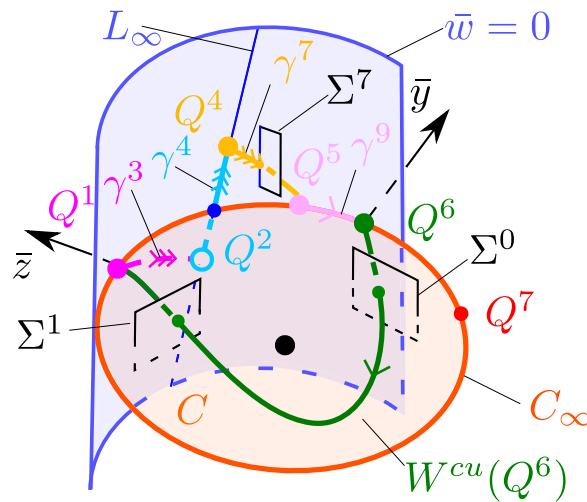
Figure 7. Illustration of the singular cycle Γ_0 on the Poincaré sphere for $\xi < \alpha < 1$. For $\alpha = 1$, γ^7 connects directly to Q^6 and therefore γ^9 'disappears' whereas for $\alpha > 1$, γ^7 connects to C_∞ with $\bar{z} < 0$ so that γ^9 gets 'flipped' on C_∞ relative to Q^6. This change in the singular cycle can be observed in bifurcation diagrams, see figure 30. In this figure, we deviate slightly from the notation in remark 1.1, insofar that we use single-headed and tripple-headed arrows to separate 'slow' pieces from 'fast' ones, respectively. That is with respect to t in (1.3), the time spend near $\gamma^3 \cup \gamma^4 \cup \gamma^7 \cup \gamma^9$ tends to zero as $\epsilon \to 0$. However, everything within $\bar{w} = 0$ is completely degenerate, and we only obtain the 'fast dynamics' upon several blowup transformations.

such that sign $\left(\frac{\mathrm{d}}{\mathrm{d}t} H(y, z)\right) = -\text{sign}(\alpha - \xi)$ for all $y, z \neq 0$ and $\alpha \neq \xi$. Therefore for $\alpha > \xi$, H increases monotonically along all orbits ($\neq (y, z)(t) \equiv (0, 0)$) of (1.8). Therefore limit cycles cannot exist. Recall that Q^1 is a stable node on the Poincaré sphere, while Q^7 is an unstable node. By Poincaré–Bendixson, $W^{cu}(Q^6)$ is asymptotic to Q^1 when $\alpha > \xi$. The approach is similar for $\alpha < \xi$. □

By this lemma, we obtain the global phase portraits in figure 6 for the reduced problem (1.8).

In [3], the authors also apply Poincaré compactification of the full system (1.3) defining $\Phi : S^3 \cap \{\bar{w} > 0\} \to \mathbb{R}^3$, $S^3 = \{(\bar{x}, \bar{y}, \bar{z}, \bar{w}) \,|\, \bar{x}^2 + \bar{y}^2 + \bar{z}^2 + \bar{w}^2 = 1\}$ by

$$(\bar{x}, \bar{y}, \bar{z}, \bar{w}) \mapsto \begin{cases} x &= \bar{w}^{-1}\bar{x}, \\ y &= \bar{w}^{-1}\bar{y}, \\ z &= \bar{w}^{-1}\bar{z}. \end{cases} \tag{1.16}$$

By (1.11) and (1.9), we obtain

$$C := \{(\bar{x}, \bar{y}, \bar{z}, \bar{w}) \in S^3 \,|\, \bar{y} + (\bar{x} + \bar{z})\xi^{-1} = 0, \, \bar{w} > 0\}, \tag{1.17}$$

as an embedded ellipsoid (or actually a hemisphere hereof) within $S^3 = \{(\bar{x}, \bar{y}, \bar{z}, \bar{w}) \,|\, \bar{x}^2 + \bar{y}^2 + \bar{z}^2 + \bar{w}^2 = 1\}$, the equator of which, along $\overline{w} = 0$, contains the corresponding points Q^1, Q^3, Q^6 and Q^7 along the boundary

$$C_\infty := \{(\bar{x}, \bar{y}, \bar{z}, \bar{w}) \in S^3 \,|\, \bar{y} + (\bar{x} + \bar{z})\xi^{-1} = \bar{w} = 0\}, \tag{1.18}$$

of C, recall also (1.6). For simplicity, we have here used the same symbols for these points as a subset S^3.

We use the directional charts

$$\phi_1 : S^3 \cap \{\bar{y} > 0\} \to \mathbb{R}^3,$$
$$\phi_3 : S^3 \cap \{\bar{z} > 0\} \to \mathbb{R}^3,$$

in the following, defined by

$$(\bar{x}, \bar{y}, \bar{z}, \bar{w}) \mapsto \begin{cases} x_1 &=& \bar{y}^{-1}\bar{x}, \\ z_1 &=& \bar{y}^{-1}\bar{z}, \\ w_1 &=& \bar{y}^{-1}\bar{w}, \end{cases} \tag{1.19}$$

$$(\bar{x}, \bar{y}, \bar{z}, \bar{w}) \mapsto \begin{cases} x_3 &=& \bar{z}^{-1}\bar{x}, \\ y_3 &=& \bar{z}^{-1}\bar{y}, \\ w_3 &=& \bar{z}^{-1}\bar{w}, \end{cases} \tag{1.20}$$

respectively (where we again misuse notation slightly by reusing the symbols in (1.12) and (1.13) for the new charts). Notice that the coordinate transformation between ϕ_1 and ϕ_3 can be derived from the expressions

$$x_1 = y_3^{-1}x_3,$$
$$z_1 = y_3^{-1}, \tag{1.21}$$
$$w_1 = y_3^{-1}w_3,$$

for $z_1 > 0$ and $y_3 > 0$. Furthermore, the coordinates in ϕ_1 and ϕ_3 and the original coordinates (x, y, z) are related as follows

$$x = w_1^{-1}x_1 = w_3^{-1}x_3,$$
$$y = w_1^{-1} \quad = w_3^{-1}y_3, \tag{1.22}$$
$$z = w_1^{-1}z_1 = w_3^{-1},$$

using (1.16).

Under the compactification defined by (1.16), the critical manifold $C \cup C_\infty$ is also compactified. However, by working in the directional charts, [3] shows that the manifold is nonhyperbolic along its boundary C_∞ due to the non-trivial eigenvalue $\lambda \to 0$, exponentially, as points on C approach C_∞. See also section 3 below.

Following [3], we define a 'singular' cycle as follows:

Definition 1.3 ([3, definition 1]). Let the points $Q^{1,2,4,5,6}$ be given by

$$Q_3^1 = (-1, 0, 0),$$
$$Q_3^2 = (-1 - \alpha, 0, 0),$$
$$Q_3^4 = \left(-1 - \alpha, \frac{2\alpha}{\xi}, 0\right),$$

in the coordinates (x_3, y_3, w_3) of chart ϕ_3, see (1.20),

$$Q_1^5 = \left(-\frac{\xi}{2\alpha}(1+\alpha), \frac{\xi}{2\alpha}(1-\alpha), 0 \right),$$
$$Q_1^6 = (-\xi, 0, 0), \tag{1.23}$$

in the coordinates (x_1, z_1, w_1) of chart ϕ_1, see (1.19). Then for any $\alpha > \xi$, we define the (singular) cycle Γ_0 as follows

$$\Gamma_0 = \gamma^3 \cup \gamma^4 \cup \gamma^7 \cup \gamma^9 \cup W^{cu}(Q^6), \tag{1.24}$$

where

- γ^3 connects Q^1 and Q^2. In the (x_3, y_3, w_3)-coordinates it is given as

$$\gamma_3^3 = \{(x_3, y_3, w_3) \,|\, x_3 \in (-1-\alpha, -1], y_3 = w_3 = 0\}. \tag{1.25}$$

- γ^4 connects Q^2 with Q^4. In the (x_3, y_3, w_3)-coordinates it is given as

$$\gamma_3^4 = \{(x_3, y_3, w_3) \,|\, x_3 = -1-\alpha, w_3 = 0, y_3 \in [0, 2\alpha/\xi)\}.$$

- γ^7 connects Q^4 with Q^5. In the (x_1, z_1, w_1)-coordinates it is given as

$$\gamma_1^7 = \left\{ (x_1, z_1, w_1) \,|\, x_1 = -\frac{\xi}{2\alpha}(1+\alpha), \right.$$
$$\left. z_1 \in \left(\frac{\xi}{2\alpha}(1-\alpha), \frac{\xi}{2\alpha} \right], w_1 = 0 \right\}. \tag{1.26}$$

- γ^9 connects Q^5 with Q^6 on C_∞. In the (x_1, z_1, w_1)-coordinates it is given as

$$\gamma_1^9 = \left\{ (x_1, z_1, w_1) \,|\, x_1 = -\xi - z_1, \right.$$
$$\left. z_1 \in \left(0, \frac{\xi}{2\alpha}(1-\alpha) \right], w_1 = 0 \right\}, \tag{1.27}$$

for $0 < \alpha < 1$. For $\alpha = 1$, γ_1^9 is the empty set, and for $\alpha > 1$ the interval for z_1 has to be swapped around such that $z_1 \in [\xi(1-\alpha)/(2\alpha), 0)$.

- $W^{cu}(Q^6)$ is the unique center manifold of Q^6 for the reduced problem (1.8), described in lemma 1.2, connecting Q^6 with Q^1 (given that $\alpha > \xi$) in forward (slow) time.

The segment γ^4 belongs to a curve L_∞, that the authors in [3], upon blowup (using the adapted version in [22] to handle the exponentials), identified as a set of partially hyperbolic equilibria (see also proposition 4.8 below for further details). In the (x_3, y_3, w_3)-coordinates, it is given as the line

$$L_{\infty,3} = \{(x_3, y_3, w_3) \,|\, x_3 = -1-\alpha, w_3 = 0, y_3 \in I\}, \tag{1.28}$$

where $I \subset \mathbb{R}$ is a large interval. γ^3 is given by the contraction towards this manifold. The segment γ^7 connects Q^4 on L_∞ with a point Q^5 on C_∞. The final segment γ^9 is a segment on C_∞ following the 'desingularized' reduced slow flow on C_∞ (basically using the time that produces figure 6). We illustrate Γ_0 and the segments in figure 7. Here we represent C as a disk and the equator sphere $\bar{w} = 0$ (locally) as a cylindrical object containing C_∞ as a circle.

In figure 3, we illustrate the set L in the (x, y, z)-coordinates obtained by extending (1.28) for $w_3 > 0$ sufficiently small and applying the coordinate change (1.22):
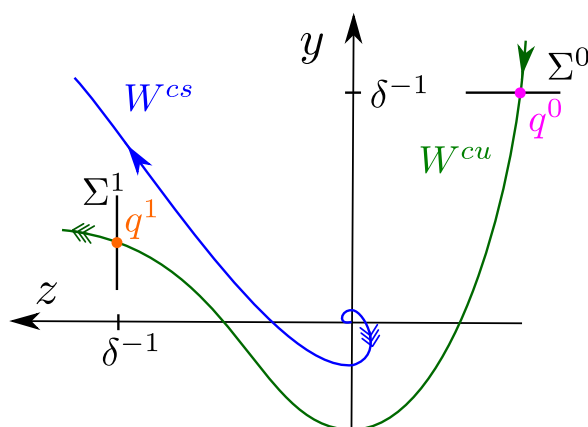
Figure 8. Illustration of the sections Σ^0 and Σ^1 at $y = \delta^{-1}$ and $z = \delta^{-1}$, respectively, used in the proof of theorem 1.5. Both sections are transverse to the reduced flow on C and intersect W^{cu} in their interior. Also Σ^1 is small enough so that it does not contain W^{cs}.

$$L = \{(x, y, z) \,|\, x = (-1 - \alpha)z, \, y/z \in I, \, z \gg 0\}. \tag{1.29}$$

The role of this set (and therefore also the role of L_∞, given that the amplitude increases as $\epsilon \to 0$) is clearly visible in these diagrams.

Remark 1.4. [3] presents a heuristic argument for how L appears which we for convenience also include here. Divide the right hand side of (1.3) by e^z and suppose that $e^{-2z} \ll \epsilon$. Then

$$\begin{aligned}
\dot{x} &= -(x + (1 + \alpha)z), \\
\dot{y} &= 1, \\
\dot{z} &= 0
\end{aligned} \tag{1.30}$$

to 'leading order'. The set $x = (-1 - \alpha)z$, producing (1.29), is an invariant set of (1.30), along which y increases monotonically. But notice that this naive approach does not explain how orbits leave a neighborhood of L. For this we need a more detailed analysis, which we provide in the present paper.

1.3. Main results

In this paper, we prove the following result, conjectured in [3].

Theorem 1.5. *Fix $\xi > 0$ and any compact set K in $\mathbb{R}^3$. Then for all $\alpha > \xi$ the following holds:*

(a) *There exists an $\epsilon_0 > 0$ such that system (1.3) has an attracting limit cycle Γ_ϵ for all $0 < \epsilon \leqslant \epsilon_0$. Furthermore, no limit cycles exist within K. In particular, $\Gamma_\epsilon \not\subset K$.*

(b) *Moreover, on the Poincaré sphere S^3, recall (1.16), Γ_ϵ converges in Hausdorff distance to the singular cycle Γ_0 as $\epsilon \to 0$.*

For $\alpha < \xi$, the omega limit set $\omega(K)$ of K is the unique equilibrium $(x, y, z) = (0, 0, 0)$.

Since the statement about $\alpha < \xi$ follows directly from Fenichel's theory and the reduced problem, see figure 6(a), we will from now on focus on the statements (a) and (b) for $\alpha > \xi$. The main difficulty in proving this result is that C on $S^3 \cap \{\bar{w} > 0\}$, see (1.17), loses hyperbolicity at $\bar{w} = 0$ due to the exponential decay of the single (recall (1.7)) non-zero eigenvalue. To deal with this type of loss of hyperbolicity, we use the method in [22], developed by the present author, to gain hyperbolicity in an extended space.

Besides providing all the details of the analysis to obtain a rigorous proof of theorem 1.5 we also provide a better overview of the analysis and the many blowup steps (we count 16 in total). We lay out the geometry of the blowups and detail the charts and the corresponding coordinate transformations. Also, in the present manuscript we provide a complete analysis of the dynamics near Q^6 for $\epsilon > 0$, which is missing at any level of formality in [3]. Our blowup approach allows us to identify an improved singular cycle, consisting of 12 segments, with better hyperbolicity properties. The additional segments $\gamma^{1,2,5,6,8,10,11}$, not visible in the 'blown down' version of Γ_0 in figure 7, see definition 1.3 and (1.24), are described carefully in sections 4 and 7, see also figures 15 and 25 from the perspective of ϕ_1 and ϕ_3, respectively. A corollary of our results, is that the amplitude of the relaxation oscillations grows like $\mathcal{O}(\log \epsilon^{-1})$ as $\epsilon \to 0$, see remark 5.2 for details.

2. Proof of the main theorem

To prove theorem 1.5, we first consider the reduced problem (1.8) and $\alpha > \xi$. Then by lemma 1.2, $W^{cu}(Q^6)$ intersects $y = \delta^{-1}$ in a single point

$$q^0 = (x^0, \delta^{-1}, z^0), \tag{2.1}$$

with

$$z^0 \approx -\log(\delta^{-1}) \left(1 + \frac{\alpha\delta}{\xi}\right),$$

see (1.14), and $x^0 = m(\delta^{-1}, z^0)$, for $\delta > 0$ sufficiently small. Let N^0 be a small neighborhood of (x^0, z^0) in $\mathbb{R}^2$. We therefore define a section Σ^0 as follows

$$\Sigma^0 = \{(x, y, z) \mid y = \delta^{-1}, (x, z) \in N^0\}. \tag{2.2}$$

By lemma 1.2 again, $W^{cu}(Q^6)$ also intersects $z = \delta^{-1}$ in a single point $q^1 = (x^1, y^1, \delta^{-1})$ with $y^1 > 0$ and $x^1 = m(y^1, \delta^{-1})$ for $\delta > 0$ sufficiently small, recall (1.9). See also [3, proposition 5.2]. Then we define a section Σ^1 as follows

$$\Sigma^1 = \{(x, y, z) \mid z = \delta^{-1}, (x, y) \in N^1\}, \tag{2.3}$$

where N^1 is a small neighborhood of (x^1, y^1) in $\mathbb{R}^2$. See figure 8. Notice that (1.5) is transverse to Σ^0. Also the reduced flow on C is transverse to Σ^1.

2.1. The transition map $\Pi^0 : \Sigma^0 \to \Sigma^1$

Let $\Pi^0 : \Sigma^0 \to \Sigma^1$ be defined for $0 < \epsilon \ll 1$ as the transition mapping obtained by the first intersection through the forward flow of (1.3). For $\epsilon = 0$, we similarly define $\Pi^0 : \Sigma^0 \to \Sigma^1$ as the composition of the following mappings: (a) the projection $(x, \delta^{-1}, z) \mapsto (x, \delta^{-1}, \tilde{m}(x, \delta^{-1}))$ onto C defined by the stable, critical fibers. Here $\tilde{m}(x, y) := -x - \xi y$, obtained by solving

the equation (1.9) for z. (b): the mapping obtained from $(x, \delta^{-1}, \tilde{m}(x, \delta^{-1})) \in \Sigma^0$ by the first intersection with Σ^1 through the forward flow of the reduced problem on C. Hence Π^0 only depends upon x for $\epsilon = 0$:

$$\Pi^0(x, \delta^{-1}, z; 0) = \Pi^0(x, \delta^{-1}, \tilde{m}(x, \delta^{-1}); 0) \in C \cap \Sigma^1,$$

for all $(x, \delta^{-1}, z) \in \Sigma^0$. Notice, we write $\Pi^0(\cdot; \epsilon)$ to highlight the dependency of Π^0 on ϵ (as a parameter).

Lemma 2.1. *Suppose $\alpha > \xi$. Then for N^0 sufficiently small there exists an $\epsilon_0 > 0$ such Π^0 is well-defined and $C^{k \geqslant 1}$-smooth, even in $\epsilon \in [0, \epsilon_0]$. In particular*

$$\Pi^0(x, \delta^{-1}, z; \epsilon) = \Pi^0(x, \delta^{-1}, \tilde{m}(x, \delta^{-1}); 0) + \mathcal{O}(\epsilon).$$

Proof. The result follows directly from Fenichel's theory [12–14, 20]. Indeed, following the analysis of the reduced problem, the mapping $\Pi^0(\cdot; 0)$ is described over a compact sub-manifold $S_0 \subset C$. Since C is normally hyperbolic, S_0 and the smooth foliation of its stable manifold therefore perturb by Fenichel's theory. In particular, there exists a locally invariant slow manifold S_ϵ for all $0 \leqslant \epsilon \ll 1$ which is diffeomorphic to—and smoothly $\mathcal{O}(\epsilon)$-close to—S_0. The reduced flow on S_ϵ is therefore smoothly $\mathcal{O}(\epsilon)$-close to the reduced flow on S_0 given by (1.8). Using the smooth fiber projections, the result then follows. $\qquad\square$

2.2. The transition map $\Pi^1 : \Sigma^1 \to \Sigma^0$

The main problem of the proof of theorem 1.5 is to prove the following result: let

$$\Pi^1 : \; \Pi^0(\Sigma^0) \subset \Sigma^1 \to \Sigma^0, \tag{2.4}$$

be the mapping obtained by the first intersection by the forward flow. Then the following result will enable a proof of theorem 1.5:

Lemma 2.2. *There exist a $\delta > 0$, a sufficiently small set N^0, and an $\epsilon_0 > 0$ such that the mapping $\Pi^1(\cdot; \epsilon)$ is well-defined and C^1 for all $0 < \epsilon \leqslant \epsilon_0$. In particular, $\Pi^1(x, y, \delta^{-1}; \epsilon)$ is C^1 $o(1)$-close to the constant function q^0 as $\epsilon \to 0$.*

Proof of theorem 1.5. Let $\Pi = \Pi^1 \circ \Pi^0$. Then by lemmas 2.1 and 2.2, Π is a contraction for $\epsilon \ll 1$. The existence of an attracting limit cycle Γ_ϵ in theorem 1.5(*a*) therefore follows from the contraction mapping theorem—the attracting limit cycle being obtained as the forward flow of the unique fix-point of Π.

The unboundedness of Γ_ϵ in (x, y, z) follows from the convergence $\Gamma_\epsilon \to \Gamma_0$ as $\epsilon \to 0$ on the Poincaré sphere. The latter—being the content of theorem 1.5(*b*)—is a consequence of our approach. We actually first 'derive' an improved version of Γ_0 using successive blowup transformations (working in the charts ϕ_3 and ϕ_1) that allow us to prove lemma 2.2 using several applications of standard, local, hyperbolic methods of dynamical systems theory. This gives Γ_ϵ as a 'perturbation' of (the blown up) Γ_0. In more details, we further decompose Π^1 into two parts Π^{17} and Π^{70} where $\Pi^{17} : D(\Pi^{17}) \subset \Sigma^1 \to \Sigma^7$ and $\Pi^{70} : \Sigma^7 \to \Sigma^0$. Here Σ^7 is an appropriate 2D-section, transverse to γ^7 (1.26), contained within $y_3 = \frac{2\alpha(1+\nu)}{\xi}$ for $\nu > 0$ small, see figure 7 for an illustration. We describe these mappings in details in the following sections, see lemmas 5.1 and 8.1. Lemma 2.2 is a consequence of these two intermediate results (see end of section 8). $\qquad\square$

2.3. Outline

In the remainder of this paper, we prove lemma 2.2. Following the proof of theorem 1.5, the analysis of Π^1 is split into two parts: one part in ϕ_3 (relevant for the description of the mapping Π^{17}) and another in ϕ_1 (relevant for the description of the other half of Π^1, Π^{70}). In section 3, we first describe the blowup analysis in ϕ_3, summarizing the results in section 3.4 before providing all the details of the analysis in section 4. In section 5, we combine the results of the analysis into a rigorous statement on the transition map Π^{17}, see lemma 5.1. The blowups we describe in section 3 is (in practice) the result of calculations done in charts. However, given the complicated nature of the problem and the repeated blowups required, we feel that presenting these transformations—and the associated geometry—in section 3 before the details in section 4 is useful for the readability of the paper. In section 6, we adopt a similar approach by first describing the blowup analysis in the chart ϕ_1. However, due to the special essential singularity at Q^6 on C_∞, this blowup analysis will be further divided into three separate steps following a 'blowup' of $(\bar{y}, \bar{z}, \bar{w}) = (1, 0, 0)$. Again, in section 3.4, the results of the blowup analysis are summarized before all the details are provided, see section 7. In section 8, we finally combine the results of the analysis into a rigorous statement on the transition map Π^{70}, see lemma 8.1. We end this section with a proof of lemma 2.2. In section 9, we discuss some consequences of theorem 1.5 and directions for future work on the topic.

3. Blowup analysis in chart ϕ_3

In this chart, we obtain the following equations

$$
\begin{aligned}
\dot{x}_3 &= -\epsilon(x_3 + 1 + \alpha) + x_3 e^{-2/w_3}\left(y_3 + \frac{x_3 + 1}{\xi}\right), \\
\dot{y}_3 &= \epsilon w_3(1 - e^{-1/w_3}) + y_3 e^{-2/w_3}\left(y_3 + \frac{x_3 + 1}{\xi}\right), \\
\dot{w}_3 &= w_3 e^{-2/w_3}\left(y_3 + \frac{x_3 + 1}{\xi}\right),
\end{aligned}
\tag{3.1}
$$

using the coordinates (x_3, y_3, w_3), recall (1.20). Here we cover the part of the critical manifold C (1.6) with $z > 0$ as follows

$$
C_3 = \left\{(x_3, y_3, w_3) \,\middle|\, y_3 + \frac{x_3 + 1}{\xi} = 0, w_3 > 0\right\}.
\tag{3.2}
$$

This manifold is still a normally hyperbolic and attracting critical manifold of (3.1) in the present chart: the linearization about any point in C_3 gives

$$
-\xi^{-1} e^{-2/w_3} < 0,
\tag{3.3}
$$

for $w_3 > 0$, as a single nonzero eigenvalue. But we now also obtain $\{w_3 = 0\}$, corresponding (by (1.20)) to the subset of the equator $S^3 \cap \{\bar{w} = 0\}$ with $\bar{z} > 0$, as a set of fully nonhyperbolic critical points for $\epsilon = 0$. Indeed, the linearization about any point in $\{w_3 = 0\}$ only has zero eigenvalues for $\epsilon = 0$. The boundary of C_3 along $w_3 = 0$:

$$
C_{\infty,3} = \left\{(x_3, y_3, w_2) \,\middle|\, y_3 + \frac{x_3 + 1}{\xi} = 0, w_3 = 0\right\}
\tag{3.4}
$$

is therefore also fully nonhyperbolic for $\epsilon = 0$. The exponential decay of (3.3) complicates the blowup analysis and the study of what happens near $\{w_3 = 0\}$ and $C_{\infty,3}$ for $0 < \epsilon \ll 1$. We

follow the blowup approach in [22], also used in [3], and extend the phase space dimension by introducing

$$q_3 = e^{-2/w_3}. \tag{3.5}$$

By implicit differentiation, we obtain

$$\dot{q}_3 = 2w_3^{-2}e^{-2/w_3}\dot{w}_3 = 2w_3^{-1}q_3^2\left(y_3 + \frac{x_3 + 1}{\xi}\right).$$

We therefore consider the extended system

$$
\begin{aligned}
\dot{x} &= -\epsilon w(x + 1 + \alpha) + xwq\left(y + \frac{x+1}{\xi}\right), \\
\dot{y} &= \epsilon w^2(1 - e^{-1/w}) + ywq\left(y + \frac{x+1}{\xi}\right), \\
\dot{w} &= w^2 q\left(y + \frac{x+1}{\xi}\right), \\
\dot{q} &= 2q^2\left(y + \frac{x+1}{\xi}\right), \\
\dot{\epsilon} &= 0,
\end{aligned}
\tag{3.6}
$$

having here dropped the subscripts, introduced ϵ as a dynamic variable and finally multiplied the right hand side by $w = w_3$ (to ensure that $w = 0$ is well-defined). This multiplication 'trick' is used frequently in the sequel (and in GSPT, in particular blowup, in general [19, 21]). It is important to note that it corresponds to a transformation of time for $w > 0$, and the systems are therefore equivalent there. Now, by construction, the set

$$\{(x, y, w, q, \epsilon) \,|\, q = e^{-2/w}\}, \tag{3.7}$$

is an invariant set for this system. But this invariance is implicit in the system (3.6) and we shall use it only when needed. Now, we (re-)define C by

$$C = \left\{(x, y, w, q, \epsilon) \,\Big|\, y + \frac{x+1}{\xi} = 0, w > 0, q > 0, \epsilon = 0\right\}, \tag{3.8}$$

in the extended system, using, for simplicity, the same symbol. It is still a hyperplane within $\epsilon = 0$ of partially hyperbolic critical points, now of dimension three, since the linearization about any point in C has one single nonzero eigenvalue $-wq/\xi$. Intersecting (3.8) with the set defined in (3.7) gives a 2D manifold which projects to (3.2) (upon removing the subscripts) in the (x, y, w)-space. Similarly, $\{w = \epsilon = 0\}$ and $\{q = \epsilon = 0\}$ are fully nonhyperbolic sets of equilibria for (3.6). The system is therefore very degenerate near

$$C_\infty = \left\{(x, y, w, q, \epsilon) \,\Big|\, y + \frac{x+1}{\xi} = 0, w = q = 0, \epsilon = 0\right\}, \tag{3.9}$$

where these degenerate objects intersect the boundary of (3.8): $C_\infty = \overline{C} \cap \{w = \epsilon = 0\} \cap \{q = \epsilon = 0\}$. Notice (3.9) projects to (3.4) (upon removing the subscripts) in the (x, y, w)-space (which is why we use the same symbol in (3.8)). But the system (3.6) is now algebraic to leading order and therefore we can (in principle) apply the classical blowup method of [8, 26] to study the dynamics near C_∞.

3.1. The blowup method

Before applying the blowup method to (3.6), we will first briefly review this approach in the simple context of a nonhyperbolic equilibrium point $z = 0$ for a general system $\dot{z} = h(z)$ on a neighborhood $\mathcal{U} \subset \mathbb{R}^n$ and where $h : \mathcal{U} \to \mathbb{R}^n$ is smooth. For further details see e.g. [8, 9, 26, 28]. We assume (after center manifold reduction) that $z = 0$ is fully nonhyperbolic with its linearization having only zero eigenvalues. In this paper, I will then say that a *blowup* of $z = 0$ is a *generalized polar coordinate transformation* $\Psi : [0, r_0) \times S^{n-1} \to \mathcal{U}$ defined by:

$$(r, \bar{z}) \mapsto \begin{cases} z_1 & = r^{\alpha_1} \bar{z}_1, \\ z_2 & = r^{\alpha_2} \bar{z}_2, \\ \quad \vdots \\ z_n & = r^{\alpha_n} \bar{z}_n, \end{cases}$$

where

$$\bar{z} \in S^{n-1} := \left\{ (\bar{z}_1, \bar{z}_2, \dots, \bar{z}_n) \in \mathbb{R}^n \mid \sum_{i=1}^{n} \bar{z}_i^2 = 1 \right\},$$

and the *weights*: $\alpha = (\alpha_1, \dots, \alpha_n) \in \mathbb{N}^n$, such that the following holds: there exists a $k \in \mathbb{N}$ so that

$$\widehat{h} := r^{-k} \overline{h}, \quad \overline{h} = \Psi^* h, \tag{3.10}$$

is well-defined on $[0, r_0) \times S^{n-1}$; specifically

$$\widehat{h}|_{r=0} \neq 0. \tag{3.11}$$

In (3.10), $\overline{h}$ is the pull-back of h by Ψ. Furthermore, the division of $\overline{h}$ by r^k in (3.10) is called *desingularization*, and $\widehat{h}$ is said to be the *desingularized vector-field*. By (3.11), singularities of $\widehat{h}$ will (or more accurately: may, in dimensions $n \geqslant 3$) have improved hyperbolicity properties, making the analysis of $\widehat{h}$ simpler than that of h. Notice also that $\widehat{h}$ and h are equivalent for $r > 0$, and we can therefore obtain a complete local description of h near $z = 0$ by studying $\widehat{h}$ with $r \in [0, r_0)$. The caveat is obviously that we have transformed a local problem near $z = 0$ to a global one on $[0, r_0) \times S^{n-1}$. For the analysis and for computations, one will typically describe $\widehat{h}$ in the local coordinates provided by the directional charts, see section 3.3 below.

I will call the transformation Ψ the *blowup transformation* (despite the fact that it is Ψ^{-1} —and not Ψ—that is blowing up $z = 0$ to $\{r = 0\} \times S^{n-1}$). Any invariant manifold $\overline{M}$ of $\widehat{h}$ on $[0, r_0) \times S^{n-1}$ gives rise to an invariant 'manifold' $M = \Psi(\overline{M})$ of h on $\mathcal{U}$. We say that $\overline{M}$ becomes M upon *blowing down*.

If $\alpha_1 = \alpha_2 = \cdots = \alpha_n$ (without loss of generality $\alpha_i \equiv 1$ for all $i = 1, 2, \dots, n$) then Ψ is said to be *homogeneous*. Otherwise it is called *quasi-homogeneous*. Relevant to the present paper, it is also possible to apply the blowup approach to study sets (lines, planes or more generally sub-manifolds) of nonhyperbolic points. The procedure is the same, we just apply a blowup of each point in the set. In this way, the sets of nonhyperbolic points are blown up to generalized cylinders, see e.g. [21, 23, 24].

Upon blowup additional fully nonhyperbolic singularities may be encountered, see [9, 28] and [24] for an example. In these situations, blowup has to be used successively. This is also the case in the present ϕ_3-chart. In fact, we will have to use five consecutive blowup transformations to achieve desirable hyperbolicity properties. In anticipation of the details in section 4, we describe these blowup transformations in the following section. In section 3.3, we describe the local coordinates used in our analysis. Here we also present two tables, see
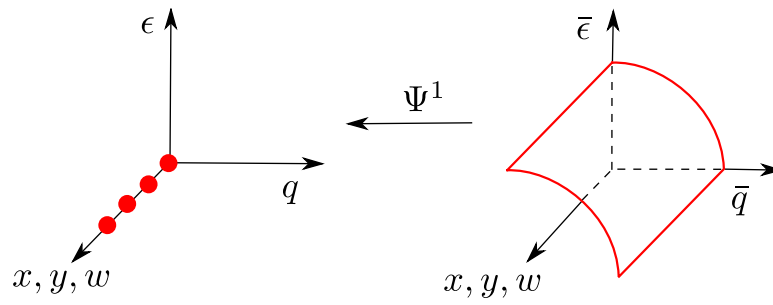
Figure 9. First cylindrical blowup of $q = \epsilon = 0$.

tables 1 and 2, to help track of the different coordinates, the coordinate changes and the resulting differential equations.

3.2. Blowup transformations in chart ϕ_3

In the first step of our blowup procedure, we blowup the set of degenerate equilibria $\{q = \epsilon = 0\}$ of (3.6). Let

$$P = \left\{ (x, y, w, q, \epsilon) \in \mathbb{R}^2 \times [0, \infty)^3 \right\}.$$
$$P^1 = \left\{ (x, y, w, r, (\bar{q}, \bar{\epsilon})) \in \mathbb{R}^2 \times [0, \infty)^2 \times S^1 \right\}.$$

Then we blowup the set $\{(x, y, w, q, \epsilon) \in P \,|\, q = \epsilon = 0\}$ to a cylinder through the following blowup transformation

$$\Psi^1 : P^1 \to P,$$

which fixes x, y and z and takes

$$(r, (\bar{q}, \bar{\epsilon})) \mapsto (q, \epsilon) = r(\bar{q}, \bar{\epsilon}), \quad r \geqslant 0, \ (\bar{q}, \bar{\epsilon}) \in S^1. \tag{3.12}$$

Clearly, only $\bar{q} \geqslant 0$, $\bar{\epsilon} \geqslant 0$ will be relevant. Furthermore, Ψ^1 simply corresponds to introducing polar coordinates in the (q, ϵ)-plane. We can therefore study a small neighborhood of $(q, \epsilon) = 0$ by studying any $(r, (\bar{q}, \bar{\epsilon})) \in [0, \infty) \times S^1$ with $r \geqslant 0$ small. But the preimage of $\{q = \epsilon = 0\}$ is a cylinder $(x, y, w, (\bar{q}, \bar{\epsilon})) \in \mathbb{R}^2 \times [0, \infty) \times S^1$. (This is in the sense that we understand blowup.) The mapping Ψ^1 produces a vector-field $\overline{X}^1$ on P^1 by pull-back of the vector-field (3.6) on P. More importantly, the desingularized vector-field $\widehat{X}^1 = r^{-1}\overline{X}^1$ is well-defined and non-zero—this is straightforward to see from (3.6). It is therefore $\widehat{X}^1$ that we shall study in the following.

We illustrate the blowup transformation defined by (3.12) in figure 9. Notice how we artistically combine the *xyw*-space into a single coordinate axis. We use red colours and lines, also in the following, to indicate what variables and coordinate axes that are included in each blowup in figure 9. Specifically, points that are blown up are given red dots. Since we are working in five dimensions, some of the figures that will appear in the following will be fairly caricatured. We cannot capture everything with these figures. To obtain a more detailed understanding, these attempts of 'global figures' have to be combined with the 'local' ones in section 4.

Now, although the set defined by $(\bar{q}, \bar{\epsilon}) = (1, 0)$, $r = 0$ is partially hyperbolic for $\widehat{X}_1$ (which we will use later in section 4.7, see also figure 20), this set loses hyperbolicity along the line

(a)

(b)
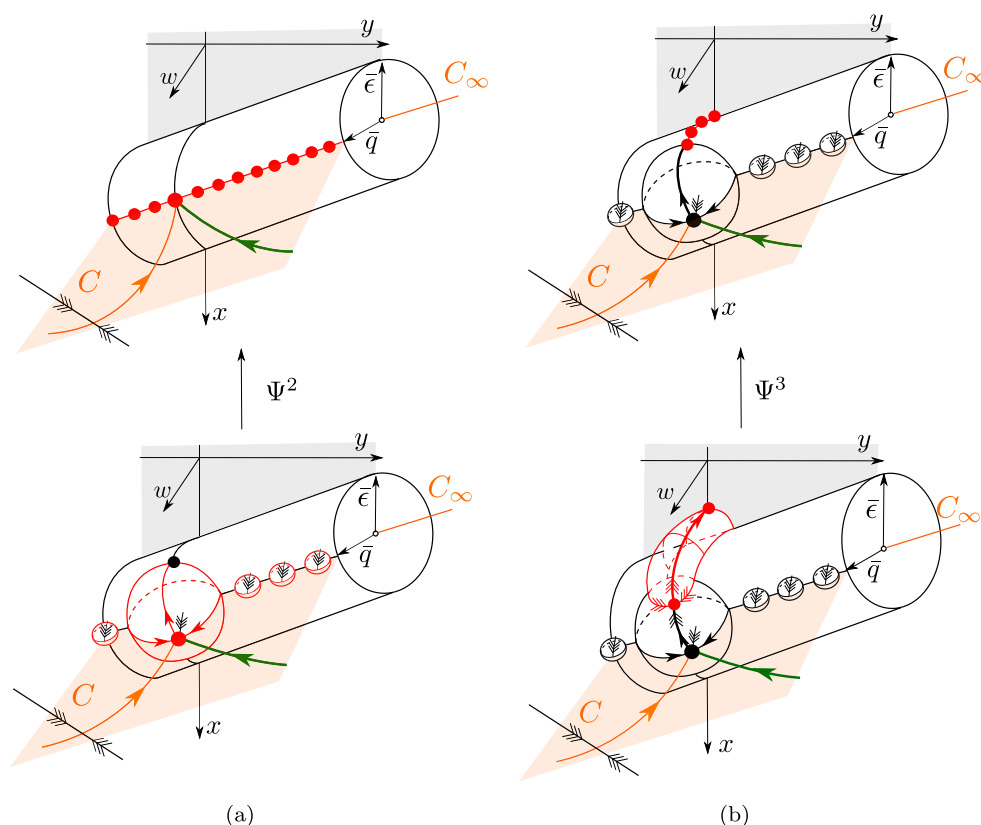
Figure 10. In these figures, the 'blown down' diagrams are on top while the corresponding 'blown up' pictures are sketched below. A similar convention will appear in later figures, although sometimes we will rotate the diagram, recall figure 9. Notice that our view is from $w > 0$, the w-axis coming out of the picture. The directions of the remaining x- and y-axes are indicated. In particular, the x-axis is directed downwards. In (a): second blowup of C_∞, see (3.9), along $\bar{q} = 1$. The spheres indicated below are blown versions of the (red) points on C_∞ shown on top, each involving the extra dimensions due to q and ϵ, see details in (3.13). The sphere at $y = 0$ (enlarged) is extra special since this point, corresponding to Q^1, is a stable node of the reduced problem. The blowup produces normal hyperbolicity of C all the way up to (an improved version of) C_∞ (indicated by smaller triple-headed arrows). This enables an extension of the slow manifold, in the usual way [26]. In (b): third blowup step. Here we blowup a line of equilibria (indicated by red points in the top half of the figure), emanating from the fully nonhyperbolic 'north pole' of the sphere obtained in the second step, see figure (a). This gives rise to a cylinder (also in red in the blowup figure below), its axis being formed by the quarter circle with $\bar{q} \geqslant 0, \bar{\epsilon} \geqslant 0$.

defined by $x = -1 - \xi y$, $w = 0$ for each y (corresponding to C_∞ (3.9)). In the next step, we therefore blowup this set. Let

$$P^2 = \left\{ (y, r, \rho, (\bar{x}, \bar{w}, \bar{\bar{\epsilon}})) \in \mathbb{R} \times [0, \infty)^2 \times S^2 \right\}.$$

We then apply the blowup transformation

$$\Psi^2 : P^2 \to P^1,$$

which fixes y and r and takes

$$
(y, \rho, (\bar{x}, \bar{w}, \bar{\bar{\epsilon}})) \mapsto \begin{cases} x & = & -1 - \xi y + \rho \bar{x}, \\ w & = & \rho \bar{w}, \\ \bar{q}^{-1} \bar{\epsilon} & = & \rho \bar{\bar{\epsilon}}. \end{cases} \qquad \rho \geqslant 0, (\bar{x}, \bar{w}, \bar{\bar{\epsilon}}) \in S^2. \quad (3.13)
$$

Clearly, we can study a small neighborhood of $x = -1 - \xi y$, $w = 0$, $(\bar{q}, \bar{\epsilon}) = (1, 0)$ by studying $(\rho, (\bar{x}, \bar{w}, \bar{\bar{\epsilon}})) \in [0, \infty) \times S^2$ with $\rho \geqslant 0$ small for any y. As before, the mapping Ψ^2 gives rise to a vector-field $\overline{X}^2 = \Psi^{2*}(\widehat{X}^1)$ on P^2 by pull-back of $\widehat{X}^1$ on P^1. Now, for example by working in the local charts described below, we find that $\overline{X}^2$ has ρ as a common factor and we therefore study $\widehat{X}^2 = \rho^{-1} \overline{X}^2$ in the following. For this $\widehat{X}^2$, we find an improved partially hyperbolic version of C_∞, which allow us to extend the slow manifold up close to Q^1, in the usual way see [26]. See an illustration of the second blowup step in figure 10(a).

Let

$$
P^3 = \left\{ (y, r, \rho, \varrho, (\bar{\bar{x}}, \bar{\bar{w}})) \in \mathbb{R} \times [0, \infty)^3 \times S^1 \right\}.
$$

Then in the third step, we find that $\bar{x} = \bar{w} = 0, \bar{\bar{\epsilon}} = 1$, $\rho \geqslant 0$ for each y is a set of nonhyperbolic points within P^2 for $\widehat{X}^2$. We therefore blowup this set through the following quasi-homogeneous blowup transformation

$$
\Psi^3 : P^3 \to P^2
$$

which fixes y, r and ρ and takes

$$
(\varrho, (\bar{\bar{x}}, \bar{\bar{w}})) \mapsto \begin{cases} \bar{\bar{\epsilon}}^{-1} \bar{x} & = & \varrho \bar{\bar{x}}, \\ \bar{\bar{\epsilon}}^{-1} \bar{w} & = & \varrho^2 \bar{\bar{w}}, \end{cases} \qquad \varrho \geqslant 0, (\bar{\bar{x}}, \bar{\bar{w}}) \in S^1. \quad (3.14)
$$

We illustrate this in figure 10(b). Clearly, we can study a small neighborhood of $(\bar{x}, \bar{w}, , \bar{\bar{\epsilon}}) = (0, 0, 1)$ by studying $(\varrho, (\bar{\bar{x}}, \bar{\bar{w}})) \in [0, \infty) \times S^2$ with $\varrho \geqslant 0$ small. Ψ^3 gives a vector-field $\overline{X}^3 = \Psi^{3*}(\widehat{X}^2)$ on P^3 by pull-back of $\widehat{X}^2$ on P^2. The weights on ϱ in (3.14) are so that $\overline{X}^3$ has ϱ as a common factor and we therefore study the 'improved' vector-field defined by $\widehat{X}^3 = \varrho^{-1} \overline{X}^3$.

In the following, we define

$$
\Psi^{12} : P^2 \to P
$$

and

$$
\Psi^{123} : P^3 \to P
$$

by the compositions

$$
\Psi^{12} = \Psi^1 \circ \Psi^2, \quad \Psi^{123} = \Psi^{12} \circ \Psi^3.
$$

Therefore by (3.12)–(3.14) (see also remark 3.1)

$$
\Psi^{12} : (y, r, \rho, (\bar{x}, \bar{w}, \bar{\bar{\epsilon}})) \mapsto \begin{cases} x & = & -1 - \xi y + \rho \bar{x}, \\ y & = & y \\ w & = & \rho \bar{w}, \\ q & = & \frac{r}{\sqrt{1 + \rho^2 \bar{\bar{\epsilon}}^2}}, \\ \epsilon & = & \frac{r \rho \bar{\bar{\epsilon}}}{\sqrt{1 + \rho^2 \bar{\bar{\epsilon}}^2}}, \end{cases} \quad (3.15)
$$

(a)

(b)
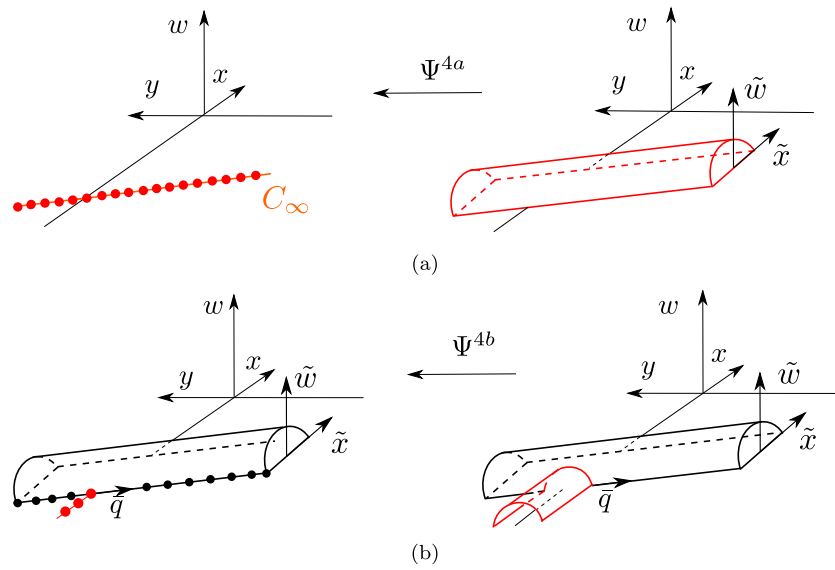
Figure 11. In these figures, the 'blown down' pictures are on the left, whereas the 'blown up' versions are on the right (as in figure 9). In both figures, we show a view from $x < 0$, the x-axis 'entering' the page. The directions of the remaining axes w and y are indicated by arrows. In (a): fourth blowup step, part a, blowing up C_∞ (red points in the 'blown down' picture on the left), see (3.9), to a cylinder (in red in the 'blown up' picture on the right). In (b): fourth blowup step, part b. Here we blow up a line of equilibria (red points on the left) $\bar{q} = 0$, $\tilde{w} = 0$ on the cylinder (also on the right in figure (a)) producing a new cylinder (also in red on the right) along the negative x-direction.

$$
\Psi^{123} : (y, r, \rho, \varrho, (\bar{\bar{x}}, \bar{\bar{w}})) \mapsto
\begin{cases}
x &= -1 - \xi y + \dfrac{\rho \varrho \bar{\bar{x}}}{\sqrt{1 + \varrho^2 \bar{\bar{x}}^2 + \varrho^4 \bar{\bar{w}}^2}}, \\[3mm]
y &= y \\[2mm]
w &= \dfrac{\rho \varrho^2 \bar{\bar{w}}}{\sqrt{1 + \varrho^2 \bar{\bar{x}}^2 + \varrho^4 \bar{\bar{w}}^2}}, \\[3mm]
q &= \dfrac{r}{\sqrt{1 + \dfrac{\rho^2}{1 + \varrho^2 \bar{\bar{x}}^2 + \varrho^4 \bar{\bar{w}}^2}}}, \\[5mm]
\epsilon &= \dfrac{r\rho \dfrac{1}{\sqrt{1 + \varrho^2 \bar{\bar{x}}^2 + \varrho^4 \bar{\bar{w}}^2}}}{\sqrt{1 + \dfrac{\rho^2}{1 + \varrho^2 \bar{\bar{x}}^2 + \varrho^4 \bar{\bar{w}}^2}}}.
\end{cases}
\tag{3.16}
$$

Remark 3.1. The expressions in (3.15) and (3.16) follow from simple calculations. For example, given that $(\bar{q}, \bar{\epsilon}) \in S^1$, it follows from the last equality in (3.13) that

$$
(\bar{q}, \bar{\epsilon}) = \left(\sqrt{1 + \rho^2 \bar{\bar{\epsilon}}^2}, \frac{\rho \bar{\bar{\epsilon}}}{\sqrt{1 + \rho^2 \bar{\bar{\epsilon}}^2}} \right).
$$

Similarly, since $(\bar{x}, \bar{w}, \bar{\bar{\epsilon}}) \in S^2$ we can also write the right hand side of (3.14) as
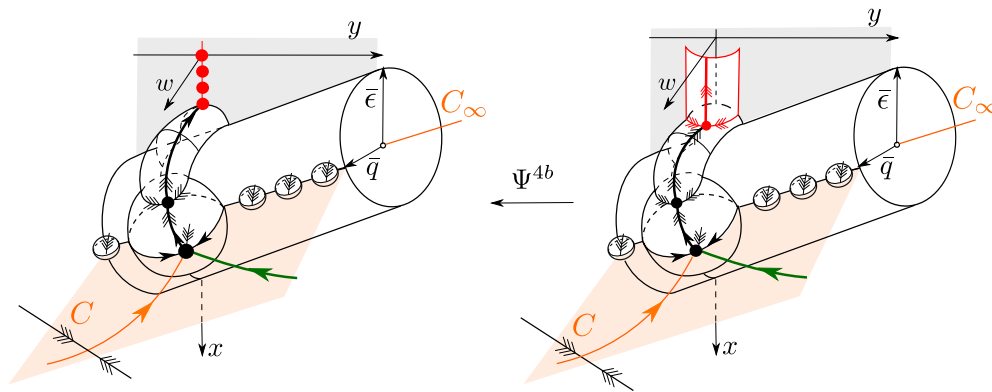
Figure 12. Similar to figure 11(b), but now—following lemma 3.3—using the viewpoint in figure 10(b).

$$\left(\bar{x}, \bar{w}, \bar{\bar{\epsilon}} \right) = \left(\frac{\varrho \bar{\bar{x}}}{\sqrt{1 + \varrho^2 \bar{\bar{x}}^2 + \varrho^4 \bar{\bar{w}}^2}}, \frac{\varrho^2 \bar{\bar{w}}}{\sqrt{1 + \varrho^2 \bar{\bar{x}}^2 + \varrho^4 \bar{\bar{w}}^2}}, \frac{1}{\sqrt{1 + \varrho^2 \bar{\bar{x}}^2 + \varrho^4 \bar{\bar{w}}^2}} \right).$$

In the fourth step, we first return to P^1 near $(\bar{q}, \bar{\epsilon}) = (0, 1)$. Notice that this implies ρ large in (3.13). We therefore proceed as follows in two steps (enumerated a and b). (Eventually in lemma 3.3 we will connect these steps with Φ^{123}, see also figure 11(c).) Let

$$P^{4a} = \left\{ (y, r, \sigma, (\tilde{x}, \tilde{w}), (\bar{q}, \bar{\epsilon})) \in \mathbb{R} \times [0, \infty)^2 \times S^1 \times S^1 \right\}.$$

Then, we first blowup the set C_∞ of nonhyperbolic points of $\widehat{X}^1$ defined by $x = -1 - \xi y$, $w = 0$ through the blowup transformation

$$\Psi^{4a} : P^{4a} \rightarrow P^1,$$

which fixes y, r and $(\bar{q}, \bar{\epsilon})$ and takes

$$(y, \sigma, (\tilde{x}, \tilde{w})) \mapsto \begin{cases} x &=& -1 - \xi y + \sigma \tilde{x}, \\ w &=& \sigma^2 \tilde{w}. \end{cases} \tag{3.17}$$

Crucially, the exponents of σ in (3.17) coincide with the exponents on ϱ in (3.14). For $r = 0$, (3.17) is still a blowup of C_∞. We illustrate the blowup in figure 11(a). Ψ^{4a} gives a vector-field $\overline{X}^{4a} = \Psi^{4a*}(\widehat{X}^1)$ on P^{4a} by pull-back of $\widehat{X}^1$ on P^1. Here $\overline{X}^{4a} = \sigma \widehat{X}^{4a}$, with $\widehat{X}^{4a}$ well-defined. It is $\widehat{X}^{4a}$ that we shall study.

Next, let

$$P^{4b} = \left\{ (y, r, \sigma, \pi, (\tilde{\tilde{w}}, \tilde{\tilde{q}})) \in \mathbb{R} \times [0, \infty)^3 \times S^1 \right\}.$$

Then we blowup the set of nonhyperbolic points for $\widehat{X}^{4a}$ defined by $\tilde{x} = -1$, $\tilde{w} = 0$, $\bar{\epsilon}^{-1} \bar{q} = 0$ within P^{4a} for each y through the blowup transformation $\Psi^{4b} : P^{4b} \rightarrow P^{4a}$ which fixes y, r and σ and takes

$$(\pi, (\tilde{\tilde{w}}, \tilde{\tilde{q}})) \mapsto \begin{cases} \tilde{x}^{-2} \tilde{w} &=& \pi \tilde{\tilde{w}}, \\ \bar{\epsilon}^{-1} \bar{q} &=& \pi \tilde{\tilde{q}}, \end{cases} \quad \pi \geqslant 0, (\tilde{\tilde{w}}, \tilde{\tilde{q}}) \in S^1. \tag{3.18}$$

We illustrate the fourth blowup step in figure 11, see also figure 12, using the viewpoint of figure 10(b). (See also lemma 3.3 below).

Ψ^{4b} gives $\overline{X}^{4b} = \Psi^{4b*}(\widehat{X}^{4a})$ on P^{4b} by pull-back of $\widehat{X}^{4a}$ on P^{4a}. Now, $\overline{X}^{4b} = \pi\widehat{X}^{4b}$ and it is $\widehat{X}^{4b}$ that we study.

We now define

$$\Psi^{14a} : P^{4a} \to P, \quad \Psi^{14a4b} : P^{4b} \to P,$$

as the compositions

$$\Psi^{14a} = \Psi^1 \circ \Psi^{4a}, \quad \Psi^{14a4b} = \Psi^1 \circ \Psi^{4a} \circ \Psi^{4b}.$$

Therefore by (3.12), (3.17) and (3.18) (see also remark 3.2)

$$\Psi^{14a} : (y, r, \sigma, (\tilde{x}, \tilde{w}), (\bar{q}, \bar{\epsilon})) \mapsto \begin{cases} x & = & -1 - \xi y + \sigma\tilde{x}, \\ y & = & y \\ w & = & \sigma^2\tilde{w}, \\ q & = & r\bar{q}, \\ \epsilon & = & r\bar{\epsilon}, \end{cases}$$

and

$$\Psi^{14a4b} : (y, r, \sigma, \pi, (\tilde{\tilde{w}}, \tilde{\tilde{q}})) \mapsto \begin{cases} x & = & -1 - \xi y + \sigma\chi\left(\pi\tilde{\tilde{w}}\right), \\ y & = & y \\ w & = & \sigma^2\chi\left(\pi\tilde{\tilde{w}}\right)^2 \pi\tilde{\tilde{w}}, \\ q & = & \frac{r\pi\tilde{\tilde{q}}}{\sqrt{1+\pi^2\tilde{\tilde{q}}^2}}, \\ \epsilon & = & \frac{r}{\sqrt{1+\pi^2\tilde{\tilde{q}}^2}}. \end{cases} \qquad (3.19)$$

Here $\chi : \mathbb{R} \to (-1, 0)$ is the unique, negative-valued, smooth function

$$\chi : \mathbb{R} \to (-1, 0), \quad \chi(p) = \begin{cases} -1 & \text{if } p = 0 \\ -\frac{\sqrt{\sqrt{4p^2+1}-1}}{\sqrt{2}\,|p|} & \text{otherwise} \end{cases},$$

satisfying $\chi(p)^2 + \chi(p)^4 p^2 = 1$.

Remark 3.2. Notice that since $(\tilde{x}, \tilde{w}) \in S^1$ and $(\bar{q}, \bar{\epsilon}) \in S^1$ it follows from simple calculations that the right hand side of (3.18) can be written as

$$(\tilde{x}, \tilde{w}) = \left(\chi\left(\pi\tilde{\tilde{w}}\right), \chi\left(\pi\tilde{\tilde{w}}\right)^2 \pi\tilde{\tilde{w}}\right),$$

$$(\bar{q}, \bar{\epsilon}) = \left(\frac{\pi\tilde{\tilde{q}}}{\sqrt{1+\pi^2\tilde{\tilde{q}}^2}}, \frac{1}{\sqrt{1+\pi^2\tilde{\tilde{q}}^2}}\right).$$

Lemma 3.3. *Let*

$$U^3 = \{(y, r, \rho, \varrho, (\bar{\bar{x}}, \bar{\bar{w}})) \in P^3 \mid \rho > 0, \varrho > 0, \bar{\bar{x}} < 0, \bar{\bar{w}} > 0\},$$

and

$$V^{4b} = \{(y, r, \sigma, \pi, (\tilde{\tilde{w}}, \tilde{\tilde{q}})) \in P^{4b} \mid \pi > 0, \tilde{\tilde{w}} > 0, \tilde{\tilde{q}} > 0\}.$$

$$\overline{X}^3|_{U^3} \xrightarrow{\quad M_* \quad} \overline{X}^{4b}|_{V^{4b}}$$

$$U^3 \subset P^3 \xrightarrow{\quad M \quad} V^{4b} \subset P^{4b}$$

$$\Phi^{123}|_{U^3} \searrow \qquad \swarrow \Phi^{14a4b}|_{V^{4b}}$$

$$P$$
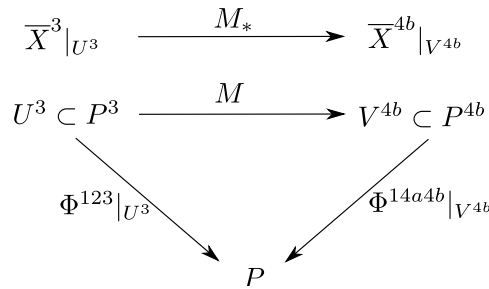
Figure 13. Commutative diagram.

Then there exists a diffeomorphism $M : U^3 \subset P^3 \to V^{4b} \subset P^{4b}$ such that

$$\Psi^{13}|_{U^3} = \Psi^{14a4b} \circ M.$$

Proof. Clearly, M fixes y and r and takes

$$(r, \rho, \varrho, (\bar{\bar{x}}, \bar{\bar{w}})) \mapsto (\sigma, \pi, (\tilde{\tilde{w}}, \tilde{\tilde{q}})).$$

We solve for $(\sigma, \pi, (\tilde{\tilde{w}}, \tilde{\tilde{q}}))$ directly using (3.16) and (3.19). This gives,

$$
\begin{aligned}
x^{-2}w &= \sqrt{1 + \varrho^2\bar{\bar{x}}^2 + \varrho^4\bar{\bar{w}}^2}\,\rho^{-1}\bar{\bar{x}}^{-2}\bar{\bar{w}} = \pi\tilde{\tilde{w}}, \\
\epsilon^{-1}q &= \sqrt{1 + \varrho^2\bar{\bar{x}}^2 + \varrho^4\bar{\bar{w}}^2}\,\rho^{-1} \qquad = \tilde{\tilde{q}}\pi,
\end{aligned}
\tag{3.20}
$$

the first set of equalities due to (3.16), the latter ones due to (3.19). Therefore by division

$$\tilde{\tilde{q}}^{-1}\tilde{\tilde{w}} = \bar{\bar{x}}^{-2}\bar{\bar{w}},$$

and hence we obtain a unique $(\tilde{\tilde{q}}, \tilde{\tilde{w}}) \in S^1$ with $\tilde{\tilde{q}} > 0, \tilde{\tilde{w}} > 0$ for every $(\bar{\bar{x}}, \bar{\bar{w}}) \in S^1$ with $\bar{\bar{x}} > 0$ and $\bar{\bar{w}} > 0$. From here π can be determined by

$$\pi = \tilde{\tilde{w}}^{-1}\sqrt{1 + \varrho^2\bar{\bar{x}}^2 + \varrho^4\bar{\bar{w}}^2}\,\rho^{-1}\bar{\bar{x}}^{-2}\bar{\bar{w}},$$

using (3.20). Finally,

$$\sigma = \chi(\pi\tilde{\tilde{w}})^{-1}\rho\varrho\bar{\bar{x}}/\sqrt{1 + \varrho^2\bar{\bar{x}}^2 + \varrho^4\bar{\bar{w}}^2}.$$

Similar calculations gives the inverse of M on $M(U) = V^{4b}$. □

This result means that the diagram in figure 13 commutes and that we can study $\widehat{X}^3$ on U^3 using $\widehat{X}^{4b}$ on $M(U^3) = V^{4b}$ since $\overline{X}^{4b} = M_*(\overline{X}^4)$ there. The latter property is important for connecting results for $\widehat{X}^3$ on P^3 with results for $\widehat{X}^{4b}$ on P^{4b}.

In the analysis of the fourth blowup, we will find that σ eventually increases while π remains small. To cover this part, where C_∞ plays no role, it is easiest to skip the first part of the fourth blowup (3.17), see also local form in (3.29) below, and just do a polar blowup of $w = 0, (\bar{\epsilon}, \bar{q}) = (1, 0)$ as follows:

$$\Psi^5 : (\mu, (\tilde{w}, \tilde{q})) \mapsto (w, \bar{\epsilon}^{-1}q) = \mu(\tilde{w}, \tilde{q}), \quad \mu \geqslant 0, (\tilde{w}, \tilde{q}) \in S^1,$$

fixing x, y and r_2. Here $\Psi^5 : P^5 \to P^1$ where
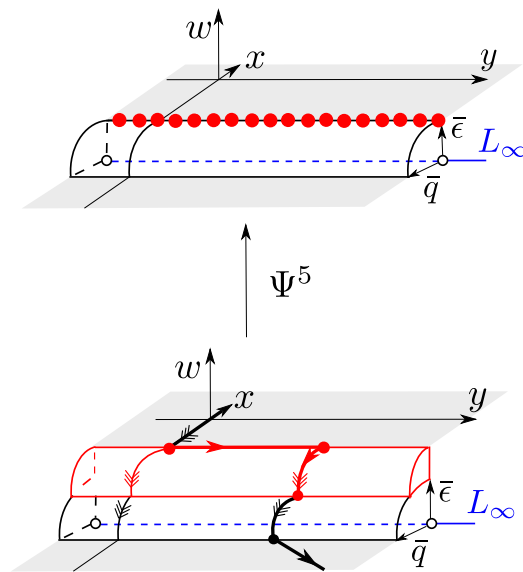
Figure 14. Fifth blowup step near L_∞, see (3.21), where this blowup is used. We view the system from the $x < 0$ side, the x-axis 'entering' the page. In this picture, we blowup $w = \bar{q} = 0$ to a circle. Geometrically, this produces the red cylinder and dynamically it injects partial hyperbolicity (indicated by black triple-headed arrow) of an improved version of L_∞. This gives rise to a slow flow on L_∞ (indicated by the thick red orbit with a single-headed arrow). We also indicate two important planes $\bar{q} = w = 0$ (furthest away) and $\bar{\epsilon} = w = 0$ (nearest) by gray shading. An essential step in our construction of the improved singular cycle, will be a transition between these planes. Basically, the dynamics near L_∞ occurs close to the former whereas the dynamics close to C_∞ occurs along the latter.

$$P^5 = \{(x, y, r_2, \mu, (\tilde{w}, \tilde{\bar{q}})) \in \mathbb{R}^2 \times [0, \infty]^2 \times S^1\}.$$

We put $\Psi^{15} = \Psi^1 \circ \Psi^5$. We illustrate this final blowup in figure 14 near

$$L_\infty := \{(x, y, w, q, \epsilon) \mid x = -1 - \alpha, y \in I, w = q = \epsilon = 0\}, \tag{3.21}$$

recall also (1.28) and remark 1.4.

3.3. Local charts and the corresponding directional blowup transformations

We use separate directional charts to describe the blowup transformations defined in the previous section. For the first blowup Ψ^1, for example, we will use two separate charts obtained by central projections onto the planes $\bar{q} = 1$ and $\bar{\epsilon} = 1$, respectively. We call these charts $(\bar{q} = 1)_1$ and $(\bar{\epsilon} = 1)_2$, respectively. The mapping from local coordinates to (q, ϵ) is obtained by setting $\bar{q} = 1$ and $\bar{\epsilon} = 1$, respectively, in (3.12). These charts therefore give the following local forms of the blowup Ψ^1:

$$\Psi^1_1 : (r_1, \epsilon_1) \mapsto \begin{cases} q &=& r_1, \\ \epsilon &=& r_1 \epsilon_1, \end{cases} \tag{3.22}$$

$$\Psi^1_2 : (r_2, q_2) \mapsto \begin{cases} q &=& r_2 q_2, \\ \epsilon &=& r_2 \end{cases} \tag{3.23}$$

where $(x, y, w, r_1, \epsilon_1)$ and (x, y, w, r_2, q_2) are the local coordinates in the two charts. We can change coordinates between these charts through the following expressions:

$$r_2 = r_1 \epsilon_1,$$
$$q_2 = \epsilon_1^{-1}, \tag{3.24}$$

for $\epsilon_1 > 0$. For the second blowup Ψ^2, described by the equation (3.13), we work in the chart $(\bar{q} = 1)_1$ such that $\bar{q}^{-1} \bar{\epsilon} = \epsilon_1 \geqslant 0$. Subsequently we then use local charts to describe $(\bar{x}, \bar{w}, \bar{\bar{\epsilon}}) \in S^2$ by setting $\bar{w} = 1$, $\bar{\bar{\epsilon}} = 1$ and finally $\bar{x} = 1$. We refer to each of these local charts as $(\bar{q} = 1, \bar{w} = 1)_{11}$, $(\bar{q} = 1, \bar{\bar{\epsilon}} = 1)_{12}$ and $(\bar{q} = 1, \bar{x} = 1)_{13}$, respectively. They produce the following local forms of the second blowup $\Psi^{12} = \Psi^1 \circ \Psi^2$:

$$\Psi_{11}^{12} : (y, r_1, \rho_1, x_1, \epsilon_{11}) \mapsto \begin{cases} x &= -1 - \xi y + \rho_1 x_1, \\ w &= \rho_1 \\ q &= r_1, \\ \epsilon &= r_1 \rho_1 \epsilon_{11}, \end{cases} \tag{3.25}$$

$$\Psi_{12}^{12} : (y, r_1, \rho_2, x_2, w_2) \mapsto \begin{cases} x &= -1 - \xi y + \rho_2 x_2, \\ w &= \rho_2 w_2, \\ q &= r_1, \\ \epsilon &= r_1 \rho_2, \end{cases} \tag{3.26}$$

using $(y, r_1, \rho_1, x_1, \epsilon_{11})$ and $(y, r_1, \rho_2, x_2, w_2)$, as the local coordinates in these charts $(\bar{q} = 1, \bar{w} = 1)_{11}$, $(\bar{q} = 1, \bar{\bar{\epsilon}} = 1)_{12}$, respectively. We can change coordinates between $(\bar{q} = 1, \bar{w} = 1)_{11}$ and $(\bar{q} = 1, \bar{\bar{\epsilon}} = 1)_{12}$ through the following expressions:

$$\rho_2 = \rho_1 \epsilon_{11},$$
$$x_2 = \epsilon_{11}^{-1} x_1, \tag{3.27}$$
$$w_2 = \epsilon_{11}^{-1},$$

for $\epsilon_{11} > 0$. We summarize the information about the charts used for the first two blowups in table 1.

For the third blowup Ψ^3, we work in the chart $(\bar{q} = 1, \bar{\bar{\epsilon}} = 1)_{12}$ where

$$\bar{\bar{\epsilon}}^{-1} \bar{x} = x_2, \quad \bar{\bar{\epsilon}}^{-1} \bar{w} = w_2.$$

Then we plug in $\bar{\bar{w}} = 1$ into (3.14) and obtain the chart $(\bar{q} = 1, \bar{\bar{\epsilon}} = 1, \bar{\bar{w}} = 1)_{122}$, respectively. Within this charts we obtain the following local form of the blowup $\Psi^{123} = \Psi^1 \circ \Psi^2 \circ \Psi^3$:

$$\Psi_{122}^{123} : (y, r_1, \rho_2, \varrho_2, x_{22}) \mapsto \begin{cases} x &= -1 - \xi y + \rho_2 \varrho_2 x_{22}, \\ w &= \rho_2 \varrho_2^2 \\ q &= r_1, \\ \epsilon &= r_1 \rho_2, \end{cases} \tag{3.28}$$

using $(y, r_1, \rho_2, \varrho_2, x_{22})$ as local coordinates.

For the fourth blowup Ψ^4, we first work in the chart $(\bar{\epsilon} = 1)_2$. Then we plug in $\tilde{x} = -1$ into (3.17) to obtain a chart for the description of $(\tilde{x}, \tilde{w}) \in S^1$ in a neighborhood of $(\tilde{x}, \tilde{w}) = (-1, 0)$. This produces the local chart $(\bar{\epsilon} = 1, \tilde{x} = -1)_{21}$ in which $\Psi^{14a} = \Psi^1 \circ \Psi^{4a}$ takes the following local form

$$\Psi_{21}^{14a} : (y, r_2, \sigma_1, w_1, q_2) \mapsto \begin{cases} x &= -1 - \xi y - \sigma_1, \\ w &= \sigma_1^2 w_1, \\ q &= r_2 q_2, \\ \epsilon &= r_2, \end{cases} \tag{3.29}$$

Table 1. Details about the charts used for the first two blowups. The second to last row ('Equations') contains the equation numbers of the local forms of the desingularized vector-fields, and the corresponding section numbers where these systems are analyzed. The last row ('Coordinate changes') contains the equation numbers for the coordinate changes between the corresponding columns.

	1st blowup		2nd blowup	
	$(\bar{q} = 1)_1$	$(\bar{\epsilon} = 1)_2$	$(\bar{q} = 1, \bar{w} = 1)_{11}$	$(\bar{q} = 1, \bar{\bar{\epsilon}} = 1)_{12}$
Charts				
Coordinates	$(x, y, w, r_1, \epsilon_1)$	(x, y, w, q_2, r_2)	$(y, r_1, \rho_1, x_1, \epsilon_{11})$	$(y, r_1, \rho_2, x_2, w_2)$
Local blowup	Ψ_1^1 (3.22)	Ψ_2^1 (3.23)	Ψ_{11}^{12} (3.25)	Ψ_{12}^{12} (3.26)
Equations	(4.19), section 4.7		(4.1), section 4.1	(4.10), section 4.2
Coordinate changes	(3.24)		(3.27)	

using $(y, r_2, \sigma_1, w_1, q_2)$ as coordinates in this chart. Within $(\bar{\epsilon} = 1, \tilde{x} = -1)_{21}$ we have

$$\tilde{x}^{-2}\tilde{w} = w_1,$$
$$\bar{\epsilon}^{-1}\bar{q} = q_2,$$

and therefore (3.18) becomes

$$w_1 = \pi\tilde{\tilde{w}},$$
$$q_2 = \pi\tilde{\tilde{q}}.$$

We therefore plug in $\tilde{\tilde{q}} = 1$ and obtain the chart $(\bar{\epsilon} = 1, \tilde{x} = -1, \tilde{\tilde{q}} = 1)_{211}$ and the following local form of $\Psi^{14a4b} = \Psi^1 \circ \Psi^{4a} \circ \Psi^{4b}$:

$$\Psi_{211}^{14a4b} : (y, r_2, \sigma_1, \pi_1, w_{11}) \mapsto \begin{cases} x &=& -1 - \xi y - \sigma_1, \\ w &=& \sigma_1^2 \pi_1 w_{11}, \\ q &=& r_2 \pi_1, \\ \epsilon &=& r_2, \end{cases} \tag{3.30}$$

using $(y, r_2, \sigma_1, \pi_1, w_{11})$ as local coordinates.

Following lemma 3.3, we can change coordinates between $(\bar{\epsilon} = 1, \tilde{x} = -1, \tilde{\tilde{q}} = 1)_{211}$ and $(\bar{q} = 1, \bar{\bar{\epsilon}} = 1, \bar{\bar{w}} = 1)_{122}$ through the following expressions:

$$\pi_1 = \rho_2^{-1},$$
$$r_2 = r_1 \rho_2,$$
$$\sigma_1 = \rho_2 \varrho_2 x_{22}, \tag{3.31}$$
$$w_{11} = x_{22}^{-1}$$

for $\rho_2 > 0$ and $x_{22} > 0$.

We describe the fifth blowup transformation Ψ^5 using the chart $(\bar{\epsilon} = 1, \tilde{w} = 1)_{21}$ and $(\bar{\epsilon} = 1, \tilde{\tilde{q}} = 1)_{22}$ such that $\Psi^{15} = \Psi^1 \circ \Psi^5$ becomes

$$\Psi_{21}^{15} : (r_2, \mu_1, q_{21}) \mapsto \begin{cases} q &=& r_2 \mu_1 q_{21}, \\ \epsilon &=& r_2, \\ w &=& \mu_1, \end{cases} \tag{3.32}$$

$$\Psi_{22}^{15} : (r_2, \mu_2, w_2) \mapsto \begin{cases} q &=& r_2 \mu_2, \\ \epsilon &=& r_2, \\ w &=& \mu_2 w_2, \end{cases} \tag{3.33}$$
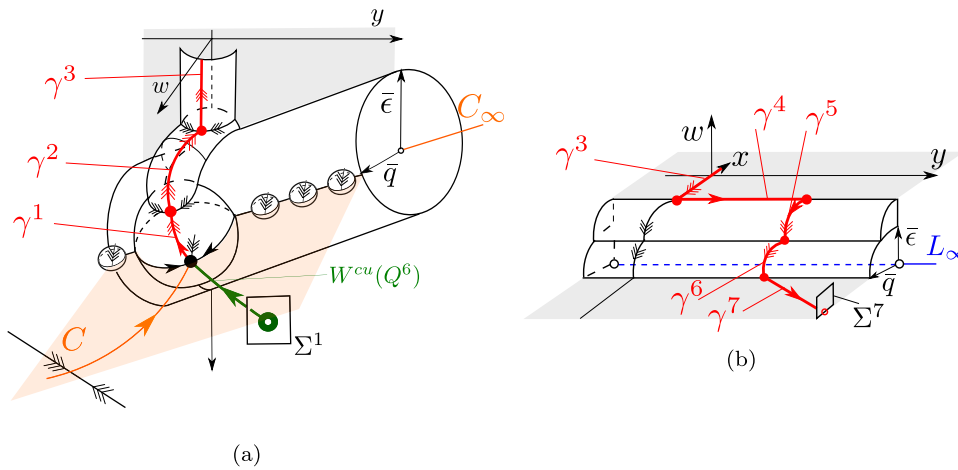
Figure 15. Parts of the blown up singular cycle visible in chart ϕ_3. The improved hyperbolicity properties of the segments γ^{1-7} allow us to prove lemma 5.1. In (a): γ^{1-3} using the viewpoint in figure 11(c). In (b): γ^{3-7} using the viewpoint in figure 11(d). Notice that in (b), γ^3 and γ^4 are contained within the plane $\bar{q} = w = 0$, whereas γ^7 is contained within $\bar{\epsilon} = w = 0$. γ^5 and γ^6 connect these orbit segments. Along these orbits, $\bar{\epsilon}$ is therefore decreasing. Essentially, γ^{1-7} provide a route from $\bar{\epsilon} = 0$, into $\bar{q} = 0$ and back again. Furthermore, the dynamics near $\bar{q} = 0$ is dominated by an 'improved L_∞' whereas the dynamics within $\bar{\epsilon} = 0$ is dominated by an improved version of C_∞. See further details in section 4; here we will also define q^i's as the points where the γ^i's 'depart' from.

in the local coordinates $(x, y, r_2, \mu_1, q_{21})$ and (x, y, r_2, μ_2, w_2), respectively. Notice, that we can change coordinates between $(\bar{\epsilon} = 1, \tilde{w} = 1)_{21}$ and $(\bar{\epsilon} = 1, \tilde{x} = -1, \tilde{\bar{q}} = 1)_{211}$ through the following expressions

$$
\begin{aligned}
\mu_1 &= \sigma_1^2 \pi_1 w_{11}, \\
q_{21} &= \sigma_1^{-2} w_{11}^{-1}, \\
x &= -1 - \xi y - \sigma_1.
\end{aligned}
\tag{3.34}
$$

Also, between $(\bar{\epsilon} = 1, \tilde{w} = 1)_{21}$ and $(\bar{\epsilon} = 1, \tilde{\bar{q}} = 1)_{22}$ we have the following equations

$$
\begin{aligned}
\mu_2 &= \mu_1 q_{21}, \\
w_2 &= q_{21}^{-1}.
\end{aligned}
\tag{3.35}
$$

We summarize the information about the charts used for the third, fourth and fifth blowup in table 2.

3.4. A summary of the findings in chart ϕ_3

The full details of the analysis of the blowup systems, working in the charts described in section 3.3, are available in section 4. Essentially, our approach injects improved hyperbolicity properties into parts of the singular cycle visible in the chart ϕ_3. In doing so, we also identify segments that are only visible upon blowup. In section 5, we combine the findings of section 4 into a result, see lemma 5.1, on the transition map Π^{17}. In the following, we will first summarise our findings, focussing in particular on the description of the hidden segments γ^{1-7} of Γ_0 obtained upon blowup. (Only γ^3 and γ^4 are visible upon blowing down, recall figure 7.)

Table 2. Details about the charts used for the third, fourth and fifth blowup. The rows have the same meaning as in table 1. In particular, the last two rows contain the equation numbers for the coordinate changes between the corresponding columns.

3rd blowup	4th blowup, part b	5th blowup	
$(\bar{q}=1, \bar{\bar{\epsilon}}=1, \bar{\bar{x}}=-1)_{122}$	$(\bar{\epsilon}=1, \tilde{x}=-1, \tilde{\tilde{q}}=1)_{211}$	$(\bar{\epsilon}=1, \tilde{w}=1)_{21}$	$(\bar{\epsilon}=1, \tilde{\tilde{q}}=1)_{22}$
$(y, r_1, \rho_2, \varrho_2, x_{22})$	$(y, r_2, \sigma_1, \pi_1, w_{11})$	$(x, y, r_2, \mu_1, q_{21})$	(x, y, r_2, μ_2, w_2)
Ψ_{122}^{13} (3.28)	Ψ_{211}^{14a14b} (3.30)	Ψ_{21}^{15} (3.32)	Ψ_{22}^{15} (3.33)
(4.11), section 4.3	(4.13), section 4.4	(4.15), section 4.5	(4.18), section 4.6
(3.31)		(3.35)	
	(3.34)		

Figure 15 provides an illustration of the blown up cycle using the viewpoints in figures 11(c) and (d).

Firstly, by working in the chart $(\overline{q}=1, \overline{w}=1)_{11}$ associated with the second blowup transformation Ψ^{12} and the vector-field $\widehat{X}^2$, we are able to extend the hyperbolicity of the critical manifold up to a neighborhood of the $\bar{\bar{\epsilon}}=0$-equator of the sphere $(\bar{x}, \bar{w}, \bar{\bar{\epsilon}}) \in S^2$. This enables us to extend the slow manifold as a center manifold, in the usual way [26], and hereby guide a neighborhood of $W^{cu}(Q^6)$ close to a heteroclinic connection γ^1 on the sphere $(\bar{x}, \bar{w}, \bar{\bar{\epsilon}}) \in S^2$, see also figure 10(a), section 4.1 and proposition 4.2. In fact, we show that the contraction of the slow flow on C towards Q^1, recall figure 6, produces a contraction towards γ^1 for $\epsilon \ll 1$, see lemma 4.4. (In turn, this gives rise to the contraction of the full return mapping $\Pi = \Pi^1 \circ \Pi^0$, which is used to prove the existence of the attracting limit cycle, recall section 2.)

By the third blowup, we gain hyperbolicity of the forward limit point of γ^1 and subsequently follow a 1D unstable manifold γ^2 (defined in (4.12) in the chart $(\bar{q}=1, \bar{\bar{\epsilon}}=1, \bar{\bar{w}}=1)_{122}$) towards $(\bar{q}, \bar{\epsilon}) = (0, 1)$. See section 4.3. We gain hyperbolicity of the forward limit point of γ^2 by the fourth blowup transformation and follow an unstable manifold γ^3 (see (4.14)). Then by working in the chart $(\bar{\epsilon}=1, \tilde{w}=1)_{21}$, we find that γ^3 is attracted towards a center manifold based on $L_\infty : x = -1 - \alpha, w = 0, y \in I$, recall (1.28); see also section 4.5. On this center manifold, we desingularize the slow flow and follow γ^4. Along γ^4, we find that y is increasing, recall remark 1.4. At $y = 2\alpha/\xi$, γ^4 ends along a line of equilibria of saddle-structure. We subsequently follow the unstable manifold γ^5, along which $\bar{q}$ is increasing. By the fifth blowup, we gain hyperbolicity of the forward limit point of γ^5 and subsequently follow an unstable manifold γ^6. See (4.16) and figure 19. γ^6 is asymptotic to a normally hyperbolic set of equilibria defined by $(\bar{q}, \bar{\epsilon}) = (1, 0)$, $r = 0$. Upon desingularization, we obtain a slow flow within this manifold which produces γ^7. These last segments are described by the chart $(\bar{\epsilon}=1, \tilde{\tilde{q}}=1)_{22}$ and by $(\bar{\epsilon}=1)_1$ in section 4.7. γ^7 is asymptotic to C_∞—where the set $(\bar{q}, \bar{\epsilon}) = (1, 0)$, $r = 0$ loses hyperbolicity—but this part is better described in chart ϕ_1, see section 6.

4. Blowup dynamics in chart ϕ_3

In this section we describe the dynamics in chart ϕ_3 using the blowup and the charts presented in section 3.

Remark 4.1. In the following, we will need to introduce several new symbols. In general, $\mathcal{M}_i$ will be reserved to denote center manifold extensions of the slow manifold S_ϵ. Here the subscript i will reflect the subscript used in the corresponding chart. However, an $\mathcal{M}_j$ with $j \neq i$ will not necessarily correspond to $\mathcal{M}_i$ in a separate chart since the domains for these
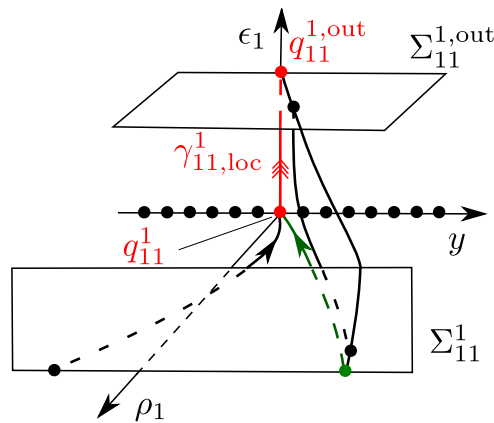
Figure 16. Illustration of the result in lemma 4.4. Our view is from $\rho_1 > 0$, the ρ_1-axis 'coming out' of the page. Within the center manifold $\mathcal{M}_{11}$, the orbit $\gamma^1_{11,loc}$, contained within $\rho_1 = 0$, is a local unstable manifold of the point q^1_{11} on the degenerate line $\rho_1 = \epsilon_1 = 0$, being defined by $(y, \rho_1, \epsilon_{11}) = (0, 0, 0)$.

(often local) manifolds will not necessarily overlap. The same applies to other objects $\mathcal{C}_i$, $\mathcal{N}_i$, $\mathcal{P}_i$, $\mathcal{L}_i$, $\mathcal{H}_i$ and $\mathcal{U}_i$ introduced in the following. Here $\mathcal{C}_i$ and $\mathcal{L}_i$ will be reserved to improved versions of C_∞ and L_∞ (that blow down to these manifolds in the (x, y, w)-space) whereas $\mathcal{P}_i$ and $\mathcal{H}_i$ will refer to various new 2D and 1D invariant manifolds that appear along the way. Important points and orbits are denoted by q^j_i and γ^j_i, where j is the number system used for the segments on the (improved) singular cycle and where i corresponds to the chart. The number system we follow is so that γ^j_i (γ^{j+1}_i) 'ends' ('begins', respectively) at q^{j+1}_i.

We will also introduce various smooth functions h_i and H_i in the following. The functions h_j and h_i with $i \neq j$ will in general denote different functions (as opposed to the same function in different coordinates). Same applies to the H_i's.

4.1. Dynamics in $(\overline{q} = 1, \overline{w} = 1)_{11}$

In this chart, we obtain the following equations

$$
\begin{aligned}
\dot{y} &= \rho_1 \left(\epsilon_{11} \rho_1 F(\rho_1) + y \frac{x_1}{\xi} \right), \\
\dot{r}_1 &= 2 r_1 \frac{x_1}{\xi}, \\
\dot{\rho}_1 &= \rho_1^2 \frac{x_1}{\xi}, \\
\dot{x}_1 &= -\frac{x_1}{\xi} - \epsilon_{11}(\rho_1 x_1 - \xi y + \alpha) + \rho_1 \epsilon_{11} \xi F(\rho_1), \\
\dot{\epsilon}_{11} &= -\epsilon_{11} \frac{x_1}{\xi}(2 + \rho_1)
\end{aligned}
\tag{4.1}
$$

by (3.6) using Ψ^{12}_{11}, see (3.25). Here $F(\rho_1) = 1 - e^{-1/\rho_1}$. Notice that r_1-decouples. At this stage, we therefore proceed with the $(y, \rho_1, x_1, \epsilon_{11})$-subsystem only. We notice that the point q^1_{11}, defined by $(y, \rho_1, x_1, \epsilon_{11}) = 0$, is an equilibrium of the system with $-\xi^{-1}$ as a single non-zero eigenvalue. We therefore obtain an extension of the slow manifold as a center manifold using standard center manifold theory:

Proposition 4.2.   *Fix $\eta \in (0,1)$. Then there exists a $\delta > 0$ and a small neighborhood $\mathcal{U}_{11}$ of $(y, \rho_1, \epsilon_{11}) = 0$ in $\mathbb{R}^3$ such that the following holds. There exists a local center manifold $\mathcal{M}_{11}$ of q_{11}^1 as a graph*

$$x_1 = -\epsilon_{11}\xi h_{11}(y, \rho_1, \epsilon_{11}), \tag{4.2}$$

over $(y, \rho_1, \epsilon_{11}) \in \mathcal{U}_{11}$. Here h_{11} is a smooth function of the following form

$$h_{11}(y, \rho_1, \epsilon_{11}) = \alpha - \xi y + \mathcal{O}(\rho_1, \epsilon_{11}). \tag{4.3}$$

Furthermore, there exists a smooth stable foliation with base $\mathcal{M}_{11}$ and 1D fibers as leaves of the foliation. Within $x_1 \in [-\delta, \delta]$, $(\rho_1, y, \epsilon_{11}) \in \mathcal{U}_{11}$, the contraction along any of these fibers is at least $e^{-\eta\xi^{-1}t}$.

Remark 4.3.   Notice, as usual [26], that $\mathcal{M}_{11}$ provides an extension of the Fenichel slow manifold as a locally invariant manifold, upon restriction to the invariant set $\{\epsilon = r_1\rho_1\epsilon_{11}, r_1 = e^{-\rho^{-1}}\}$ and blowing down, up to

$$\epsilon_{11} = \delta \Leftrightarrow \epsilon = e^{-w^{-1}}w\delta \Leftrightarrow w = W(\epsilon\delta^{-1})^{-1}.$$

Here W in the last expression is the principle-value Lambert W function W: $(-e^{-1}, \infty) \to (-1, \infty)$, defined by $z = W(ze^z)$ for all $z \in (-1, \infty)$. Using the asymptotics

$$W(w) = \log w(1 + o(1)), \tag{4.4}$$

of W for $w \to \infty$, see e.g. [32], we realise that the slow manifold by $\mathcal{M}_{11}$ is extended up to $w \approx \log^{-1}\epsilon^{-1}$.

Now, consider the following sections:

$$\Sigma_{11}^1 = \{(y, \rho_1, x_1, \epsilon_{11}) \,|\, \rho_1 = \delta, \, x_1 \in [-\beta_1, 0), \, y \in [-\beta_2, \beta_2], \, \epsilon_{11} \in (0, \beta_3]\},$$
$$\Sigma_{11}^{1,\text{out}} = \{(y, \rho_1, x_1, \epsilon_{11}) \,|\, \epsilon_{11} = \nu, \, \rho_1 \in [0, \beta_4], \, x_1 \in [-\beta_1, 0), \, y \in [-\beta_2, \beta_2]\},$$

transverse to the flow. Notice that $\rho_1 = \delta$ in Σ_{11}^1 becomes $z = 1/\delta$ in the original variables using (3.25), in agreement with Σ^1, see (5.1).

The 1D manifold

$$\gamma_{11,\text{loc}}^1 := \mathcal{M}_{11} \cap \{\rho_1 = y = 0\},$$

is invariant and by inserting $x_1 = -\epsilon_{11}\xi h_{11}(0, 0, \epsilon_{11})$ into (4.1), using (4.3), it follows that ϵ_{11} is increasing along this set for $\epsilon_{11} \neq 0$. In fact, we shall see that $\gamma_{11,\text{loc}}^1$ is a local unstable manifold of the point q_{11}^1 of a desingularized flow on $\mathcal{M}_{11}$.

$\gamma_{11,\text{loc}}^1$ intersects $\Sigma_{11}^{1,\text{out}}$ in a point $q_{11}^{1,\text{out}}$ with coordinates

$$(y, \rho_1, x_1, \epsilon_{11}) = (0, 0, -\nu\xi h_{11}(0, 0, \nu), \nu).$$

We now consider the mapping $\Pi_{11}^1 : \Sigma_{11}^1 \to \Sigma_{11}^{1,\text{out}}$ defined as the first intersection by the forward flow. See figure 16. We have the following.

Lemma 4.4.   *The mapping Π_{11}^1 is well-defined for appropriately small δ, ν and $\beta_i > 0$, $i = 1, 4$. In particular,*

$$\Pi_{11}^1(y, x_1, \delta, \epsilon_{11}) = \left(y_+(y, x_1, T(y, x_1, \epsilon_{11})), \rho_{1+}(y, x_1, T(y, x_1, \epsilon_{11})), \right.$$

$$\left. x_{1+}(y, x_1, T(x_1, \epsilon_{11})), \nu \right),$$

with y_+, ρ_{1+}, and x_{1+} being C^1 in each of their arguments:

$$\rho_{1+}(y, x_1, T) = \frac{\delta}{1 + \delta T}(1 + \mathcal{O}(\delta)),$$

$$y_+(y, x_1, T) = \frac{y}{1 + \delta T} + \frac{\delta \log(1 + \delta T)}{\alpha(1 + \delta T)} + \mathcal{O}\left(\frac{\delta}{1 + \delta T}, e^{-ce^{2T}}\right),$$

$$x_{1+}(y, x_1, T) = -\nu\xi h_{11}(\rho_{1+}(y, x_1, T), y_+(y, x_1, T), \nu) + \mathcal{O}(e^{-ce^{2T}}),$$

for some $c(\delta, \nu) > 0$ sufficiently small and where $T(y, x_1, \epsilon_{11}) > 0$ is the unique solution of the following equation

$$\tilde{\epsilon}_{11}(\rho_{1+}, y_+, x_{1+}, \nu) = \tilde{\epsilon}_{11}(\delta, y, x_1, \epsilon_{11})e^{2T(y, x_1, \epsilon_{11})}(1 + \delta T(y, x_1, \epsilon_{11})). \tag{4.5}$$

Here $\tilde{\epsilon}_{11}(\rho, y, x_1, \epsilon_{11}) = \epsilon_{11}(1 + \mathcal{O}(x_1, \epsilon_{11}\xi h_{11}(\delta, y, \epsilon_{11})))$ is a smooth function.

Substituting (4.2) into (4.1) (with r_1 decoupled) and dividing the resulting right hand side by $\epsilon_{11}h_{11}(\rho_1, y, \epsilon_{11})$, where h_{11} is defined in (4.3), produce the following equations

$$\dot{\epsilon}_{11} = \epsilon_{11}(2 + \rho_1),$$
$$\dot{\rho}_1 = -\rho_1^2,$$
$$\dot{y} = -\rho_1 F(\rho_1)\left(y - \frac{\rho_1 F(\rho_1)}{h_{11}(\rho_1, y, \epsilon_{11})}\right). \tag{4.6}$$

To prove lemma 4.4 we will then use the following result on this reduced problem on $\mathcal{M}_{11}$.

Fact. There exists two C^1, locally defined functions H_{11} and $\tilde{H}_{11}$ such that

$$y \mapsto \tilde{y} = H_{11}(y, \rho_1, \epsilon_{11}) = y + \mathcal{O}(\rho_1), \tag{4.7}$$

with inverse

$$\tilde{y} \mapsto y = \tilde{H}_{11}(\tilde{y}, \rho_1, \epsilon_{11}) = \tilde{y} + \mathcal{O}(\rho_1),$$

transforms system (4.6) into

$$\dot{\epsilon}_{11} = \epsilon_{11}(2 + \rho_1),$$
$$\dot{\rho}_1 = -\rho_1^2,$$
$$\dot{\tilde{y}} = -\rho_1\left(\tilde{y} - \frac{\rho_1}{\alpha}\right). \tag{4.8}$$

Proof of fact. The transformation (4.7) is composed of two steps. First we notice that the set defined by $\epsilon_{11} = 0$ is a normally hyperbolic invariant set for (4.6) with smooth unstable fibers. We can straighten out these fibers through a smooth transformation of the form $(\rho_1, y, \epsilon_{11}) \mapsto y_1$. Then the y_1 equation is independent of ϵ_{11}:

$$\dot{y}_1 = -\rho_1 \left(y_1 - \frac{\rho_1 F(\rho_1)}{h_{11}(\rho_1, y, 0)} \right).$$

The (ρ_1, y_1)-system therefore decouples, and with respect to the time τ defined by

$$\frac{d\tau}{dt} = \rho_1$$

this planar systems has a stable, hyperbolic node at the origin. Therefore we can linearize this system by a C^1 transformation fixing ρ and taking $(\rho, y_1) \mapsto \tilde{y}_1$. This gives the desired result.
□

Proof of lemma 4.4. First, we straighten out the stable fibers of $\mathcal{M}_{11}$ by a smooth transformation fixing x_1 and taking $(y, \rho_1, x_1, \epsilon_{11}) \mapsto (\tilde{\rho}_1, \tilde{y}, \tilde{\epsilon}_{11})$ of the form

$$\tilde{\rho}_1 = \rho_1(1 + \mathcal{O}(\rho_1)),$$
$$\tilde{y} = y + \mathcal{O}(\rho_1),$$
$$\tilde{\epsilon}_{11} = \epsilon_{11}(1 + \mathcal{O}(x_1, \epsilon_{11}\xi h_{11}(\rho_1, y, \epsilon_{11}))).$$

The transformation is close to the identity for ρ_1, x_1 and ϵ_{11} sufficiently small and hence invertible by the inverse function theorem. Then the dynamics of $(\tilde{\rho}_1, \tilde{y}, \tilde{\epsilon}_{11})$ becomes independent of x_1. Then upon dropping the tildes and dividing the right hand side by $\epsilon_{11}h_{11}(\rho_1, y, \epsilon_{11})$ we finally obtain the equations in (4.6). Following the fact above, we apply the local diffeomorphism $(\rho_1, y, \epsilon_{11}) \mapsto (\rho_1, \tilde{y}, \epsilon_{11})$, defined by (4.7), and study (4.8) instead. Integrating this equation gives

$$\rho_1(T) = \frac{\delta}{1 + \delta T},$$
$$\tilde{y}(T) = \frac{\tilde{y}_0}{1 + \delta T} + \frac{\delta \ln(1 + \delta T)}{\alpha(1 + \delta T)},$$

where T is defined by $\epsilon_{11}(T) = \tilde{\nu}$:

$$\tilde{\nu} = \tilde{\epsilon}_0 e^{2T}(1 + \delta T). \tag{4.9}$$

We now transform T back to the original time. This gives the duration of the transition in terms of this time. Using the contraction along the stable fibers, then gives the desired result. □

Now, the function T, given implicitly by (4.9), can be expressed in terms of the smooth Lambert W function as follows

$$T(y, x_1, \epsilon_{11}) = \frac{1}{2} \left(W \left(2\tilde{\nu} e^{2\delta^{-1}}/\tilde{\epsilon}_0 \right) - 2\delta^{-1} \right).$$

Using the asymptotics (4.4), we obtain the following asymptotics of T in (4.5) as $\epsilon_{11} \to 0$:

$$T(y, x_1, \epsilon_{11}) = \frac{1}{2} \log \epsilon_{11}^{-1}(1 + o(1)),$$

after substituting $\tilde{\nu} = \tilde{\epsilon}_{11}(\rho_{1+}, y_+, x_{1+}, \nu)$, $\tilde{\epsilon}_0 = \tilde{\epsilon}_{11}(\delta, y, x_1, \epsilon_{11})$. In fact, the partial derivatives of T with respect to y and x_1 satisfy an identical estimate. We therefore have the following corollary:
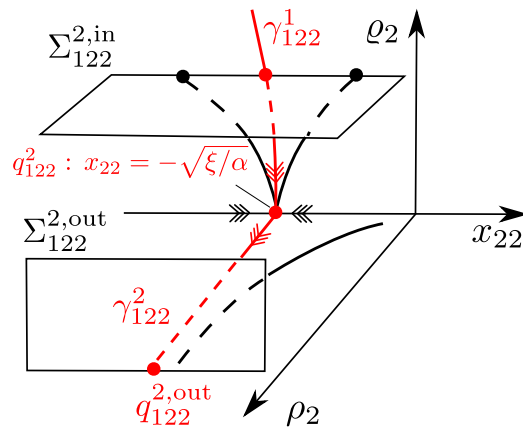
Figure 17. Illustration of the result in lemma 4.6. γ_{122}^1 is contained within $\rho_2 = 0$, approaching the point q_{122}^2 defined by $x_{22} = -\sqrt{\xi\alpha}$, $\varrho_2 = \rho_2 = y = 0$. The orbit γ_{122}^2 is the unstable manifold of the point q_{122}^2 and is contained within $\varrho_2 = 0$.

Corollary 4.5. *The mapping* $(y, x_1) \mapsto \Pi_{11}^1(y, x_1, \delta, \epsilon_{11})$ *is* C^1 $\mathcal{O}\left(\frac{\log\log\epsilon_{11}}{\log\epsilon_{11}}\right)$*-close to the constant mapping* $(y, x_1) \mapsto q_{11}^{1,\text{out}}$ *as* $\epsilon_{11} \to 0$.

4.2. Dynamics in $(\overline{q} = 1, \overline{\overline{\epsilon}} = 1)_{12}$

In this chart, we obtain the following equations

$$
\begin{aligned}
\dot{y} &= \rho_2 \left(\rho_2 w_2^2 F(\rho_2 w_2) + y w_2 \frac{x_2}{\xi} \right), \\
\dot{\rho}_2 &= -2\rho_2 \frac{x_2}{\xi}, \\
\dot{x}_2 &= \frac{2x_2^2}{\xi} - w_2 \left(\alpha - \xi y + \rho_2 x_2 \right) + w_2 \frac{x_2}{\xi} \left(\rho_2 x_1 - 1 \right) \\
&\quad + \xi \rho_2 w_2^2 F(\rho_2 w_2), \\
\dot{w}_2 &= w_2 \frac{x_2}{\xi} (2 + \rho_2 w_2),
\end{aligned}
\tag{4.10}
$$

from (3.6) using (3.26). We then transform $q_{11}^{1,\text{out}}$ from above to this chart and obtain $q_{12}^{1,\text{out}}$ with coordinates

$$
(y, \rho_2, x_2, w_2) = (0, 0, -\xi h_{11}(0, 0, \nu), \nu^{-1}),
$$

see (3.27). Setting $y = \rho_2 = 0$ in (4.10) gives

$$
\begin{aligned}
\dot{x}_2 &= \frac{2x_2^2}{\xi} - w_2 \left(\alpha - \xi y \right) - w_2 \frac{x_2}{\xi}, \\
\dot{w}_2 &= 2w_2 \frac{x_2}{\xi}.
\end{aligned}
$$

In [3], it was shown, using a simple phase portrait analysis that γ_{12}^1, which is γ_{11}^1 in the present coordinates, is asymptotic to the nonhyperbolic equilibrium $x_2 = w_2 = 0$ within the invariant subset $y = \rho_2 = 0$. Fix a large $T > 0$. Then, by regular perturbation theory, we can map a sufficiently small neighborhood of $q_{12}^{1,\text{out}}$ diffeomorphically onto a neighborhood of $\phi_T(q_{12}^{1,\text{out}})$

using the flow ϕ_t. Due to the loss of hyperbolicity we apply the third blowup transformation, see (3.14) and (3.16), of $x_2 = w_2 = 0$. We describe this in the following using the chart $(\bar{q} = 1, \bar{\bar{\epsilon}} = 1, \bar{\bar{w}} = 1)_{122}$ and the local form of the blowup (3.28).

4.3. Dynamics in $(\bar{q} = 1, \bar{\bar{\epsilon}} = 1, \bar{\bar{w}} = 1)_{122}$

Inserting (3.28) into (3.6) produces the following equations:

$$
\begin{aligned}
\dot{y} &= \rho_2 \varrho_2^2 \left(\rho_2 \varrho_2 F(\rho_2 \varrho_2^2) + y \frac{x_{22}}{\xi} \right), \\
\dot{\rho}_2 &= -2\rho_2 \frac{x_{22}}{\xi}, \\
\dot{\varrho}_2 &= \frac{1}{2} \varrho_2 \frac{x_{22}}{\xi} \left(2 + \rho_2 \varrho_2^2 \right), \\
\dot{x}_{22} &= \frac{x_{22}^2}{\xi} - (\alpha - \xi y + \rho_2 \varrho_2 x_{22}) \\
&\quad + \varrho_2 \frac{x_{22}}{\xi} \left(\frac{1}{2} \rho_2 \varrho_2 x_{22} - 1 \right) + \xi \rho_2 \varrho_2 F(\rho_2 \varrho_2^2).
\end{aligned}
\tag{4.11}
$$

Now, γ_{12}^1—in these coordinates—becomes γ_{122}^1 which is asymptotic to the equilibrium q_{122}^2 defined by $x_{22} = -\sqrt{\alpha\xi}$, $y = \rho_2 = \varrho_2 = 0$. This point is a stable node within the invariant (ϱ_2, x_{22})-plane. We therefore work in a neighborhood of this equilibrium and consider the sections

$$
\Sigma_{122}^{2,\text{in}} = \{(y, \rho_2, \varrho_2, x_{22}) \,|\, \varrho_2 = \delta, \ \rho_2 \in [0, \beta_1], \ x_{22} - \sqrt{\alpha\xi} \in [-\beta_2, \beta_2], \ y \in [-\beta_3, \beta_3]\},
$$

and

$$
\Sigma_{122}^{2,\text{out}} = \{(y, \rho_2, \varrho_2, x_{22}) \,|\, \rho_2 = \nu, \ \varrho_2 \in [0, \beta_4], \ x_{22} - \sqrt{\alpha\xi} \in [-\beta_2, \beta_2], \ y \in [-\beta_5, \beta_5]\}.
$$

Notice the graph $\mathcal{H}_{122}$, defined by $x_{22} = -\sqrt{\xi(\alpha - \xi y)}$, $y < \frac{\alpha}{\xi}$, $\rho_2 = \varrho_2 = 0$, is a curve of equilibria of (4.11). It is normally hyperbolic with a 3D stable manifold $W^s(\mathcal{H}_{122})$ within $\rho_2 = 0$ and a 2D unstable manifold $W^u(\mathcal{H}_{122})$ defined by $x_{22} = -\sqrt{\xi(\alpha - \xi y)}$, $\varrho_2 = 0$, $\rho_2 \geqslant 0$, $y < \frac{\alpha}{\xi}$. In particular,
$$
\gamma_{122}^2 = \{(y, \rho_2, \varrho_2, x_{22}) \,|\, y = \varrho_2 = 0, \ x_{22} = -\sqrt{\alpha\xi}, \ \rho_2 \geqslant 0\},
\tag{4.12}
$$
is contained within the unstable manifold and is invariant. See figure 17.

Consider the local mapping Π_{122}^2 from $\Sigma_{122}^{2,\text{in}}$ to $\Sigma_{122}^{2,\text{out}}$ obtained from the first intersection by following the forward flow.

Lemma 4.6. Π_{122}^2 *is well-defined for appropriately small* $\delta > 0$, $\nu > 0$ *and* $\beta_i > 0$, $i = 1, \dots, 5$. *In particular,*

$$
\Pi_{122}^2(y, \rho_2, \delta, x_{22}) = (y_+(y, \rho_2, x_{22}), \nu, \varrho_{2+}(\sqrt{\rho_2}), x_{22+}(y, \sqrt{\rho_2}, x_{22})),
$$

with ϱ_{2+} *a* C^1-*function,*

$$
x_{22+}(y, \sqrt{\rho_2}, x_{22}) = H_{122}(y, \rho_2) + \mathcal{O}(\sqrt{\rho_2}),
$$

with H_{122} *smooth satisfying* $H_{122}(0, 0) = -\sqrt{\alpha\xi}$. *Also*

$$
y_+(y, \rho_2, x_{22}) = y + \mathcal{O}(\ln(\rho_2)\rho_2).
$$

Furthermore, the remainder terms in x_{22+} and y_+ are C^1 with respect to x_{22} and y and the orders of these terms as $\rho_2 \to 0$ do not change upon differentiation.

Proof. We divide the right hand side by $-x_{22}/\xi$. This gives

$$\dot{\varrho}_2 = -\frac{1}{2}\varrho_2\left(2 + \rho_2\varrho_2^2\right),$$
$$\dot{\rho}_2 = 2\rho_2,$$

and new equations for x_{21} and y. It is possible to C^1 linearize the (ϱ_2, ρ_2)-subsystem by a transformation fixing ρ_2 and taking $(\varrho_2, \rho_2) \mapsto \tilde{\varrho}_2 = \varrho_2(1 + \mathcal{O}(\rho_2))$ with $(\varrho_2, 0) \mapsto \tilde{\varrho}_2 = \varrho_2$. Now, for the $\rho_2 = 0$ subsystem y is constant and $x_{22} = -\sqrt{\xi(\alpha - \xi y)}$, $\tilde{\varrho}_2 = 0$ is a hyperbolic stable node for any $y < \frac{\alpha}{\xi}$ sufficiently small. We can therefore linearize this subsystem by a C^1 transformation fixing $\tilde{\varrho}_2$ and taking $(\tilde{\varrho}_2, x_{22}) \mapsto \tilde{x}_{22}$. Applying these transformations to the full system produces

$$\dot{y} = \mathcal{O}(\rho_2\tilde{\varrho}_2^2),$$
$$\dot{\rho}_2 = 2\rho_2,$$
$$\dot{\tilde{\varrho}}_2 = -\tilde{\varrho}_2,$$
$$\dot{\tilde{x}}_{22} = -2\tilde{x}_{22} + \mathcal{O}(\rho_2\tilde{\varrho}_2).$$

Integrating these equations gives

$$\tilde{x}_{22}(T) = e^{-2T}\tilde{x}_{22}(0) + \int_0^T \mathcal{O}(e^{-2(T-s)}e^{2s}\rho_{20}e^{-s}\varrho_{20})\mathrm{d}s$$
$$= \frac{\rho_{20}}{\nu}\tilde{x}_{22}(0) + \mathcal{O}(\sqrt{\rho_{20}}\varrho_{20}) = \mathcal{O}(\sqrt{\rho_{20}}),$$
$$y(T) = y(0) + \mathcal{O}(\ln(\rho_{20}^{-1}\rho_2)\rho_{20}\varrho_{20}^2),$$

using that $e^{2T} = \nu\rho_{20}^{-1}$ and hence $\rho_{20}e^T \sim \sqrt{\rho_{20}}$. We obtain similar estimates for the derivatives. $\qquad\square$

Notice that $\Pi_{122}^2(0, \delta, x_{22}, 0) = \gamma_{122}^2 \cap \Sigma_{122}^{2,\mathrm{out}}$ for every $x_{22} - \sqrt{\alpha\xi} \in [-\beta_2, \beta_2]$. Now, along γ_{122}^2, ρ_2 is increasing for $\rho_2 \neq 0$. We therefore study the dynamics in a neighborhood of this orbit in chart $(\bar{\epsilon} = 1, \tilde{x} = -1, \tilde{\tilde{q}} = 1)_{211}$.

4.4. Dynamics in $(\bar{\epsilon} = 1, \tilde{x} = -1, \tilde{\tilde{q}} = 1)_{211}$

In this chart, we obtain the following equations

$$\dot{y} = \sigma_1^2\pi_1 w_{11}\left(-\frac{y}{\xi} + \sigma_1 w_{11}F(\sigma_1^2\rho_1 w_{11})\right),$$
$$\dot{\pi}_1 = -\frac{2\pi_1}{\xi},$$
$$\dot{\sigma}_1 = \sigma_1 w_{11} G_{211}(y, \pi_1, \sigma_1, w_{11}),$$
$$\dot{w}_{11} = w_{11}\left(\frac{2}{\xi} - w_{11}\left(2G_{211}(y, \pi_1, \sigma_1, w_{11}) + \sigma_1^2\frac{\pi_1}{\xi}\right)\right),$$

(4.13)

and $\dot{r}_2 = 0$. Notice that $r_2 \geqslant 0$ decouples and we shall therefore work within the $(y, \pi_1, \sigma_1, w_{11})$-space. Here

$$G_{211}(y, \pi_1, \sigma_1, w_{11}) = \alpha - \sigma_1 - \xi y - \sigma_1 \pi_1 (\sigma_1 + 1) - \sigma_1^2 \xi \pi_1 w_{11} F(\sigma_1^2 \rho_1 w_{11}).$$

Also γ_{122}^2 from chart $(\bar{q} = 1, \bar{\bar{\epsilon}} = 1, \bar{\bar{w}} = 1)_{122}$ becomes

$$\gamma_{211}^2 = \{(y, \pi_1, \sigma_1, w_{11}) \mid \pi_1 > 0, w_{11} = 1/(\alpha\xi), \sigma_1 = 0, y = 0\},$$

using (3.31). It is contained within the invariant set $\sigma_1 = 0$ where

$$\dot{y} = 0,$$

$$\dot{\pi}_1 = -\frac{2\pi_1}{\xi},$$

$$\dot{w}_{11} = 2w_{11}\left(\frac{1}{\xi} - w_{11}(\alpha - \xi y)\right).$$

Here the 2D graph $\mathcal{P}_{211}$, defined by $w_{11} = 1/(\xi(\alpha - \xi y))$, over $y < \frac{\alpha}{\xi}$, $\pi_1 \geqslant 0$, is invariant. This set is foliated by 1D stable manifolds $w_{11} = 1/(\xi(\alpha - \xi y)), y = \text{const}, \pi_1 \geqslant 0$ of points on the curve $\mathcal{H}_{211}$ of equilibria, defined by $w_{11} = 1/(\xi(\alpha - \xi y))$, $y < \frac{\alpha}{\xi}$, within $\pi_1 = 0$. In particular, γ_{211}^2 is contained within the stable manifold $\mathcal{W}^s(\mathcal{H}_{211})$ within $y = 0$, being asymptotic under the forward flow to the point q_{211}^3 defined by $w_{11} = 1/(\alpha\xi)$, $y = 0$, $\pi_1 = 0$ within $\mathcal{H}_{211}$.

Next, within the invariant set $\pi_1 = 0$ we have

$$\dot{y} = 0,$$

$$\dot{\sigma}_1 = \sigma_1 w_{11}(\alpha - \sigma_1 - \xi y),$$

$$\dot{w}_{11} = w_{11}\left(\frac{2}{\xi} - 2w_{11}(\alpha - \sigma_1 - \xi y)\right).$$

For this subsystem, $\mathcal{H}_{211}$ is of saddle type. Indeed, the linearization about any point in this set, gives $-2/\xi$ and $1/\xi$ as eigenvalues with the stable space purely in the w_{11}-direction and the unstable space contained in the (σ_1, w_{11})-plane. It is possible to write the individual local unstable manifolds within as graphs:

$$w_{11} = H_{211}(y, \sigma_1),$$

with H_{211} smooth, such that $H_{211}(y, 0) = 1/(\xi(\alpha - \xi y))$, for $\sigma_1 \leqslant \nu$ with $\nu > 0$ sufficiently small. Let γ_{211}^3 be the individual unstable manifold of q_{211}^3. Locally it is given as

$$\gamma_{211,\text{loc}}^3 = \{(y, \pi_1, \sigma_1, w_{11}) \mid w_{11} = H(0, \sigma_1), 0 \leqslant \sigma_1 \leqslant \nu, y = 0, \pi_1 = 0\}. \tag{4.14}$$

Therefore, we consider the following sections transverse to the flow:

$$\Sigma_{211}^{3,\text{in}} = \{(y, \pi_1, \sigma_1, w_{11}) \mid \pi_1 = \delta, w_{11} - 1/(\alpha\xi) \in [-\beta_1, \beta_1], \sigma_1 \in [0, \beta_2], y \in [-\beta_3, \beta_3]\},$$

$$\Sigma_{211}^{3,\text{out}} = \{(y, \pi_1, \sigma_1, w_{11}) \mid \pi_1 \in [0, \beta_4], \sigma_1 = \nu, w_{11} - 1/(\alpha\xi) \in [-\beta_1, \beta_1], y \in [-\beta_5, \beta_5]\}.$$

Let $\Pi_{211}^3 : \Sigma_{211}^{3,\text{in}} \to \Sigma_2^{3,\text{out}}$ be the associated map obtained by the first intersection by applying the forward flow.
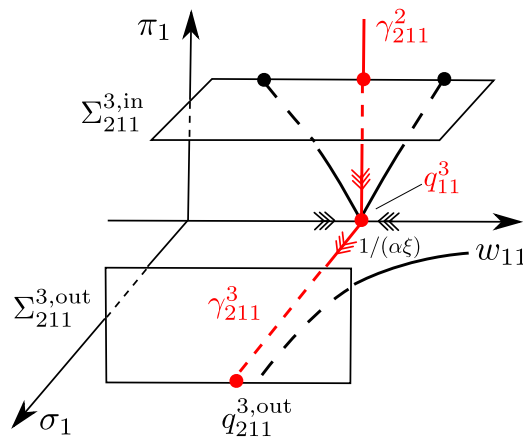
Figure 18. Illustration of the result lemma 4.7. γ^2_{211} is contained within $\sigma_1 = 0$, approaching the point q^3_{211} defined $(y, \pi_1, \sigma_1, w_{11}) = (0, 0, 0, 1/(\alpha\xi))$. The orbit γ^3_{211} is the unstable manifold of q^3_{211} and is contained within $\pi_1 = 0$.

Lemma 4.7. Π^3_{211} *is well-defined for appropriately small* $\delta > 0$, $\nu > 0$ *and* $\beta_i > 0$, $i = 1, \ldots, 5$. *In particular*

$$\Pi^3_{211}(y, \delta, \sigma_1, w_{11}) = (y_+(y, \sigma_1, w_{11}), \pi_{1+}(y, \sigma_1, w_{11}), \nu, w_{11+}(y, \sigma_1, w_{11})),$$

with

$$\pi_{1+}(y, \sigma_1, w_{11}) = \mathcal{O}(\sigma_1^2),$$
$$w_{11+}(y, \sigma_1, w_{11}) = H_{211}(y, \nu) + \mathcal{O}(\sigma_1^2),$$
$$y_{11+}(y, \sigma_1, w_{11}) = y + \mathcal{O}(\ln(\sigma^{-1})\sigma_1^2).$$

Furthermore, the remainder terms in π_{1+}, w_{11+} *and* y_{11+} *are* C^1 *with respect to* y *and* w_{11} *and the orders of these terms as* $\sigma_1 \to 0$ *do not change upon differentiation.*

Proof. The proof is similar to the proof of lemma 4.6, using partial linearization and Gronwall-like estimation of the remainder. We leave out the details. $\square$

Notice that $\Pi^3_{211}(\delta, w_{11}, 0, 0) = \gamma^3_{211} \cap \Sigma^{3,\text{out}}_{211}$. See figure 18. Notice also that $\gamma^3_{211,\text{loc}}$ in the (x, y, w)-variables becomes:

$$\gamma^3_{\text{loc}} = \{(x, y, w) \mid x \in [-1 - \nu, -1], y = w = 0\},$$

using (3.30), in agreement with (1.25). (γ^1 and γ^2, on the other hand, both 'collapse' to Q^1 at $(x, y, w) = (0, 0, 0)$ upon blowing down. See also figure 15.) To follow γ^3_{211} forward, we move to chart $(\bar{\epsilon} = 1, \tilde{w} = 1)_{21}$, see (3.32).

4.5. Dynamics in $(\bar{\epsilon} = 1, \tilde{w} = 1)_{21}$

In this chart, we obtain the following equations

$$\dot{x} = -(x + 1 + \alpha) + x\mu_1 q_{21}\left(y + \frac{x+1}{\xi}\right),$$

$$\dot{y} = \mu_1 F(\mu_1) + y\mu_1 q_{21}\left(y + \frac{x+1}{\xi}\right),$$

$$\dot{\mu}_1 = \mu_1^2 q_{21}\left(y + \frac{x+1}{\xi}\right), \tag{4.15}$$

$$\dot{q}_{21} = 2q_{21}^2\left(y + \frac{x+1}{\xi}\right)(2 - \mu_1),$$

and $\dot{r}_2 = 0$. Again, r_2 decouples and we shall therefore only work with the (x, y, μ_1, q_{21})-system. Also $\gamma^3_{211,\text{loc}}$ becomes

$$\gamma^3_{21,\text{loc}} = \left\{ (x, y, \mu_1, q_{21}) \,|\, q_{21} = \sigma_1^{-2} H(\sigma, 0), \, x = -1 - \sigma_1, \, \sigma_1 \in (0, \nu), \right.$$

$$\left. y = 0, \, \mu_1 = 0 \right\},$$

using (3.34), in the present chart. It is therefore contained within the invariant set $\mu_1 = y = 0$ where

$$\dot{x} = -(x + 1 + \alpha),$$

$$\dot{q}_{21} = 2q_{21}^2 \frac{x+1}{\xi}.$$

Notice, that starting from $x = -1 - \nu$ with $\nu > 0$ small, x and q_{21} are both monotonically decreasing towards the equilibrium q_{21}^4 defined by $(x, q_{21}) = (-1 - \alpha, 0)$. Therefore, by extending $\gamma^3_{2,\text{loc}}$ by the forward flow, we obtain an orbit that is asymptotic to this point. Since the x-direction is a stable space and the q-direction is a center space, the orbit γ^3_2 approaches q_{21}^4 as a local center manifold $x = h(q)$ over $0 \leqslant q \leqslant \delta$ which is flat at $q = 0$: $h^{(i)}(0) = 0$ for all $i \in \mathbb{N}$. In fact, we have something similar for any $y \in I$ where I is a open interval containing $[0, 2\alpha/\xi]$: the line $\mathcal{L}_{21}$, defined by $(x, \mu_1, q_{21}) = (-1 - \alpha, 0, 0)$, $y \in I$, is a set of equilibria. The linearization about any point in this set gives one single non-zero eigenvalue -1. Since $\mathcal{L}_{21}$ blows down to $L_\infty : x = -1 - \alpha$, $w = 0, y \in I$ using (3.32), we think of $\mathcal{L}_{21}$ as an improved version of this original degenerate line. Then, by center manifold theory, we have the following:

Proposition 4.8. *Fix $\eta \in (0, 1)$. Then there exists a $\delta > 0$ and a small neighborhood $\mathcal{U}_{21}$ of $(\mu_1, q_{21}) = 0$ in $\mathbb{R}^2$ such that the following holds. There exists a locally invariant center manifold $\mathcal{N}_{21}$ as a graph*

$$x = -1 - \alpha + \mu_1 h_{21}(y, \mu_1, q_{21}),$$

over $(y, \mu_1, q_{21}) \in I \times \mathcal{U}_{21}$. Here h_{21} is a smooth function. Furthermore, there exists a smooth stable foliation with base $\mathcal{N}_{21}$ and 1D fibers as leaves of the foliation. Within $x + 1 + \alpha \in [-\delta, \delta], (y, \mu_1, q_{21}) \in \mathcal{U}_{21}$, the contraction along any of these fibers is at least $e^{-\eta t}$.

Remark 4.9. Center manifold theory is (in general) a purely local result [4], that can be applied to any partially hyperbolic equilibrium. However, in proposition 4.8 we use the fact
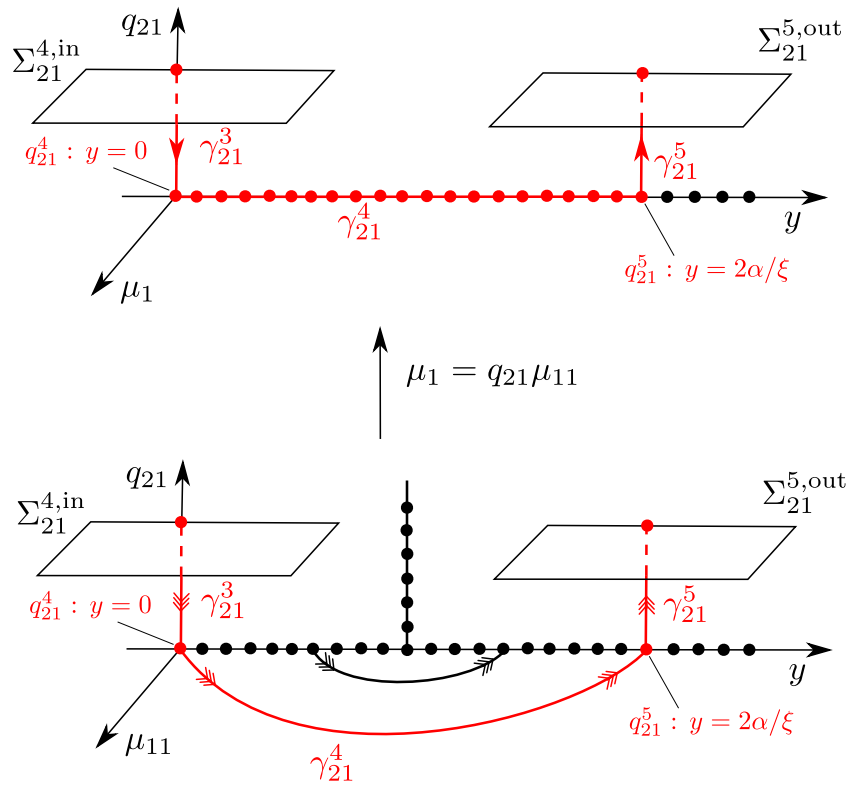
Figure 19. Illustration of the result in lemma 4.10. Our view is from $\mu_1 > 0$ on top and from $\mu_{11} > 0$ below. In the (y, μ_1, q_{21})-variables, the y-axis is a line of equilibria (it is a projection of $\mathcal{L}_{21}$). Upon the blowup $(q_{21}, \mu_{11}) \mapsto \mu_1 = q_{21}\mu_{11}$, which fixes q_{21}, this line has improved hyperbolicity properties, in particular we obtain a heteroclinic orbit γ_{21}^4—contained within $q_{21} = 0$, see also expression (4.16)—between equilibria $(0, 0, 0)$ and $q_{21}^5 : (2\alpha/\xi, 0, 0)$ on this axis. It connects γ_{21}^3 with γ_{21}^5, the former being the stable manifold of $(0, 0, 0)$ while the latter is the unstable manifold of $(2\alpha/\xi, 0, 0)$. For simplicity, we use the same symbols in the two figures (although the axes are different).

that the center manifold theory can be applied to any point on the line $\mathcal{L}_{21}$. This gives the desired 'global' center manifold $\mathcal{N}_{21}$ in proposition 4.8 by the same theory (in the same way that a slow manifold S_ϵ of (1.1) can be obtained as an ϵ-section of a center manifold $\{S_\epsilon \times \{\epsilon\} \mid \epsilon \in (-\epsilon_0, \epsilon_0)\}$, only truly local in ϵ, of the critical manifold $S_0 \times \{0\}$ in the extended space $\{(x, y, \epsilon)\}$, obtained by adding $\epsilon' = 0$ to the fast time version of (1.1)).

Next, consider the following sections

$$\Sigma_{21}^{4,\text{in}} = \{(x, y, \mu_1, q_{21}) \mid q_{21} = \delta, \, x + 1 + \alpha \in [-\beta_1, \beta_1], \, \mu_1 \in [0, \beta_2], \, y \in [-\beta_3, \beta_3]\},$$

$$\Sigma_{21}^{5,\text{out}} = \{(x, y, \mu_1, q_{21}) \mid q_{21} = \delta, \, x + 1 + \alpha \in [-\beta_1, \beta_1], \, \mu_1 \in [0, \beta_4], \, y - \frac{2\alpha}{\xi} \in [-\beta_5, \beta_5]\},$$

and let $\Pi_{21}^{45} : \Sigma_{21}^{4,\text{in}} \to \Sigma_{21}^{5,\text{out}}$ be the associated mapping obtained by the first intersection of the forward flow. By reducing the dynamics to the center manifold $\mathcal{N}_{21}$ (and applying a subsequent blowup) we will then show that we can guide the forward flow along the following lines

$$\gamma_{21}^4 = \{(x,y,\mu_1,q_{21}) \,|\, x = -1 - \alpha, \, y \in [0, 2\alpha/\xi), \mu_1 = q_{21} = 0\},$$
$$\gamma_{21}^5 = \{(x,y,\mu_1,q_{21}) \,|\, x = -1 - \alpha, \, y = 2\alpha/\xi, \mu_1 = 0, q_{21} \geqslant 0\}. \tag{4.16}$$

See figure 19. Notice that γ_{21}^4 belongs to $\mathcal{L}_{21}$ and is obtained through a desingularized (slow) flow on $\mathcal{N}_{21}$, see details below. Recall also figure 7. Then we have

Lemma 4.10. Π_{21}^{45} *is well-defined for appropriately small* $\delta > 0$, $\nu > 0$ *and* $\beta_i > 0$, $i = 1, \ldots, 5$. *In particular,*

$$\Pi_{21}^{45}(x,y,\mu_1,\delta) = (x_+(x,y,\mu_1), y_+(x,y,\mu_1), \mu_{1+}(x,y,\mu_1), \delta),$$

with μ_{1+} *a* C^l-*function with* $\mu_{1+} = \mu_1(1 + o(1))$,

$$x_+(x,y,\mu_1) = -1 - \alpha + \mu_{1+}(x,y,\mu_1)\nu h_{21}(\mu_{1+}(x,y,\mu_1), \delta, y_+(x,y,\mu_1)) + \mathcal{O}(e^{-\eta/\mu_1}),$$

$$y_+(x,y,\mu_1) = \frac{2\alpha}{\xi} - y + \mathcal{O}(\mu_1 \log \mu_1),$$

as $\mu_1 \to 0$. *Furthermore, the remainder terms in* x_+ *and* y_+ *are* C^l *with respect to* x *and* y *and the orders of these terms as* $\mu_1 \to 0$ *do not change upon differentiation.*

Proof. Working in a small neighborhood of $\mathcal{N}_{21}$, we can straighten out the stable fibers by a smooth transformation fixing x and taking $(x,y,\mu_1,q_{21}) \mapsto (\tilde{y}, \tilde{\mu}_1, \tilde{q}_{21})$ where

$$\tilde{y} = y + \mathcal{O}(\mu_1),$$
$$\tilde{\mu}_1 = \mu_1 + \mathcal{O}(\mu_1^2 q_{21}),$$
$$\tilde{q}_{21} = q_{21} + \mathcal{O}(q_{21}^2).$$

We drop the tildes henceforth and therefore consider the following reduced system on $\mathcal{N}_{21}$.

$$\dot{y} = \mu_1\left(F(\mu_1) + y q_{21}\left(\xi y - \alpha + \mu_1 h_2(\mu_1, q_{21}, y)\right)/\xi\right),$$
$$\dot{\mu}_1 = \mu_1^2 q_{21}\left(\xi y - \alpha + \mu_1 h_2(\mu_1, q_{21}, y)\right)/\xi,$$
$$\dot{q}_{21} = q_{21}^2\left(\xi y - \alpha + \mu_1 h_2(\mu_1, q_{21}, y)\right)/\xi(2 - \mu_1).$$

Here $\mu_1 = q_{21} = 0$, $y \in I$, where I is some appropriate interval, is a line of equilibria (it is a projection of $\mathcal{L}_{21}$, so we will use reuse this symbol in the following). It is not normally hyperbolic since the linearization about any point in $\mathcal{L}_{21}$ only has zero as an eigenvalue. We can gain hyperbolicity by applying the directional blowup, setting:

$$\mu_1 = q_{21}\mu_{11}.$$

Inserting this into the reduced equations we obtain

$$\dot{y} = \mu_{11}\left(F(q_{21}\mu_{11}) + y q_{21}\left(\xi y - \alpha + q_{21}\mu_{11} h_2(q_{21}\mu_{11}, q_{21}, y)\right)/\xi\right),$$
$$\dot{\mu}_{11} = 2\mu_{11}\left(\xi y - \alpha + q_{21}\mu_{11} h_2(q_{21}\mu_{11}, q_{21}, y)\right)(-1 + q_{21}\mu_{11})/\xi, \tag{4.17}$$
$$\dot{q}_{21} = q_{21}\left(\xi y - \alpha + q_{21}\mu_{11} h_2(q_{21}\mu_{11}, q_{21}, y)\right)(2 - \mu_1)/\xi,$$

after division of the right hand side by q_{21}. Now, the line $\widehat{\mathcal{L}}_{21}$ defined $\mu_1 = q_{21} = 0$, $y \in I$ is an improved version of $\mathcal{L}_{21}$, being normally hyperbolic for any $y \neq \alpha/\xi$. Indeed, the linearization about any point gives $\pm 2(\xi y - \alpha)$ as nonzero eigenvalues. Within the invariant set $\mu_1 = 0$ we obtain

$$\dot{y} = 0,$$
$$\dot{q}_{21} = q_{21}\left(\xi y - \alpha\right)/\xi.$$

Along $y = \alpha/\xi, q_{21} \geqslant 0$ every point is an equilibrium. For $y < \alpha/\xi$, q_{21} contracts exponentially towards $q_{21} = 0$. On the hand, for $y > \alpha/\xi$, q_{21} expands exponentially. Next, within $q_{21} = 0$ we obtain from (4.17)

$$\dot{y} = \mu_{11},$$
$$\dot{\mu}_{11} = 2\mu_{11}\left(\xi y - \alpha\right)/\xi.$$

Writing

$$\frac{\mathrm{d}\mu_{11}}{\mathrm{d}y} = 2\left(\xi y - \alpha\right)/\xi,$$

we realise that every point $\mu_{11} = 0, y = y_0 < \alpha/\xi$, is heteroclinic with $\mu_{11} = 0, y = y_1 > \alpha/\xi$ where $y_1 = 2\alpha/\xi - y_0$. See figure 19.

Now, to describe the mapping Π_{21}^{45}, we proceed as follows. We first work locally near $y = 0$ and consider a mapping from $q_{21} = \delta$ to $\mu_{11} = \nu$. From there we then apply a finite time flow map by following the heteroclinic orbits within $\mu_{11} = 0$ up to a neighborhood of the point q_{21}^5 defined by $\mu_{11} = 0$, $q_{21} = 0$, $y = 2\alpha/\xi$. From here, we then consider a mapping $\mu_{11} = \nu$ to $q_{21} = \delta$ working near the normally hyperbolic line $\mu_{11} = q_{21} = 0$, $y \approx 2\alpha/\xi$.

For the first part, near $y = 0$, we divide the right hand side by

$$(\xi y - \alpha + q_{21}\mu_{11}h_2(q_{21}\mu_{11}, q_{21}, y))\left(-1 + q_{21}\mu_{11}\right)/\xi > 0.$$

This gives

$$\dot{y} = \mu_{11}(-1 + q_{21}\mu_{11})^{-1}\left((\xi y - \alpha + q_{21}\mu_{11}h_2(q_{21}\mu_{11}, q_{21}, y))^{-1}\xi F(q_{21}\mu_{11}) + yq_{21}\right),$$
$$\dot{\mu}_{11} = 2\mu_{11},$$
$$\dot{q}_{21} = q_{21}(1 - q_{21}\mu_{11})^{-1}(-2 + \mu_1).$$

Now we straighten out the unstable fibers within the unstable manifold $q_{21} = 0$ by performing a transformation of the form $(y, \mu_{11}) \mapsto \tilde{y}$ such that

$$\dot{\tilde{y}} = \mathcal{O}(\mu_{11}q_{21}),$$
$$\dot{\mu}_{11} = 2\mu_{11},$$
$$\dot{q}_{21} = q_{21}(1 - q_{21}\mu_{11})^{-1}(-2 + \mu_1).$$

The y-variables decouples and the (μ_{11}, q_{21})-subsystem has a saddle at $p_{21} = q_{21} = 0$. We can therefore linearize this subsystem through a C^1-transformation fixing μ_1 and taking $(\mu_{11}, q_{21}) \mapsto \tilde{q}_{21} = q_{21}(1 + \mathcal{O}(\mu_{11}))$ such that

$$\dot{\tilde{y}} = \mathcal{O}(\mu_{11}\tilde{q}_{21}),$$
$$\dot{\mu}_{11} = 2\mu_{11},$$
$$\dot{\tilde{q}}_{21} = -2\tilde{q}_{21}.$$

We then integrate this system from $\tilde{q}_{21} = \tilde{\delta}$ to $\mu_{11} = \nu$. This gives

$$(\tilde{y}, \mu_{11}, \tilde{\delta}) \mapsto (y + \mathcal{O}(\mu_{11} \log \mu_{11}), \nu, \mu_{11}\nu^{-1}\tilde{\delta}).$$

We then return to (y, μ_{11}, q_{21}), by applying the C^1-inverses, and proceed with the second and third step. In the third, final step, our approach is identical to the first part, now working near the point $q_{21}^5 : y = 2\alpha/\xi$, $\mu_{11} = q_{21} = 0$. We leave out further details, but in combination, this gives the desired result. $\qquad\square$

4.6. Dynamics in $(\bar{\epsilon} = 1, \tilde{\bar{q}} = 1)_{22}$

In this chart, we obtain

$$\begin{aligned}
\dot{x} &= w_2\left(-(x+1+\alpha) + x\mu_2\left(y + \frac{x+1}{\xi}\right)\right), \\
\dot{y} &= \mu_2 w_2\left(w_2 F(\mu_2 w_2) + y\left(y + \frac{x+1}{\xi}\right)\right), \\
\dot{\mu}_2 &= 2\mu_2\left(y + \frac{x+1}{\xi}\right), \\
\dot{w}_2 &= -w_2\left(y + \frac{x+1}{\xi}\right)(2 - \mu_2 w_2),
\end{aligned}$$

(4.18)

and $\dot{r}_2 = 0$. Furthermore, γ_{21}^5 becomes

$$\gamma_{22}^5 = \{(x, y, \mu_2, w_2) \mid w_2 > 0, x = -1 - \alpha, y = 2\alpha/\xi, \mu_2 = 0\},$$

contained within the invariant set $x = -1 - \alpha, \mu_2 = 0$ where

$$\begin{aligned}
\dot{y} &= 0, \\
\dot{w}_2 &= -2w_2\left(y - \frac{\alpha}{\xi}\right)
\end{aligned}$$

γ_{22}^5 is asymptotic to the point q_{22}^6 defined by $(x, y, \mu_2, w_2) = (-1 - \alpha, 2\alpha/\xi, 0, 0)$ within the set $\mathcal{P}_{22}$ of equilibria, defined by $\mu_2 = w_2 = 0$ and (x, y) in a neighborhood of $(-1 - \alpha, 2\alpha/\xi)$. The linearization about any point within this 'plane' $\mathcal{P}_{22}$ has ± 2 as the only non-zero eigenvalues. Consequently, $\mathcal{P}_{22}$ is normally hyperbolic. Within the invariant subset defined by $w_2 = 0$, we have

$$\begin{aligned}
\dot{x} &= 0, \\
\dot{y} &= 0, \\
\dot{\mu}_2 &= 2\mu_2\left(y + \frac{x+1}{\xi}\right).
\end{aligned}$$

In particular,

$$\gamma_{22}^6 = \{(x, y, \mu_2, w_2) \mid w_2 = 0, x = -1 - \alpha, y = 2\alpha/\xi, \mu_2 \geqslant 0\},$$

is contained within the unstable manifold of $\mathcal{P}_{22}$, and is the individual unstable manifold of the base point $q_{22}^6 \in \mathcal{P}_{22}$ of γ_{22}^5 defined by $(x, y, \mu_2, w_2) = (-1 - \alpha, 2\alpha/\xi, 0, 0)$. We therefore consider the following sections

$$\Sigma_{22}^{6,\text{in}} = \{(x, y, \mu_2, w_2) \mid w_2 = \nu, \, x + 1 + \alpha \in [-\beta_1, \beta_1], \, y - 2\alpha/\xi \in [-\beta_2, \beta_2], \, \mu_2 \in [0, \beta_2]\},$$
$$\Sigma_{22}^{6,\text{out}} = \{(x, y, \mu_2, w_2) \mid \mu_2 = \delta, \, x + 1 + \alpha \in [-\beta_3, \beta_3], \, y - 2\alpha/\xi \in [-\beta_4, \beta_4], \, w_2 \in [0, \beta_5]\},$$

and let $\Pi_{22}^6 : \Sigma_{22}^{6,\text{in}} \to \Sigma_{22}^{6,\text{out}}$ the associated local mapping obtained by the forward flow. We then have

Lemma 4.11. *The mapping Π_{22}^6 is well-defined for appropriately small $\nu > 0, \delta > 0$ and $\beta_i > 0$, $i = 1, \ldots, 5$. In particular,*

$$\Pi_{22}^6(x, y, \mu_2, \nu) = (x_+(x, y, \mu_2), y_+(x, y, \mu_2), \delta, w_{2+}(\mu_2)),$$

where w_{2+} is C^l satisfying $w_{2+}(\mu_2) = \mu_2(1 + o(1))$ and

$$x_+(x, y, \mu_2) = H_{22}(x, \delta) + \mathcal{O}(\mu_2 \ln \mu_2^{-1}),$$
$$y_+(x, y, \mu_2) = y + \mathcal{O}(\mu_2 \ln \mu_2^{-1}),$$

as $\mu_2 \to 0$. Here H_{22} is smooth and satisfies $H_{22}(-1 - \alpha, \delta) = -1 - \alpha$.

Furthermore, the remainder terms in x_+ and y_+ are C^l with respect to x and y and the orders of these terms as $\mu_2 \to 0$ do not change upon differentiation.

Proof. We straighten out the individual stable manifolds of $\mathcal{P}_{22}$ within $\mu_2 = 0$ by a transformation fixing y and w_2 and taking $(w_2, x) \mapsto \tilde{x} = H_{22}(x, w_2)$. Here by the invariance of γ_{22}^5 we have $H_{22}(-1 - \alpha, w_2) = -1 - \alpha$ for any w_2. Then

$$\dot{\tilde{x}}_2 = \mathcal{O}(w_2 \mu_2).$$

Straightforward estimation gives the desired result. $\qquad\square$

See figure 15 for illustration of γ^6.

4.7. Dynamics in $(\bar{\epsilon} = 1)_1$: exit of chart ϕ_3

To follow γ_{22}^6 forward, we return to the chart $(\bar{\epsilon} = 1)_1$ and the coordinates $(x, y, w, \epsilon_1, r_1)$. In this chart, we obtain the following equations

$$\begin{aligned}
\dot{x} &= w\left(-\epsilon_1(x + 1 + \alpha) + x\left(y + \frac{x+1}{\xi}\right)\right), \\
\dot{y} &= w\left(\epsilon_1 w F(w) + y\left(y + \frac{x+1}{\xi}\right)\right), \\
\dot{w} &= w^2\left(y + \frac{x+1}{\xi}\right), \\
\dot{\epsilon}_1 &= -2\epsilon_1\left(y + \frac{x+1}{\xi}\right).
\end{aligned} \qquad (4.19)$$

Also $\dot{r}_1 = 2\epsilon_1\left(y + \frac{x+1}{\xi}\right)$ but this decouples and we shall therefore (again) just work with the (x, y, w, ϵ_1)-subsystem. In these coordinates, γ_{22}^6 becomes

$$\gamma_1^6 = \left\{(x, y, w, \epsilon_1) \mid \epsilon_1 > 0, \, x = -1 - \alpha, \, y = \frac{2\alpha}{\xi}, \, w = 0\right\}.$$

It is asymptotic to the point q_1^7 with coordinates

$$(x, y, w, \epsilon_1) = \left(-1 - \alpha, \frac{2\alpha}{\xi}, 0, 0\right). \tag{4.20}$$

We work in a neighborhood of this point where

$$y + \frac{x+1}{\xi} \approx \alpha/\xi > 0.$$

We therefore divide the right hand side of (4.19) by this quantity and consider the following system

$$\dot{x} = w\left(-\frac{\epsilon_1(x+1+\alpha)}{y + \frac{x+1}{\xi}} + x\right),$$

$$\dot{y} = w\left(\frac{\epsilon_1 w F(w)}{y + \frac{x+1}{\xi}} + y\right),$$

$$\dot{w} = w^2,$$

$$\dot{\epsilon}_1 = -2\epsilon_1.$$

Notice that $\epsilon_1 = w = 0$ is invariant. Also the linearization about any point in this set gives -2 as a single zero eigenvalue. Therefore $\epsilon_1 = 0$, $w \in [0, \beta]$ and (x, y) in a small neighborhood of $(-1 - \alpha, \frac{2\alpha}{\xi})$ is a local center manifold with smooth foliation by 1D fibers, along which orbits contract towards the center manifold with e^{-2t}. Therefore there exists a smooth, local transformation fixing w and ϵ_1 and taking $(x, y, w, \epsilon_1) \mapsto (\tilde{x}, \tilde{y}) = (x, y) + \mathcal{O}(w\epsilon_1)$ such that

$$\dot{\tilde{x}} = w\tilde{x},$$

$$\dot{\tilde{y}} = w\tilde{y}.$$

In the following, fix $y_1 > \frac{2\alpha}{\xi}$ and consider the following sections:

$$\Sigma_1^{7,\mathrm{in}} = \{(x, y, w, \epsilon_1) \,|\, \epsilon_1 = \delta, \, x + 1 + \alpha \in [-\beta_1, \beta_1], \, y - 2\alpha/\xi \in [-\beta_2, \beta_2], \, w \in [0, \beta_3]\},$$

$$\Sigma_1^7 = \{(x, y, w, \epsilon_1) \,|\, \epsilon_1 \in [0, \beta_4], \, x + 1 + \alpha \in [-\beta_5, \beta_5], \, y = y_1, \, w \in [0, \beta_6]\}.$$

Let $\Pi_1^7 : \Sigma_1^{7,\mathrm{in}} \to \Sigma_1^7$. Then, by integrating the $(\tilde{x}, \tilde{y}, w, \epsilon_1)$-system and transforming the result back to the (x, y, w, ϵ_1)-system using the implicit function theorem, we obtain the following:

Lemma 4.12. Π_1^7 *is well-defined for appropriately small* $y_1 - \frac{2\alpha}{\xi}$, $\delta > 0$ *and* $\beta_i > 0$, $i = 1, \ldots, 6$. *In particular,*

$$\Pi_1^7(x, y, w, \delta) = (x_+(x, y, w), y_1, w_+(x, y, w), \epsilon_{1+}(x, y, w)),$$

with x_+, w_+ *and* ϵ_{1+} *all* C^l *satisfying*

$$x_+(x, y, w) = \frac{x y_1}{y}(1 + \mathcal{O}(w)),$$

$$w_+(x, y, w) = \frac{w y_1}{y}(1 + \mathcal{O}(w)),$$

$$\epsilon_{1+}(x, y, w) = \mathcal{O}(e^{-c/w}),$$
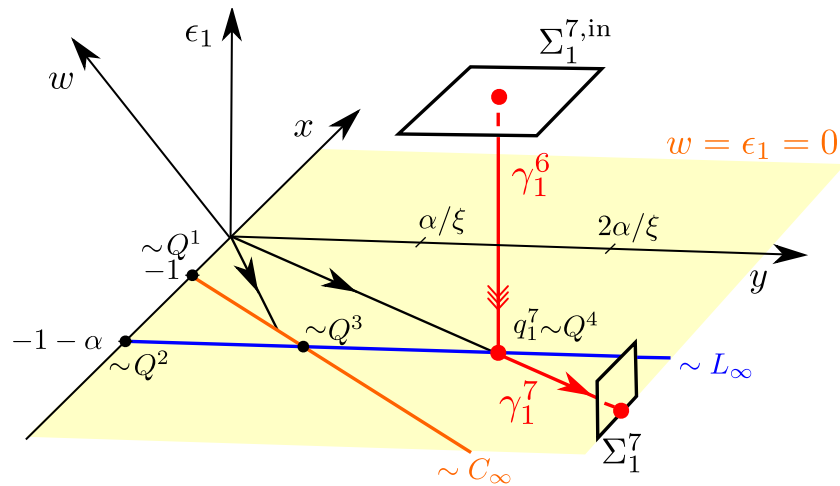
Figure 20. Illustration of the result in lemma 4.10. We try to artistically include all the four dimensions, our view being from $x < 0$. The set $\{\epsilon_1 = 0\}$ is partially hyperbolic and attracting within the region $y + (x + 1)/\xi > 0$. We can desingularize the flow within $\epsilon_1 = w = 0$ (shown in yellow) by division by w. This produces (4.22) and γ_1^7 (in red) as the flow of the base point $q_1^7 : (x, y, w, \epsilon_1) = (-1 - \alpha, 2\alpha/\xi, 0, 0)$ of γ_1^6 (also in red). The projection of this point onto (x, y, w) (which we indicate by $\sim$) is Q^4.

for some sufficiently small $c > 0$.

Define $\gamma_{1,\text{loc}}^7$ by

$$\gamma_{1,\text{loc}}^7 = \left\{ (x, y, w, \epsilon_1) \,|\, \epsilon_1 = w = 0, \, x = -\frac{\xi(1 + \alpha)}{2\alpha} y, \, y \in \left[\frac{2\alpha}{\xi}, \frac{2\alpha(1 + \nu)}{\xi} \right] \right\}. \tag{4.21}$$

It is obtained from the reduced problem of (4.19) within $\epsilon_1 = 0$:

$$\begin{aligned}
\dot{x} &= x \left(y + \frac{x + 1}{\xi} \right), \\
\dot{y} &= y \left(y + \frac{x + 1}{\xi} \right),
\end{aligned} \tag{4.22}$$

using $x(0) = -1 - \alpha, y(0) = 2\alpha/\xi$, see (4.20), upon desingularization through division by w, and subsequently letting $w = 0$. See figure 20. Then it follows that

$$\Pi_1^7(x, y, 0, \delta) = \gamma_{1,\text{loc}}^7 \cap \Sigma_1^7.$$

We can extend $\gamma_{1,\text{loc}}^7$ by the forward flow of (4.22) within $\epsilon_1 = w = 0$. We then have

Lemma 4.13. *Under the forward flow of (4.22) within $\epsilon_1 = w = 0$, γ_1^7 is bounded if and only if $\alpha < 1$. In the affirmative case, γ_1^7 is asymptotic to the point $Q^5 \in C_\infty$ with*

$$x = -\frac{1 + \alpha}{1 - \alpha}, \, y = \frac{2\alpha}{\xi(1 - \alpha)}.$$

5. The transition map $\Pi^{17} : \Sigma^1 \to \Sigma^7$

We now combine the findings in ϕ_3 into a result on the transition mapping Π^{17}. This map is defined by the first intersection of the forward flow of (3.1) from

$$\Sigma^1 = \{(x, y, w) \,|\, w = \delta,\, x - 1 - \xi y \in [-\beta_1, 0),\, y \in [-\beta_2, \beta_2]\}, \tag{5.1}$$

to $\{y = 2\alpha(1 + \nu)/\xi\}$, with $\nu > 0$ sufficiently small. It will be convenient to write the image of this mapping in terms of the coordinates (x, y, w, ϵ_1) in chart $(\bar{q} = 1)_1$. Consequently, we therefore define $\Pi^{17} : \Sigma^1 \to \Sigma_1^7$ for $0 < \epsilon \ll 1$ with

$$\Sigma_1^7 = \{(x, y, w, \epsilon_1) \,|\, y = 2\alpha(1 + \nu)/\xi,\, x + 1 + \alpha \in [-\beta_3, \beta_3],\, w \in [0, \beta_4],\, \epsilon_1 \in [0, \beta_5]\}. \tag{5.2}$$

Notice the following:

- We restrict Σ^1 to $x - 1 - \xi y \in [-\beta_1, 0)$ so that the flow is transverse to the section, see (3.1). This is clearly a subset containing $\Pi^0(\Sigma^0)$, recall (2.4).
- Using (3.5) and (3.22) we have

$$\epsilon_1 = \epsilon e^{2w^{-1}}.$$

  By describing the image in the (x, y, w, ϵ_1)-coordinates, we therefore at the same time keep track of how small w is. If w were to be too small then ϵ_1 would not be small enough for us to compose it with the subsequent mapping Π^{70}, see lemma 8.1.

We then have

Lemma 5.1. *The mapping Π^{17} is well-defined for appropriately small $\delta > 0$, $\nu > 0$ and $\beta_i > 0$, $i = 1, \ldots, 5$ and all $0 < \epsilon \ll 1$. In particular,*

$$\Pi^{17}(x, y, \delta; \epsilon) = (x_+(x, y, \epsilon), 2\alpha(1 + \nu)/\xi, w_+(x, y; \epsilon), \epsilon_{1+}(x, y; \epsilon)),$$

where x_+, w_+ and $\epsilon_{1+}(x, y; \epsilon)$ are C^1-functions in x and y, satisfying the following C^1-estimates

$$\begin{aligned}
x_+(x, y; \epsilon) &= -(1 + \alpha)(1 + \nu) + \mathcal{O}(\log^{-1} \epsilon^{-1} \log\log \epsilon^{-1}), \\
w_+(x, y; \epsilon) &= \mathcal{O}(\log^{-1} \epsilon^{-1} \log\log \epsilon^{-1}), \\
\epsilon_{1+}(x, y; \epsilon) &= \mathcal{O}(e^{-c \log \epsilon^{-1}}),
\end{aligned} \tag{5.3}$$

for $c > 0$ sufficiently small, as $\epsilon \to 0$.

Proof. The result follows from the series of lemmas: lemma 4.4, see also corollary 4.5, lemmas 4.6, lemma 4.7, 4.10–4.12, describing the relevant local transition maps in the local charts described in section 3.3 using standard hyperbolic methods to follow the segments γ^{1-7}. Notice that the mappings between the different local sections are diffeomorphism that do not change the order. □

Remark 5.2. In C^0 the estimate for w_+ in (5.3) can be improved to $\mathcal{O}(\log^{-1} \epsilon^{-1})$. In fact, this is more or less a direct consequence of our approach: setting $q = e^{-w^{-1}}$ and $q = \epsilon q_2$ gives $w = \mathcal{O}(\log^{-1} \epsilon^{-1})$ for fixed q_2 as $\epsilon \to 0$. Similarly, it follows that $\min w(t) = \mathcal{O}(\log^{-1} \epsilon^{-1})$ along a relaxation oscillation. Since $z(t) = w(t)^{-1}$ for $z(t) > 0$ this implies (more or less) that the amplitude of the limit cycles grow like $\mathcal{O}(\log \epsilon^{-1})$ as $\epsilon \to 0$.

6. Blowup analysis in chart ϕ_1

In this chart, we obtain the following equations

$$
\begin{aligned}
\dot{w}_1 &= -\epsilon w_1^2 F(z_1 w_1^{-1}), \\
\dot{x}_1 &= -\epsilon \left(w_1 x_1 F(z_1 w_1^{-1}) + (x_1 + (1+\alpha)z_1) \right), \\
\dot{z}_1 &= -\epsilon w_1 z_1 F(z_1 w_1^{-1}) - e^{-2z_1 w_1^{-1}} \left(1 + \frac{x_1 + z_1}{\xi} \right), \\
\dot{\epsilon} &= 0,
\end{aligned}
\tag{6.1}
$$

redefining $F(s) = 1 - e^{-s}$. Therefore also

$$
F(-s) = -e^s F(s).
$$

Henceforth we drop the subscripts. In this chart, we then have

$$
C = \{(w, x, z, \epsilon) \,|\, x = -\xi - z, \, w > 0, \, \epsilon = 0\},
$$

and

$$
C_\infty = \{(w, x, z, \epsilon) \,|\, x = -\xi - z, w = 0, \epsilon = 0\}.
\tag{6.2}
$$

We first notice that $e^{-zw^{-1}}$ and $e^{-2zw^{-1}}$ appearing in (6.1) are not defined along $w = 0$ for $z \leqslant 0$. We shall therefore introduce a new system by blowing up $w = z = 0$ by the polar blowup transformation

$$
(w, z) = \theta(\bar{w}, \bar{z}), \, \theta \geqslant 0, \, (\bar{w}, \bar{z}) \in S^1,
\tag{6.3}
$$

and apply appropriate 'desingularization' of the transformed vector-field to have a well-defined vector-field within $\theta = 0$. In particular, we will divide the right hand side by $e^{-2\bar{z}\bar{w}^{-1}}$ whenever $\bar{z} < 0$.

We will use three separate charts $(\bar{z} = 1)_1$, $(\bar{w} = 1)_2$ and $(\bar{z} = -1)_3$ obtained by setting $\bar{z} = 1$, $\bar{w} = 1$ and $\bar{z} = -1$, respectively, so that we have the following local forms of (6.3):

$$
w = \theta_1 w_1, \, z = \theta_1,
\tag{6.4}
$$

$$
\begin{aligned}
w &= \theta_2, \, z = \theta_2 z_2, \\
w &= \theta_3 w_3, \, z = -\theta_3,
\end{aligned}
\tag{6.5}
$$

where $(\theta_1, w_1) \in [0, \infty)^2$, $(\theta_2, z_2) \in [0, \infty) \times \mathbb{R}$, and $(\theta_3, w_3) \in [0, \infty)^2$ are the local coordinates, respectively. We consider each of these charts in the following.

6.1. Blowup analysis in chart $(\bar{z} = 1)_1$

Working in the chart $(\bar{z} = 1)_1$ is similar to the analysis of (3.6) in chart ϕ_3. Indeed, here we have $e^{-2zw^{-1}} = e^{-2w_1^{-1}}$, and as in chart ϕ_3, we therefore put

$$
q_1 = e^{-2w_1^{-1}}.
\tag{6.6}
$$
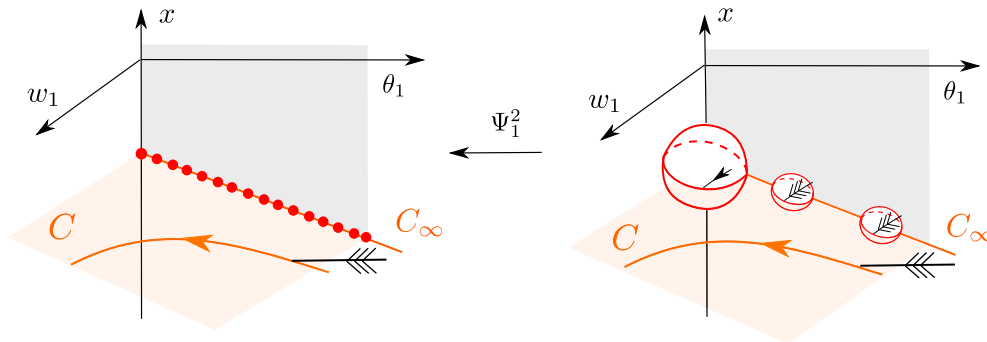
Figure 21. Blowup in chart $\bar{z} = 1$ of the line corresponding to C_∞ to a line of spheres. Our view is from $w_1 > 0$, the w_1-axis 'coming out' of the page. The gray shaded region is $w_1 = 0$ while the orange hyperplane is C. C_∞ is the intersection of C with $w_1 = 0$. As before, the spheres, seen in red on the right, are the result of blowing up the (red) points on C_∞ in the picture on the left, each involving the remaining directions due to q and ϵ (not shown), see details (6.8). By this blowup we are able to extend the hyperbolicity of C to $w_1 = 0$ for all $\theta_1 > 0$ (indicated by the tripple-headed arrows) within $\bar{\epsilon} = 0$. The sphere at $\theta_1 = 0$ (enlarged) is still degenerate.

This gives the following equations

$$\dot{x} = -\epsilon\theta_1 w_1 \left(\theta_1 w_1 x F(w_1^{-1}) + (x + (1+\alpha)\theta_1)\right),$$
$$\dot{\theta}_1 = -\theta_1 w_1 \left(\epsilon\theta_1^2 w_1 F(w_1^{-1}) + q\left(1 + \frac{x+\theta_1}{\xi}\right)\right),$$
$$\dot{w}_1 = w_1^2 q\left(1 + \frac{x+\theta_1}{\xi}\right), \tag{6.7}$$
$$\dot{q} = 2q^2\left(1 + \frac{x+\theta_1}{\xi}\right),$$
$$\dot{\epsilon} = 0,$$

by implicit differentiation and dropping the subscript on q. Here we have multiplied the right hand side by $\theta_1 w_1$ to ensure that $\theta_1 = 0$ and $w_1 = 0$ are well-defined. For this system,

$$C = \left\{(x, \theta_1, w, q, \epsilon) \,|\, 1 + \frac{x+\theta_1}{\xi} = 0, w > 0, q > 0, \epsilon = 0\right\},$$

is a partially hyperbolic set of equilibria, but still not compact. As in chart ϕ_3, the system is very degenerate near

$$C_\infty = \left\{(x, \theta_1, w, q, \epsilon) \,|\, 1 + \frac{x+\theta_1}{\xi} = 0, w_1 = q = 0, \epsilon = 0, \theta_1 \geqslant 0\right\}.$$

Then we proceed as in chart ϕ_3: let $P_1 = \{(x, \theta_1, w, q, \epsilon) \in \mathbb{R} \times [0, \infty)^4\}$, $P_1^1 = \{(x, \theta_1, w, r, (\bar{q}, \bar{\epsilon})) \in \mathbb{R} \times [0, \infty)^3 \times S^1\}$ and blowup $q = \epsilon = 0$ through the blowup transformation

$$\Psi_1^1 : P_1^1 \to P_1,$$

which fixes x, θ_1 and w and takes

$$(r, (\bar{q}, \bar{\epsilon})) \mapsto \begin{cases} q & = & r\bar{q}, \\ \epsilon & = & r\bar{\epsilon}, \end{cases} \quad r \geqslant 0, (\bar{q}, \bar{\epsilon}) \in S^1.$$
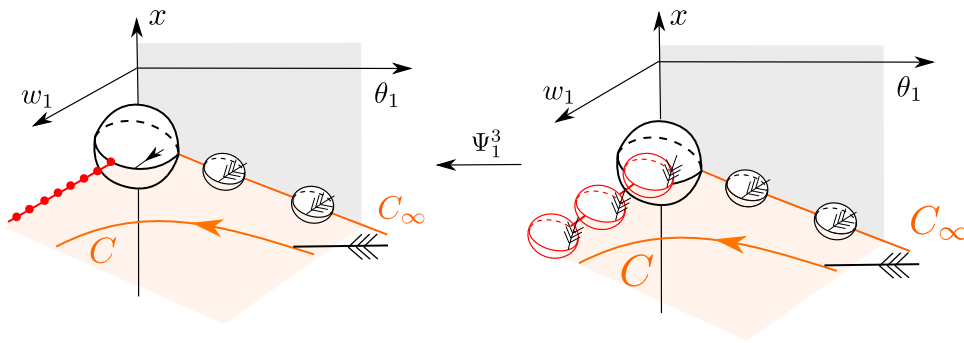
Figure 22. Blowup in chart $\bar{z} = 1$ of point on the sphere at $\theta_1 = 0$. This produces a cylinder of spheres with improved hyperbolicity properties. Again, the spheres involve directions due to q and ϵ, missing in this sketch.

Again, only $\bar{q} \geqslant 0$, $\bar{\epsilon} \geqslant 0$ is relevant. Notice that we use a notation for the blowups (i.e. Ψ_j^i) that is similar to the one used in section 3. However, we believe it will be clear from the context what blowup we are referring to. In the second blowup step, we set $P_1^2 = \{(\theta_1, r, \rho, (\bar{x}, \bar{w}, \bar{\bar{\epsilon}})) \in \mathbb{R} \times [0, \infty)^3 \times S^2\}$ and blowup C_∞ through the transformation

$$\Psi_1^2 : P_1^2 \to P_1^1,$$

which fixes θ_1 and r and takes

$$(\theta_1, \rho, (\bar{x}, \bar{w}, \bar{\bar{\epsilon}})) \mapsto \begin{cases} x & = & -\xi - \theta_1 + \rho\bar{x}, \\ w_1 & = & \rho\bar{w}_1, \\ \bar{q}^{-1}\bar{\epsilon} & = & \rho\bar{\bar{\epsilon}}, \end{cases} \quad \rho \geqslant 0, (\bar{x}, \bar{w}_1, \bar{\bar{\epsilon}}) \in S^2. \tag{6.8}$$

See figure 21. Since $(\bar{q}, \bar{\epsilon}) \in S^1$ we can write the last equality as

$$(\bar{q}, \bar{\epsilon}) = \left(\frac{1}{\sqrt{1 + \rho^2 \bar{\bar{\epsilon}}^2}}, \frac{\rho\bar{\bar{\epsilon}}}{\sqrt{1 + \rho^2 \bar{\bar{\epsilon}}^2}} \right).$$

Let $\Psi_1^{12} = \Psi_1^1 \circ \Psi_1^2$.

Due to the multiplication by θ_1 on the right hand side in the derivation of (6.7), the resulting system is still degenerate near $(\bar{x}, \bar{\bar{\epsilon}}, \bar{w}_1) = (0, 0, 1)$, $\theta_1 = 0$. Therefore let $P_1^3 = \{(r, \rho, \varrho, (\bar{\bar{x}}, \bar{\theta}_1, \bar{\bar{\bar{\epsilon}}})) \in [0, \infty)^3 \times S^2\}$. Then we apply a final blowup transformation

$$\Psi_1^3 : P_1^3 \to P_1^2,$$

which fixes r and ρ and takes

$$(\varrho, (\bar{\bar{x}}, \bar{\theta}_1, \bar{\bar{\bar{\epsilon}}})) \mapsto \begin{cases} \bar{w}_1^{-1}\bar{x} & = & \varrho\bar{\bar{x}}, \\ \theta_1 & = & \varrho\bar{\theta}_1, \\ \bar{w}_1^{-1}\bar{\bar{\epsilon}} & = & \varrho\bar{\bar{\bar{\epsilon}}}, \end{cases} \quad \varrho \geqslant 0, (\bar{\bar{x}}, \bar{\theta}_1, \bar{\bar{\bar{\epsilon}}}) \in S^2. \tag{6.9}$$

See figure 22. Since $(\bar{x}, \bar{w}_1, \bar{\bar{\epsilon}}) \in S^2$ we can write the right hand side as

$$(\bar{x}, \bar{w}_1, \bar{\bar{\epsilon}}) = \left(\frac{\varrho\bar{\bar{x}}}{\sqrt{1 + \varrho^2\bar{\bar{x}}^2 + \varrho^2\bar{\bar{\bar{\epsilon}}}^2}}, \frac{1}{\sqrt{1 + \varrho^2\bar{\bar{x}}^2 + \varrho^2\bar{\bar{\bar{\epsilon}}}^2}}, \frac{\varrho\bar{\bar{\bar{\epsilon}}}}{\sqrt{1 + \varrho^2\bar{\bar{x}}^2 + \varrho^2\bar{\bar{\bar{\epsilon}}}^2}} \right).$$

Let $\Psi_1^{123} = \Psi_1^{12} \circ \Psi_1^3$.

6.1.1. Local charts and the corresponding directional blowup transformations. To describe
the blowups Ψ_1^1, Ψ_1^{12} and Ψ_1^{123} we again use local directional charts. For Ψ_1^1 we will only work
in the chart $(\bar{z} = 1, \bar{q} = 1)_{11}$ obtained by setting $\bar{q} = 1$ so that

$$\Psi_{11}^1 : (r_1, \epsilon_1) \mapsto \begin{cases} q &=& r_1, \\ \epsilon &=& r_1\epsilon_1, \end{cases} \tag{6.10}$$

in the local coordinates $(r_1, \epsilon_1) \in [0, \infty)^2$. Then to describe Ψ_1^{12}, we use two separate charts
$(\bar{z} = 1, \bar{q} = 1, \bar{x} = 1)_{111}$ and $(\bar{z} = 1, \bar{q} = 1, \bar{w} = 1)_{112}$ obtained by setting $\bar{x} = 1$ and $\bar{w}_1 = 1$ in
(6.8):

$$\Psi_{111}^{12} : (r_1, \theta_1, \rho_1, w_{11}, \epsilon_{11}) \mapsto \begin{cases} x &=& -\xi - \theta_1 + \rho_1, \\ w_1 &=& \rho_1 w_{11}, \\ q &=& r_1, \\ \epsilon &=& r_1 \rho_1 \epsilon_{11}, \end{cases} \tag{6.11}$$

$$\Psi_{112}^{12} : (r_1, \theta_1, \rho_2, x_2, \epsilon_{12}) \mapsto \begin{cases} x &=& -\xi - \theta_1 + \rho_2 x_2, \\ w_1 &=& \rho_2, \\ q &=& r_1, \\ \epsilon &=& r_1 \rho_2 \epsilon_{12}. \end{cases} \tag{6.12}$$

The coordinate changes between these two charts are given by

$$\begin{aligned} \rho_1 &= \rho_2 x_2, \\ w_{11} &= x_2^{-1}, \\ \epsilon_{11} &= \epsilon_{12} x_2^{-1}. \end{aligned} \tag{6.13}$$

Remark 6.1. Notice that there exists a smooth change of coordinates between the coor-
dinates $(r_1, \theta_1, \rho_1, w_{11}, \epsilon_{11})$ in $(\bar{z} = 1, \bar{q} = 1, \bar{x} = 1)_{111}$ and the coordinates $(x, y, w, r_1, \epsilon_1)$ in
$(\bar{\epsilon} = 1)_1$ (3.22) in ϕ_3 given by

$$\begin{aligned} \theta_1 &= y^{-1}, \\ \rho_1 &= y^{-1} + y^{-1}x + \xi, \\ w_{11} &= \rho_1^{-1} w, \\ \epsilon_{11} &= \rho_1^{-1} \epsilon_1. \end{aligned} \tag{6.14}$$

(It is easy to see that the r_1's are same as those in (3.22).) This is important when transforming
the analysis in the exit of ϕ_3 in section 4.7 to the entrance in chart ϕ_1, see section 7.1.

For Ψ_1^{123}, we will only consider the chart $(\bar{z} = 1, \bar{q} = 1, \bar{w}_1 = 1, \bar{\theta}_1 = 1)_{1121}$ obtained by set-
ting $\bar{\theta}_1 = 1$ in (6.9):

$$\Psi_{1121}^{123} : (r_1, \rho_2, \varrho_1, x_{21}, \epsilon_{121}) \mapsto \begin{cases} x &=& -\xi - \varrho_1 + \rho_2 \varrho_1 x_{21}, \\ \theta_1 &=& \varrho_1, \\ w_1 &=& \varrho_1 \rho_2, \\ q &=& r_1, \\ \epsilon &=& r_1 \rho_2 \varrho_1 \epsilon_{121}, \end{cases} \tag{6.15}$$

such that

Table 3. Details about the charts used to describe the blowups in ϕ_1. The first row divide the table into three parts, corresponding to the three directional charts associated with the initial 'blowup' (6.3). The remaining rows have the same meaning as in table 1. In particular, the last two rows provide the equation numbers for the equations describing the coordinate changes between the charts in the corresponding columns.

$(\bar{z}=1)_1$			$(\bar{w}=1)_2$	$(\bar{z}=-1)_3$
$(\cdot,\bar{q}=1,\bar{x}=1)_{111}$	$(\cdot,\bar{q}=1,\bar{x}=1)_{112}$	$(\cdot,\bar{q}=1,\bar{w}_1=1,\bar{\theta}_1=1)_{1121}$	$(\cdot,\bar{\theta}_2=1)_{21}$	$(\cdot,\bar{\theta}_3=1,\bar{w}_3=1)_{311}$
$(r_1,\theta_1,\rho_1,w_{11},\epsilon_{11})$	$(r_1,\theta_1,\rho_2,x_2,\epsilon_{12})$	$(r_1,\rho_2,\varrho_1,x_{21},\epsilon_{121})$	$(z_2,\sigma_1,x_1,\epsilon_1)$	$(\pi_1,\mu_1,x_{11},\epsilon_{11})$
Ψ_{111}^{12} (6.11)	Ψ_{112}^{12} (6.12)	Ψ_{1121}^{123} (6.15)	Ψ_{21}^{1} (6.18)	Ψ_{311}^{12} (6.22)
(7.1), section 7.1	(7.4), section 7.2	(7.7), section 4	(7.10), section 7.4	(7.13), section 7.5
(6.13)				(6.23)
	(6.16)			

$$
\begin{aligned}
\theta_1 &= \varrho_1, \\
x_2 &= \varrho_1 x_{21}, \\
\epsilon_{12} &= \varrho_1 \epsilon_{121}.
\end{aligned}
\qquad (6.16)
$$

See table 3 for a summary.

6.2. Blowup analysis in chart $(\bar{w}=1)_2$

The analysis in this chart is more standard because here $\mathrm{e}^{-zw^{-1}}=\mathrm{e}^{-z_2}$ is regular. We have

$$
\begin{aligned}
\dot{x} &= -\epsilon\theta_2\left(\theta_2 x F(z_2) + (x_1 + (1+\alpha)\theta_2 z_2)\right), \\
\dot{\theta}_2 &= -\epsilon\theta_2^3 F(z_2), \\
\dot{z}_2 &= -\mathrm{e}^{-2z_2}\left(1 + \frac{x+\theta_2 z_2}{\xi}\right), \\
\dot{\epsilon} &= 0,
\end{aligned}
\qquad (6.17)
$$

after multiplication of the right hand side by θ_2. Within $\theta_2 = \epsilon = 0$, we find

$$
\begin{aligned}
\dot{x} &= 0, \\
\dot{z}_2 &= -\mathrm{e}^{-2z_2}\left(1 + \frac{x}{\xi}\right),
\end{aligned}
$$

so that $\dot{z}_2 < 0$ for $x > \xi$ and $\dot{z}_2 > 0$ for $x < \xi$. Hence $x = -\xi$, $\theta_2 = \epsilon = 0$, $z_2 \in \mathbb{R}$ is a line of degenerate equilibria, which we—for obvious reasons—also call C_∞. Since it is fully nonhyperbolic we will blowup this set through the following blowup transformation $\Psi_2^1 : P_2^1 \to P_2$, where $P_2 = \{(x,\theta_2,z_2,\epsilon) \in \mathbb{R} \times [0,\infty) \times \mathbb{R} \times [0,\infty)\}$, $P_2^1 = \{(z_2,\sigma,(\bar{x},\bar{\theta}_2,\bar{\epsilon})) \in \mathbb{R} \times [0,\infty) \times S^2\}$, which fixes z_2 and takes

$$
(z_2,\sigma,(\bar{x},\bar{\theta}_2,\bar{\epsilon})) \mapsto
\begin{cases}
x &= -\xi - \sigma\bar{\theta}_2 z_2 + \sigma\bar{x}, \\
\theta_2 &= \sigma\bar{\theta}_2, \\
\epsilon &= \sigma\bar{\epsilon},
\end{cases}
\quad \sigma \geqslant 0, (\bar{x},\bar{\theta}_2,\bar{\epsilon}) \in S^2.
$$

In this way, we gain hyperbolicity, allowing us to extend slow manifold into this chart, see the illustration in figure 23.
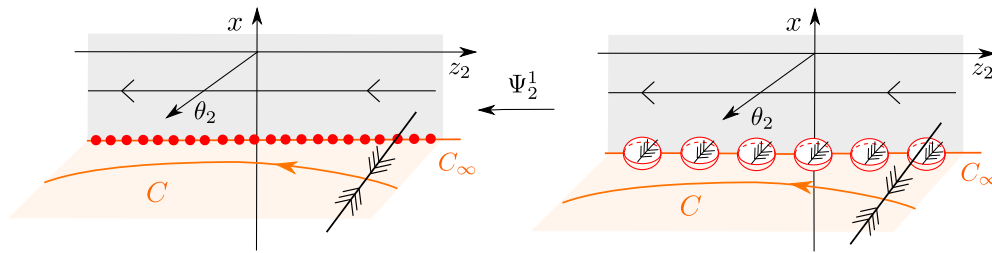
Figure 23. Blowup in chart $\bar{w} = 1$. Our view is from $\theta_2 > 0$, the θ_2-axis 'coming out' of the diagram. We blowup a line corresponding to C_∞ to a cylinder of spheres involving ϵ. This enable us to extend the hyperbolicity of C (in orange) up an improved version of C_∞. This is indicated by tripple-headed arrows. The shaded gray area is $\theta_2 = 0$, $x > -\xi$ where $\dot{z}_2 < 0$, $\dot{x} = 0$ as indicated by the single orbit (in black).

6.2.1. Local charts and the corresponding directional blowup transformations. We only need to consider the single chart $(\bar{w} = 1, \bar{\theta}_2 = 1)_{21}$ obtained by setting $\bar{\theta}_2 = 1$. This gives the following local form of Ψ_2^1

$$\Psi_{21}^1 : (z_2, \sigma_1, x_1, \epsilon_1) \mapsto \begin{cases} x & = & -\xi - \sigma_1 z_2 + \sigma_1 x_1 \\ \theta_2 & = & \sigma_1, \\ \epsilon & = & \sigma_1 \epsilon_1. \end{cases} \tag{6.18}$$

Notice, that we can change coordinates between the chart $(\bar{z} = 1, \bar{q} = 1, \bar{x} = 1, \bar{\theta}_1 = 1)_{1121}$ and $(\bar{w} = 1, \bar{\theta}_2 = 1)_{21}$, using (6.15), as follows

$$\begin{aligned} \epsilon_1 &= \exp(-2\rho_2^{-1})\epsilon_{121}, \\ \sigma_1 &= \varrho_1 \rho_2, \\ z_2 &= \rho_2^{-1}, \\ x_1 &= x_{21}, \end{aligned} \tag{6.19}$$

for $\rho_2 > 0$. See table 3 for a summary.

6.3. Blowup analysis in chart $(\bar{z} = -1)_3$

In this chart we have

$$\begin{aligned} \dot{x} &= \epsilon \theta_3 e^{-w_3^{-1}} \left(\theta_3 w_3 x F(w_3^{-1}) - e^{-w_3^{-1}}(x - (1 + \alpha)\theta_3) \right), \\ \dot{\theta}_3 &= \theta_3 \left(\epsilon \theta_3^2 e^{-w_3^{-1}} F(w_1^{-1}) + 1 + \frac{x - \theta_3}{\xi} \right), \\ \dot{w}_3 &= -w_3 \left(1 + \frac{x - \theta_3}{\xi} \right), \\ \dot{\epsilon} &= 0, \end{aligned} \tag{6.20}$$

after division of the right hand side by $\theta_3^{-1} e^{2w_3^{-1}}$ to ensure that $w_3 = 0$ is well-defined. For the analysis in this chart, we will have to keep track of exponentially small remainders in center manifold calculations. Standard power series expansion will therefore have to be adapted. For this purpose it is useful to again introduce a flat function $q(w_3)$ as follows

$$q_3 = w_3^{-1} e^{-w_3^{-1}}. \tag{6.21}$$

It is also possible to use the seemingly more natural choice $q_3 = e^{-w_3^{-1}}$ but the calculations are slightly simpler with (6.21). Implicit differentiation of (6.21) gives the following system after multiplication by w_3 on the right hand side to ensure that $w_3 = 0$ is well-defined:

$$\dot{x} = \epsilon \theta_3^2 w_3^2 q \left(\theta_3 w_3 x (1 - w_3 q) - w_3 q (x - (1 + \alpha)\theta_3) \right),$$

$$\dot{\theta}_3 = \theta_3 w_3 \left(\epsilon \theta_3^2 w_3 q (1 - w_3 q) + 1 + \frac{x - \theta_3}{\xi} \right),$$

$$\dot{w}_3 = -w_3^3 \left(1 + \frac{x - \theta_3}{\xi} \right),$$

$$\dot{q} = -q \left(1 + \frac{x - \theta_3}{\xi} \right) (1 - w_3),$$

$$\dot{\epsilon} = 0.$$

Here we have dropped the subscript on q and used (6.21) to write $e^{-w_3^{-1}} = w_3 q$. Let $P_3 = \{(x, \theta_3, w_3, q, \epsilon) \in \mathbb{R} \times [0, \infty)^4\}$, $P_3^1 = \{(\pi, w_3, q, (\bar{x}, \bar{\theta}_3, \bar{\epsilon})) \in [0, \infty)^2 \times S^2\}$. Fix any w_3, q. Then the linearization about any equilibrium point with $x = -\xi$, $\theta_3 = \epsilon = 0$ has only zero eigenvalues. We therefore perform a blowup transformation

$$\Psi_3^1 : P_3^1 \to P_3,$$

of $x = -\xi$, $\theta_3 = 0$, $\epsilon = 0$, defined by fixing w_3 and q and taking

$$(\pi, (\bar{x}, \bar{\theta}, \bar{\epsilon})) \mapsto \begin{cases} x &=& -\xi + \pi\bar{\theta} + \pi\bar{x}, \\ \theta_3 &=& \pi\bar{\theta}, \\ \epsilon &=& \pi\bar{\epsilon}. \end{cases}$$

In this way, we gain hyperbolicity of C_∞, but $w_3 = 0$ is still degenerate. Subsequently, we therefore blowup $\bar{\theta}_3^{-1}\bar{x} = 0$, $w_3 = 0$, $\bar{\theta}_3^{-1}\bar{\epsilon} = 0$ through the blowup transformation

$$\Psi_3^2 : P_3^2 \to P_3^1,$$

where $P_3^2 = \{(\pi, \mu, q, (\bar{\bar{x}}, \bar{w}_3, \bar{\bar{\epsilon}})) \in [0, \infty)^2 \times S^2\}$, which fixes π and q and takes

$$(\mu, (\bar{\bar{x}}, \bar{w}, \bar{\bar{\epsilon}})) \mapsto \begin{cases} \bar{\theta}_3^{-1}\bar{x} &=& \mu\bar{\bar{x}}, \\ w_3 &=& \mu\bar{w}_3, \quad \mu \geqslant 0, (\bar{x}, \bar{\theta}, \bar{\epsilon}) \in S^2. \\ \bar{\theta}_3^{-1}\bar{\epsilon} &=& \mu\bar{\bar{\epsilon}}, \end{cases}$$

We illustrate the blowup in figure 24. Let $\Psi_3^{12} = \Psi_3^1 \circ \Psi_3^2$.

6.3.1. Local charts and the corresponding directional blowup transformations. To describe the blowup Ψ_3^1 we will only consider the following chart $(\bar{z} = -1, \bar{\theta}_3 = 1)_{31}$ obtained by setting $\bar{\theta} = 1$:

$$\Psi_{31}^1 : (\pi_1, x_1, \epsilon_1) \mapsto \begin{cases} x &=& -\xi + \pi_1 + \pi_1 x_1, \\ \theta_3 &=& \pi_1, \\ \epsilon &=& \pi_1 \epsilon_1, \end{cases}$$

using the local coordinates $\pi_1 \geqslant 0, x_1 \in \mathbb{R}, \epsilon_1 \geqslant 0$.

For Ψ_3^{12} we use the single chart $(\bar{z} = -1, \bar{\theta}_3 = 1, \bar{w}_3 = 1)_{311}$ obtained by setting $\bar{w}_3 = 1$:
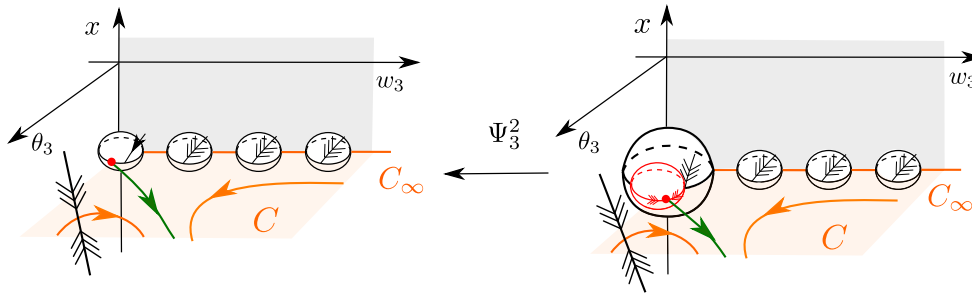
Figure 24. Blowup in chart $\bar{z} = -1$. Our view is from $\theta_3 > 0$, the θ_3-axis 'coming out' of the page. The gray shaded region is $\theta_3 = 0$ whereas the orange hyperplane is C. In diagram, we blowup a degenerate point on the sphere at $\theta_3 = w_3 = 0$ to another sphere. This provides improved hyperbolicity properties of C_∞. In fact, the reduced flow on this extended critical manifold, produces the set $W^{cu}(Q^6)$ (in green) as a unique center manifold.

$$\Psi^{12}_{311} : (\pi_1, \mu_1, x_{11}, \epsilon_{11}) \mapsto \begin{cases} x & = & -\mu + \pi_1 + \pi_1\mu_1 x_{11}, \\ \theta_3 & = & \pi_1, \\ w_3 & = & \mu_1, \\ \epsilon & = & \pi_1\mu_1\epsilon_{11} \end{cases} \tag{6.22}$$

using the local coordinates $\pi_1 \geqslant 0, \mu_1 \geqslant 0, x_{11} \in \mathbb{R}, \epsilon_{11} \geqslant 0$. Notice that we can write the right hand side of (6.22) as

$$x = -\xi - z + wx_{11},$$
$$\epsilon = w\epsilon_{11},$$

after eliminating π_1 and μ_1 and using that $\theta_3 = -z$. Notice also that we can change coordinates between $(\bar{w} = 1, \bar{\theta}_2 = 1)_{21}$ and $(\bar{z} = -1, \bar{\theta}_3 = 1, \bar{w}_3 = 1)_{311}$ as follows

$$\begin{aligned} \pi_1 &= -\sigma_1 z_2, \\ \mu_1 &= -1/z_2, \\ x_{11} &= x_1, \\ \epsilon_{11} &= \epsilon_1, \end{aligned} \tag{6.23}$$

for $z_2 < 0$. We summarize the results on the charts in table 3.

6.4. A summary of the findings in chart ϕ_1

The full details of the analysis of the blowup systems in chart ϕ_1 is available in section 7. The findings are combined into a result, lemma 8.1, in section 8 below on the transition map Π^{70}. Here we will first try to summarize the findings. For simplicity, we restrict to the case where

$$\alpha < 1. \tag{6.24}$$

$\alpha > 1$ is easier, while $\alpha = 1$ is a special case, see appendix.

The blowup approach provides improved hyperbolicity properties of parts of the singular cycle visible in the chart ϕ_1. We illustrate all the segments, including the new segments only visible upon blowup, in figure 25 using the viewpoints in figures 22–24. In figure 25(a) we illustrate the parts visible in the chart $(\bar{z} = 1)_1$. All orbits are contained within the subset defined by $(\bar{q}, \bar{\epsilon}) = (1, 0)$ and $r = 0$. γ^7 is asymptotic to a partially hyperbolic point $(1, 0, 0)$ on the sphere $(\bar{x}, \bar{w}, \bar{\epsilon}) \in S^2$. From here γ^8 is an unstable manifold which is asymptotic to a
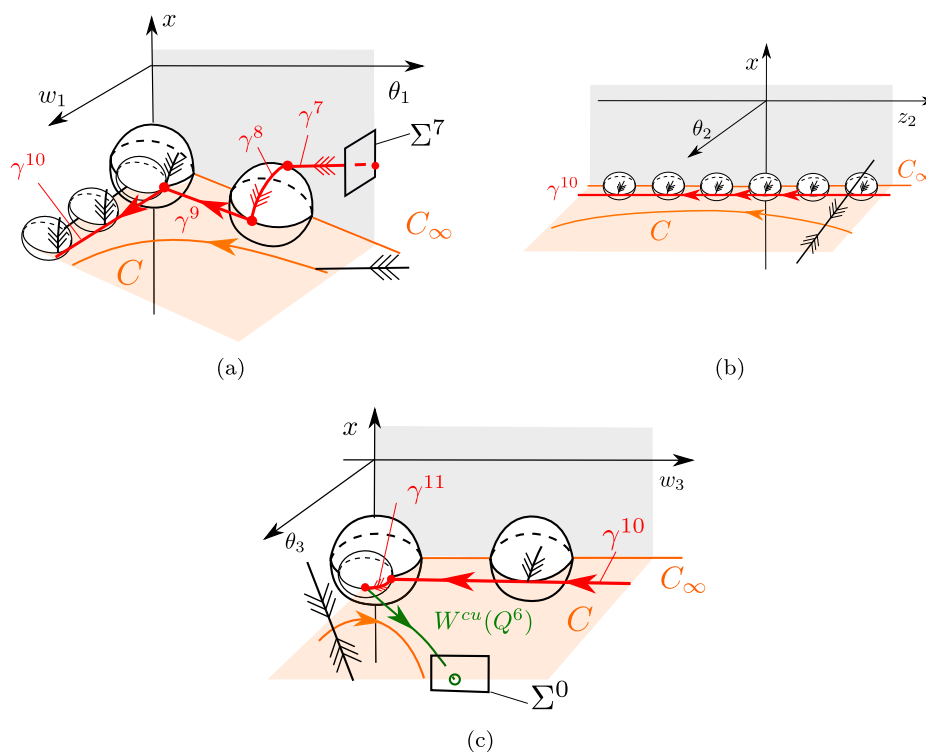
Figure 25. Improved singular orbit segments of the blowup in ϕ_1. In (a)–(c) from the viewpoints of the three direction charts associated with (6.3).

point within $\bar{w} = 1$ on a center manifold. This center manifold provides an extension of the slow manifold in the usual way, see e.g. [26]. By desingularization of the slow flow on this center manifold we obtain an orbit γ^9 which is asymptotic to a partially hyperbolic equilibrium on $\theta_1 = 0$. From here γ^{10} is an unstable manifold that we follow forward into $(\bar{w} = 1)_2$, see figure 25(b), by following the slow flow on the center manifold. This orbit eventually brings us into $(\bar{z} = -1)_3$ where we finally obtain a heteroclinic γ^{11} connecting the end of γ^{10} with $W^{cu}(Q^6)$, obtained as a center submanifold of the reduced problem on the larger center manifold (that provided an extension of the slow manifold). In fact, γ^{11} is only visible upon further use of a blowup involving exponentially small terms. The illustration in figure 25(c) is therefore (extra) caricatured. We combine the information in each of the charts into a single figure in figure 26.

7. Blowup dynamics in chart ϕ_1

In this section, we describe the dynamics in chart ϕ_1 using the blowup and the charts presented in section 6. We follow the notation in remark 4.1.

7.1. Dynamics in $(\bar{z} = 1, \bar{q} = 1, \bar{x} = 1)_{111}$

In this chart we obtain, using (6.11), the following equations
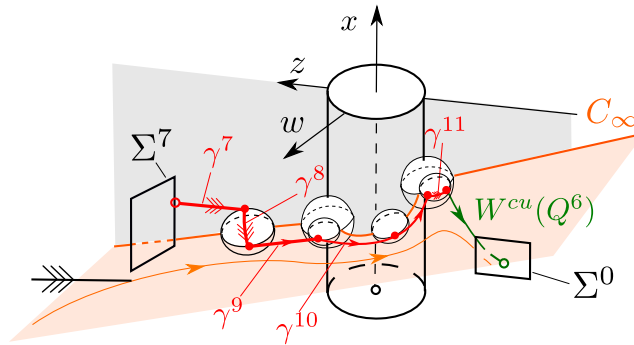
Figure 26. Improved singular orbit segments of the blowup in ϕ_1, combining figures 25(a)–(c) into a global picture.

$$\dot{\theta}_1 = \rho_1 w_{11} \theta_1 \left(-1/\xi - \epsilon_{11} \theta_1^2 \rho_1 w_{11} F(\rho_1^{-1} w_{11}^{-1}) \right),$$
$$\dot{\rho}_1 = \rho_1 w_{11} G_{111}(\theta_1, \epsilon_{11}, \rho_1, w_{11}),$$
$$\dot{w}_{11} = -w_{11}^2 G_{111}(\theta_1, \epsilon_{11}, \rho_1, w_{11}) + \rho_1 w_{11}^2/\xi, \tag{7.1}$$
$$\dot{\epsilon}_{11} = \epsilon_{11} \left(-2/\xi - G_{111}(\theta_1, \epsilon_{11}, \rho_1, w_{11}) w_{11} \right),$$

where

$$G_{111}(\theta_1, \rho_1, w_{11}, \epsilon_{11}) = -\theta_1/\xi - \epsilon_{11} \theta_1 \left(-\xi + \rho_1 + \alpha\theta_1 \right) + \epsilon_{11} \rho_1 w_{11} F(\rho_1^{-1} w_{11}^{-1})(\xi - \rho_1).$$

In these coordinates, using (6.14), γ_1^7 becomes

$$\gamma_{111}^7 = \left\{ (\theta_1, \rho_1, w_{11}, \epsilon_{11}) \,|\, \rho_1 = \frac{\xi(\alpha - 1)}{2\alpha} + \theta_1, \, \theta_1 \in \left(\frac{\xi(1 - \alpha)}{2\alpha}, \frac{\xi}{2\alpha} \right), \, w_{11} = \epsilon_{11} = 0 \right\},$$

for $\alpha < 1$, recall the assumption (6.24). It is asymptotic to the point q_{11}^8 with coordinates

$$(\theta_1, \rho_1, w_{11}, \epsilon_{11}) = \left(\frac{\xi(1 - \alpha)}{2\alpha}, 0, 0, 0 \right). \tag{7.2}$$

Now, we notice that $\{\epsilon_{11} = 0, w_{11} \in [0, \beta_5]\}$, with $\beta_5 > 0$ sufficiently small, is an attracting center manifold. The (center-)stable manifold has a smooth foliation by stable fibers as leaves of the foliation. We can straighten out these fibers through a transformation which fixes ϵ_{11} and takes $(\theta_1, \rho_1, w_{11}, \epsilon_{11}) \mapsto (\tilde{\theta}_1, \tilde{\rho}_1, \tilde{w}_{11}) = (\theta_1, \rho_1, w_{11}) + \mathcal{O}(w_{11}\epsilon_{11})$. This gives

$$\dot{\theta}_1 = -\rho_1 w_{11} \theta_1/\xi,$$
$$\dot{\rho}_1 = -\rho_1 w_{11} \theta_1/\xi, \tag{7.3}$$
$$\dot{w}_{11} = w_{11}^2 \left(\theta_1 + \rho_1 \right)/\xi,$$

upon dropping the tildes. We see that w_{11} is a common factor and therefore divide this out on the right hand side. This gives

$$\dot{\rho}_1 = -\rho_1 \theta_1/\xi,$$
$$\dot{w}_{11} = w_{11} \left(\theta_1 + \rho_1 \right)/\xi,$$
$$\dot{\theta}_1 = -\rho_1 \theta_1/\xi,$$

with respect to the new time. Now, the line $\mathcal{H}_{111}$, defined by $\rho_1 = 0$, $w_{11} = 0$, $\theta_1 > 0$ is a line of equilibria. It is normally hyperbolic, being of saddle type. γ_{111}^7 is contained in the stable manifold of $\mathcal{H}_{111}$ within $w_{11} = 0$, being asymptotic to the base point q_{111}^8 with $\rho_1 = 0$, $\theta_1 = \frac{\xi(1-\alpha)}{2\alpha}$, recall (7.2). From this point, there is also an individual unstable manifold within $W^u(\mathcal{H}_{111})$:

$$\gamma_{111}^8 = \left\{ (\theta_1, \rho_1, w_{11}, \epsilon_{11}) \,\middle|\, \rho_1 = \epsilon_{11} = 0, \; \theta_1 = \frac{\xi(1-\alpha)}{2\alpha}, \; w_{11} \geqslant 0 \right\},$$

of the base point q_{111}^8. In the following, we work in a neighborhood of the point q_{111}^8. Let

$$\Sigma_{111}^{8,\text{in}} = \left\{ (\theta_1, \rho_1, w_{11}, \epsilon_{11}) \,\middle|\, \rho_1 = \delta, \; \theta_1 - \frac{\xi(1-\alpha)}{2\alpha} \in [-\beta_1, \beta_1], w_{11} \in [0, \beta_3], \epsilon_{11} \in [0, \beta_4] \right\},$$

$$\Sigma_{111}^{8,\text{out}} = \left\{ (\theta_1, \rho_1, w_{11}, \epsilon_{11}) \,\middle|\, w_{11} = \nu, \; \rho_1 \in [0, \beta_5], \; \theta_1 - \frac{\xi(1-\alpha)}{2\alpha} \in [-\beta_6, \beta_6], \epsilon_{11} \in [0, \beta_4] \right\},$$

transverse to the flow and $\Pi_{111}^8 : \Sigma_{111}^{8,\text{in}} \to \Sigma_{111}^{8,\text{out}}$ the associated mapping obtained by the first intersection of the forward flow. Then we have

Lemma 7.1. Π_{111}^8 *is well-defined for appropriately small δ, ν and $\beta_i > 0$, $i = 1, 5$. In particular,*

$$\Pi_{111}^8(\theta_1, \delta, w_{11}, \epsilon_{11}) = (\theta_{1+}(\theta_1, w_{11}, \epsilon_{11}), \rho_{1+}(\theta_1, w_{11}, \epsilon_{11}), \nu, \epsilon_{11+}(\theta_1, w_{11}, \epsilon_{11})),$$

where ρ_{1+}, ϵ_{11+} and θ_{1+} are C^l and satisfy

$$\theta_{1+}(\theta_1, w_{11}, \epsilon_{11}) = \theta_1 - \delta + \mathcal{O}(w_{11}),$$
$$\rho_{1+}(\theta_1, w_{11}, \epsilon_{11}) = \mathcal{O}(w_{11}),$$
$$\epsilon_{11+}(\theta_1, w_{11}, \epsilon_{11}) = \mathcal{O}(\epsilon_{11} e^{-c w_{11}^{-1}}),$$

for some $c > 0$ sufficiently small.

Proof. We integrate (7.3) from $\rho_1(0) = \delta$ to $w_{11}(T) = \nu$. This gives

$$\theta_1(T(\theta_1(0), w_{11}(0))) = \theta_1(0) - T(\delta_1(0), w_{11}(0)),$$
$$\rho_1(T(\theta_1(0), w_{11}(0))) = \delta - T(\theta_1(0), w_{11}(0)),$$

where

$$T(\theta_1, w_{11}) = \frac{1}{2}(\delta + \theta_1) - \frac{1}{2}(\theta_1 - \delta)\sqrt{1 + \frac{4\delta\theta_1 w_{11}}{\nu(\theta_1^2 - \delta^2)}}.$$

Notice that $T(\theta_1, 0) = \delta$. Returning to the original variables gives the desired result upon using the exponential contraction towards $\epsilon_{11} = 0$. ▢

It follows that the image of $\gamma_{111}^7 \cap \Sigma_{111}^{8,\text{in}}$ under Π_{111}^8 is $\gamma_{111}^8 \cap \Sigma_{111}^{8,\text{out}}$. See figure 27.

7.2. Dynamics in $(\bar{z} = 1, \bar{q} = 1, \bar{w}_1 = 1)_{112}$

In this chart, we obtain the following:
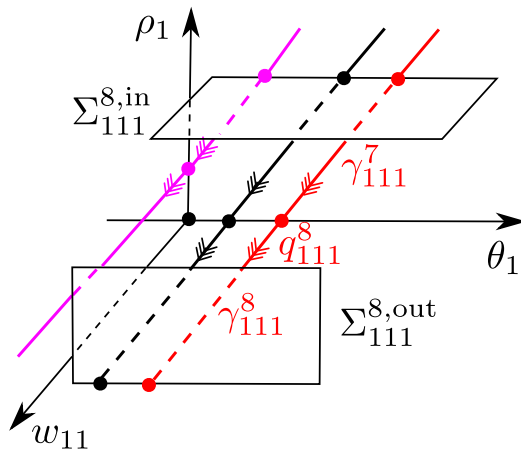
Figure 27. Illustration of the result in lemma 7.1 within $\epsilon_{11} = 0$. Our view is from $w_{11} > 0$, the w_{11}-axis 'coming out' of the page. γ^7_{111} is within the subset $w_{11} = 0$, approaching the point q^8_{111} on the line of equilibria defined by $\rho_1 = w_{11} = 0$. In contrast, γ^8_{111} belongs to $\rho_1 = 0$. The purple point is a partially hyperbolic point on the ρ_1-axis. The purple orbits shown in the figure, which are relevant for the case $\alpha > 1$, see appendix, are the stable and unstable manifolds of this point contained within $w_{11} = 0$ and $\theta_1 = 0$, respectively.

$$
\begin{aligned}
\dot{\theta}_1 &= \rho_2 \theta_1 \left(\rho_2 \theta_1^2 \epsilon_{12} F(\rho_2^{-1}) + x_2/\xi \right), \\
\dot{\rho}_2 &= \rho_2^2 \frac{x_2}{\xi}, \\
\dot{x}_2 &= \rho_2 \epsilon_{12} \theta_1^2 F(\rho_2^{-1})(\xi - \rho_2 x_2) - \theta_1 \epsilon_{12} \left(-\xi + \rho_2 x_2 + \alpha \theta_1 \right) - x_2 \left(\theta_1 + \rho_2 x_2 \right)/\xi, \\
\dot{\epsilon}_{12} &= -\epsilon_{12} x_2/\xi \left(2 + \rho_2 \right).
\end{aligned}
\tag{7.4}
$$

In these coordinates, γ^8_{111} takes the following form:

$$
\gamma^8_{112} = \left\{ (\theta_1, \rho_2, x_2, \epsilon_{12}) \,|\, x_2 > 0, \, \rho_2 = 0, \, \theta_1 = \frac{\xi(1-\alpha)}{2\alpha}, \, \epsilon_{12} = 0 \right\},
$$

using the coordinate change $x_2 = w_{11}^{-1}$ between the charts, recall (6.13). The dynamics on γ^8_{112} is asymptotic to the point q^9_{112} defined by

$$
(\theta_1, \rho_2, x_2, \epsilon_{12}) = \left(\frac{\xi(1-\alpha)}{2\alpha}, 0, 0, 0 \right).
$$

This point becomes Q^5 upon blowing down to (x, z, w), see (1.23). The set $\mathcal{C}_{112}$, defined by $\rho_2 = \epsilon_2 = x_2 = 0$, $\theta_1 \in [0, \infty)$, is a line of equilibria for (7.4). Upon blowing down, using (6.12) and (6.4), it becomes the subset of C_∞, see (6.2), with $z \geqslant 0$. But within this blowup chart, the linearization about any point on $\mathcal{C}_{112}$ now has one single non-zero eigenvalue $-\theta_1/\xi$ for $\theta_1 > 0$. We therefore think of $\mathcal{C}_{112}$ as an improved version of C_∞. This produces an extension of the slow manifold as an ϵ-section of a center manifold by standard center manifold theory in the usual way (recall remark 4.9):

Proposition 7.2. *Fix a closed interval $I \subset (0, \infty)$. Then there exists a $\delta > 0$ and a neighborhood $\mathcal{U}_{112}$ of $(\rho_2, \epsilon_{12}) = 0$ in $\mathbb{R}^2$ such that the following holds. There exists a locally invariant center manifold $\mathcal{M}_{112}$ of $\mathcal{C}_{112}$ as a graph*

$$x_2 = \epsilon_{12}\xi^2 \left(1 - \xi^{-1}\alpha\theta_1 + \epsilon_{12}h_{112}(\epsilon_{12}, \rho_2, \theta_1) \right), \tag{7.5}$$

over $(\theta_1, \rho_2, \epsilon_{12}) \in I \times \mathcal{U}_{112}$. *Here* h_{112} *is a smooth function. Furthermore, there exists a smooth stable foliation with base* $\mathcal{M}_{112}$ *and 1D fibers as leaves of the foliation. Within* $x_2 \in [-\delta, \delta], (\theta_1, \rho_2, \epsilon_{12}) \in I \times \mathcal{U}_{112}$, *the contraction along any of these fibers is at least* e^{-ct} *with* $c(I) > 0$.

The reduced problem on $\mathcal{M}_{112}$ is

$$
\begin{aligned}
\dot{\theta}_1 &= -\rho_2\theta_1 \left(1 + \frac{\rho_2\theta_1^2 F(\rho_2^{-1})}{\xi(1 - \xi^{-1}\alpha\theta_1 + \epsilon_{12}h_{112}(\epsilon_{12}, \rho_2, \theta_1))} \right), \\
\dot{\rho}_2 &= \rho_2^2, \\
\dot{\epsilon}_{12} &= -\epsilon_{12}(2 + \rho_2),
\end{aligned}
\tag{7.6}
$$

after division of the right hand side by x_2/ξ. Notice that by (7.5) this quantity is positive for θ_1 sufficiently small and $\epsilon_{12} > 0$ sufficiently small. For $\epsilon_{12} = 0$, (7.6), after division by ρ_2 on the right hand side, therefore provides a desingularized system on the center manifold, which we shall study in the following. Within $\epsilon_{12} = \rho_2 = 0$, we therefore see that θ_1 is decreasing and hence we put

$$\gamma_{112,\text{loc}}^9 = \left\{ (\theta_1, \rho_2, x_2, \epsilon_{12}) \,|\, \theta_1 \in \left[\nu, \frac{\xi(1-\alpha)}{2\alpha} \right], x_1 = \epsilon_{12} = \rho_2 = 0 \right\},$$

and consider the sections

$$\Sigma_{112}^{9,\text{in}} = \left\{ (\theta_1, \rho_2, x_2, \epsilon_{12}) \,|\, x_2 = \delta, \, \rho_2 \in [0, \beta_1], \, \epsilon_{12} \in [0, \beta_2], \, \theta_1 - \frac{\xi(1-\alpha)}{2\alpha} \in [-\beta_3, \beta_3] \right\},$$

$$\Sigma_{112}^{9,\text{out}} = \left\{ (\theta_1, \rho_2, x_2, \epsilon_{12}) \,|\, \theta_1 = \nu, \, \rho_2 \in [0, \beta_4], \, \epsilon_{12} \in [0, \beta_2], \, x_2 \in [-\beta_5, \beta_5] \right\},$$

and let $\Pi_{112}^9 : \Sigma_{112}^{9,\text{in}} \to \Sigma_{112}^{9,\text{out}}$ be the associated mapping obtained by the first intersection of the forward flow. We then have

Lemma 7.3. *The mapping* Π_{112}^9 *is well-defined for appropriately small* $\delta > 0$, $\nu > 0$ *and* $\beta_i > 0$, $i = 1, \ldots, 5$. *In particular,*

$$\Pi_{112}^9(\theta_1, \rho_2, \nu, \epsilon_{12}) = (\nu, \rho_{2+}(\rho_2, \theta_1, \epsilon_{12}), x_{2+}(\rho_2, \theta_1, \epsilon_{12}), \epsilon_{12+}(\rho_2, \theta_1, \epsilon_{12})),$$

with each ρ_{2+}, x_{2+}, ϵ_{12+} *being smooth and satisfying*

$$
\begin{aligned}
\rho_{2+}(\rho_2, \theta_1, \epsilon_{12}) &= \mathcal{O}(\rho_2), \\
x_{2+}(\rho_2, \theta_1, \epsilon_{12}) &= \mathcal{O}(\epsilon_{12}e^{-c\rho_2^{-1}}), \\
\epsilon_{1+}(\rho_2, \theta_1, \epsilon_{12}) &= \mathcal{O}(\epsilon_{12}e^{-c\rho_2^{-1}}),
\end{aligned}
$$

for $c > 0$ *sufficiently small.*

Proof. We consider the reduced problem (7.6). Here the set defined by $\epsilon_2 = 0, \rho_2 \in [0, \beta_1]$ is an attracting center manifold with smooth foliation by stable fibers. We straighten out the fibers by a transformation fixing ρ_2, ϵ_{12} and taking $(\theta_1, \rho_2, \epsilon_{12}) \mapsto \tilde{\theta}_1 = \theta_1 + \mathcal{O}(\rho_1^2\theta_1^3\epsilon_{12})$ and obtain the following

$$\dot{\rho}_2 = \rho_2,$$

$$\dot{\theta}_1 = -\theta_1 \left(1 + \frac{\rho_2 \theta_1^2 F(\rho_2^{-1})}{\xi(1 - \xi^{-1}\alpha\theta_1)} \right),$$

after dropping the tildes. On this time scale, the mapping from $\Sigma_{112}^{9,\text{in}}$ to $\Sigma_{112}^{9,\text{out}}$ takes $\mathcal{O}(1)$ time. We now work our way backwards and obtain the desired result. $\square$

See illustration in figure 28.

7.3. Dynamics in $(\overline{z} = 1, \overline{q} = 1, \overline{w}_1 = 1, \overline{\theta}_1 = 1)_{1121}$

In this chart we obtain

$$\begin{aligned}
\dot{\rho}_2 &= \rho_2^2 \frac{x_{21}}{\xi}, \\
\dot{\varrho}_1 &= -\varrho_1^2 \left(\rho_2 x_{21}/\xi + \varrho_1^2 \rho_2^2 \epsilon_{121} F(\rho_2^{-1}) \right), \\
\dot{x}_{21} &= \rho_2 \varrho_1 \epsilon_{121} F(\rho_2^{-1})\xi - \epsilon_{121}\left(-\xi + \rho_2 \varrho_1 x_{21} + \alpha\theta_1 \right) - x_{21}/\xi, \\
\dot{\epsilon}_{121} &= -\epsilon_{121}\left(2x_{21}/\xi - \varrho_1^2 \rho_2 \epsilon_{12} F(\rho_2^{-1}) \right),
\end{aligned} \tag{7.7}$$

from (6.7) using (6.15). Here the set $\mathcal{C}_{1121}$, defined by $x_{21} = \epsilon_{121} = \rho_2 = 0$, $\varrho_1 \in [0, \delta]$, is a line of equilibria. The linearization about any point in $\mathcal{C}_{1121}$ gives on single non-zero eigenvalue $-1/\xi$ for any $\varrho_1 \geqslant 0$. Also, since it blows down to C_∞, we think of it as an improved version of C_∞. Furthermore, it agrees upon coordinate transformation with $\mathcal{C}_{112}$ from the previous chart. By center manifold theory, we obtain a center manifold—which we shall call $\mathcal{M}_{1121}$ —of partially hyperbolic set $\mathcal{C}_{1121}$. This manifold therefore also provides an extension of the center manifold $\mathcal{M}_{112}$ into this chart as follows.

Proposition 7.4. *Fix $\eta \in (0, 1)$. Then there exists a $\delta > 0$ and a small neighborhood $\mathcal{U}_{1121}$ of $(\varrho_1, \rho_2, \epsilon_{121}) = 0$ in $\mathbb{R}^3$ such that the following holds. There exists a locally invariant center manifold $\mathcal{M}_{1121}$ as a graph*

$$x_{21} = \epsilon_{121}\xi^2 \left(1 - \xi^{-1}\alpha\varrho_1 + \epsilon_{121} h_{21}(\epsilon_{121}, \rho_2, \varrho_1) \right),$$

over $(\varrho_1, \rho_2, \epsilon_{121}) \in \mathcal{U}_{1121}$. Here h_{21} is a smooth function. Furthermore, there exists a smooth stable foliation with base $\mathcal{M}_{1121}$ and 1D fibers as leaves of the foliation. Within $x_{21} \in [-\delta, \delta]$, $(\varrho_1, \rho_2, \epsilon_{121}) \in \mathcal{U}_{1121}$, the contraction along any of these fibers is at least $e^{-\eta/\xi t}$.

The reduced problem on $\mathcal{M}_{1121}$ is

$$\begin{aligned}
\dot{\rho}_2 &= \rho_2^2, \\
\dot{\varrho}_1 &= -\rho_2 \varrho_1 \left(1 + \frac{\rho_2 \varrho_1^2 F(\rho_2^{-1})}{\xi(1 - \xi^{-1}\alpha\varrho_1 + \epsilon_{121}h_{21}(\epsilon_{121}, \rho_2, \varrho_1))} \right), \\
\dot{\epsilon}_{121} &= -\epsilon_{121} \left(2 - \frac{\varrho_1^2 \rho_2 F(\rho_2^{-1})}{\xi(1 - \xi^{-1}\alpha\varrho_1 + \epsilon_{121}h_{21}(\epsilon_{121}, \rho_2, \varrho_1))} \right).
\end{aligned} \tag{7.8}$$

Here $\epsilon_{121} = 0$, $\rho_2 \in [0, \beta_1]$ is a center manifold with smooth foliation by stable fibers. We straighten out these fibers by a transformation fixing ρ_2, ϵ_{121} and taking $(\rho_2, \varrho_1, \epsilon_{121}) \mapsto \tilde{\varrho}_1 = \varrho_1 + \mathcal{O}(\rho_2^2 \varrho_1^3 \epsilon_{121})$ such that
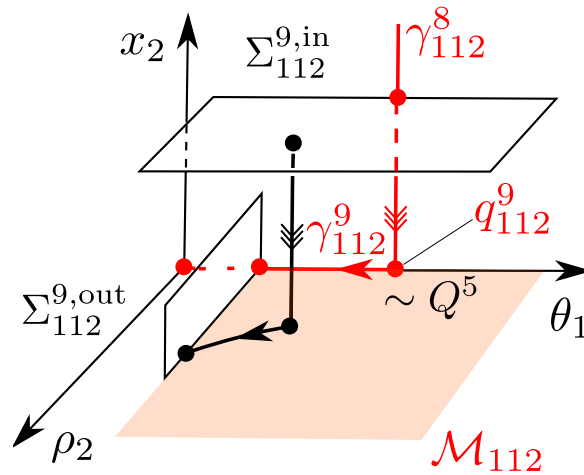
Figure 28. Illustration of the result in lemma 7.3 within $\epsilon_{11} = 0$. Our view is from $\rho_2 > 0$, the ρ_2-axis 'coming out' of the page. The red shaded region is contained within $x_2 = 0$. In particular, γ_{112}^8 is contained within $\rho_2 = 0$, asymptotic to the partially hyperbolic point q_{112}^9 along $\rho_2 = x_2 = 0$. Notice that this point becomes Q^5 in figure 7 upon blowing down (indicated by $\sim$) to the (x, z, w)-space. The segment γ_{112}^9 is an orbit segment of a desingularized flow and is contained within $\rho_2 = x_2 = 0$.

$$\dot{\rho}_2 = \rho_2,$$
$$\dot{\varrho}_1 = -\varrho_1 \left(1 + \frac{\rho_2 \varrho_1^2 F(\rho_2^{-1})}{\xi(1 - \xi^{-1}\alpha\varrho_1)} \right), \tag{7.9}$$

after dropping the tilde, and dividing the right hand side by ρ_2. In these coordinates, $\gamma_{112,\mathrm{loc}}^9$ therefore becomes

$$\gamma_{1121}^9 = \left\{ (\rho_2, \varrho_1, x_{21}, \epsilon_{121}) \, | \, x_{21} = \epsilon_{121} = \rho_2 = 0, \; \varrho_1 \in \left(0, \frac{\xi(1-\alpha)}{2\alpha} \right] \right\},$$

upon using the flow of (7.9) to extend the forward orbit. It is asymptotic to $x_{21} = \epsilon_{121} = \rho_2 = \varrho_1 = 0$ and becomes γ^9 in (1.27) upon blowing down using (6.15). From (7.9), we have an unstable manifold

$$\gamma_{1121,\mathrm{loc}}^{10} = \{ (\rho_2, \varrho_1, x_{21}, \epsilon_{121}) \, | \, x_{21} = \epsilon_{121} = \varrho_1 = 0, \; \rho_2 \in [0, \nu] \},$$

with $\nu > 0$ sufficiently small. We therefore consider the following sections

$$\Sigma_{1121}^{10,\mathrm{in}} = \{ (\rho_2, \varrho_1, x_{21}, \epsilon_{121}) \, | \, \varrho_1 = \delta, \rho_2 \in [0, \beta_1], \; x_{21} \in (\beta_2], \; \epsilon_{121} \in [0, \beta_3] \},$$
$$\Sigma_{1121}^{10,\mathrm{out}} = \{ (\rho_2, \varrho_1, x_{21}, \epsilon_{121}) \, | \, \rho_2 = \nu, \; \varrho_1 \in [0, \beta_4], \rho_2 \in [0, \beta_1], \; x_{21} \in [-\beta_2, \beta_2], \; \epsilon_{121} \in [0, \beta_3] \}$$

transverse to γ_{1121}^9 and γ_{1121}^{10}, respectively. We let Π_{1121}^{10} be the associated mapping obtained by the first intersection of the forward flow.

Lemma 7.5. Π_{1121}^{10} *is well-defined for appropriately small* $\delta > 0$, $\nu > 0$ *and* $\beta_i > 0$, $i = 1, \ldots, 4$. *In particular,*

$$\Pi_{1121}^{10}(\rho_2, x_{21}, \nu, \epsilon_{121}) = (\nu, x_{21+}(\rho_2, x_{21}, \epsilon_{121}), \varrho_{1+}(\rho_2, x_{21}, \epsilon_{121}), \epsilon_{121+}(\rho_2, \theta_1, \epsilon_{12})),$$

with each x_{21+}, ϱ_{1+}, ϵ_{121+} being C^l and satisfying

$$x_{21+}(\rho_2, \theta_1, \epsilon_{12}) = \mathcal{O}(\epsilon_{121}\mathrm{e}^{-c\rho_2^{-1}}),$$
$$\varrho_{1+}(\rho_2, x_{21}, \epsilon_{121}) = \mathcal{O}(\rho_2),$$
$$\epsilon_{1+}(\rho_2, \theta_1, \epsilon_{12}) = \mathcal{O}(\epsilon_{121}\mathrm{e}^{-c\rho_2^{-1}}),$$

for some $c > 0$ sufficiently small.

Proof. Similar to previous results in the manuscript, we perform a C^1-linearization of the (ρ_1, ϱ_1)-subsystem in (7.9). Working backwards we then obtain the result. $\qquad\square$

Notice that the image of $\gamma_{1121}^9 \cap \Sigma_{1121}^{10,\mathrm{in}}$ under Π_{1121}^{10} is $\gamma_{1121,\mathrm{loc}}^{10} \cap \Sigma_{1121}^{10,\mathrm{out}}$, as desired.

7.4. Dynamics in $(\overline{w} = 1, \overline{\theta}_2 = 1)_{21}$

In this chart, we obtain the following equations:

$$\begin{aligned}
\dot{\sigma}_1 &= -\sigma_1^3 \epsilon_1 F(z_2), \\
\dot{z}_2 &= -\mathrm{e}^{-2z_2} x_1/\xi, \\
\dot{x}_1 &= \sigma_1 \epsilon_1 \xi - \epsilon_1 \left(-\xi + \sigma_1 x_1 + \alpha\sigma_1 z_2\right) \\
&\quad - \mathrm{e}^{-2z_2} x_1/\xi + \sigma_1^2 \epsilon_1 x_1 F(z_2), \\
\dot{\epsilon}_1 &= \sigma_1^2 \epsilon_1^2 F(z_2)
\end{aligned} \tag{7.10}$$

from (6.17) using (6.18). Let $I = [-c_1, c_1] \subset \mathbb{R}$ be a fixed, large interval. Then there is a sufficiently small neighborhood $\mathcal{U}_{21}$ of $(0,0)$ in $\mathbb{R}^2$ such that there exists a center manifold $\mathcal{M}_{21}$ (of an improved version of C_∞) as a graph

$$x_1 = \epsilon_1 \mathrm{e}^{2z_2} \xi^2 (1 + \sigma_1 F(z_2) - \xi^{-1}\alpha\sigma_1 z_2 + \epsilon_1 h_{21}(\sigma_1, z_2, \epsilon_1)),$$

over $(z_2, \sigma_1, \epsilon_1) \in I \times \mathcal{U}_{21}$. This is completely analogous to proposition 7.2, see also remark 4.9. The center manifold $\mathcal{M}_{21}$ gives an extension of the slow manifold into this chart. On $\mathcal{M}_{21}$, we obtain the following reduced problem

$$\begin{aligned}
\dot{\sigma}_1 &= -\frac{\sigma_1^3 \mathrm{e}^{-2z_2} F(z_2)}{\xi(1 + \sigma_1 - \xi^{-1}\alpha\sigma_1 z_2 + \epsilon_1 h_{21}(\sigma_1, z_2, \epsilon_1))}, \\
\dot{z}_2 &= -\mathrm{e}^{-2z_2}, \\
\dot{\epsilon}_1 &= \frac{\sigma_1^2 \mathrm{e}^{-2z_2} \epsilon_1 F(z_2)}{\xi(1 + \sigma_1 - \xi^{-1}\alpha\sigma_1 z_2 + \epsilon_1 h_{21}(\sigma_1, z_2, \epsilon_1))},
\end{aligned} \tag{7.11}$$

upon dividing the right hand side by $x_1/\xi > 0$. Clearly, z_2 is decreasing. We then get a mapping from $\{z_2 = \nu^{-1}\}$ to $\{z_2 = -\nu^{-1}\}$ using regular perturbation theory. In particular, we notice that by using (6.19), γ_{1121}^{10} becomes

$$\gamma_{21}^{10} = \{(\sigma_1, z_2, x_1, \epsilon_1) \,|\, \sigma_1 = x_1 = \epsilon_1 = 0, z_2 \in \mathbb{R}\}, \tag{7.12}$$

upon extension by the forward flow of (7.11).

7.5. Dynamics in $(\overline{z} = -1, \overline{\theta} = 1, \overline{w}_3 = 1)_{311}$

In this chart, we obtain the following

$$\begin{aligned}
\dot{x}_{11} &= -x_{11}/\xi + \epsilon_{11}\mu_1^2 q\left(-\xi\pi_1(1-\mu_1 q) - q(-\xi + \pi_1\mu_1 x_{11} - \alpha\pi_1)\right), \\
\dot{\pi}_1 &= \pi_1\mu_1\left(\pi_1^2\epsilon_{11}\mu_1^2 q(1-\mu_1 q) + x_{11}/\xi\right), \\
\dot{\mu}_1 &= -\mu_1^2 x_{11}/\xi, \\
\dot{q} &= -q x_{11}(1-\mu_1)/\xi, \\
\dot{\epsilon}_{11} &= -\pi_1^2\mu_1^3 q\epsilon_{11}^2(1-\mu_1 q).
\end{aligned} \tag{7.13}$$

Recall that the equation

$$q = \mu_1^{-1}\mathrm{e}^{-\mu_1^{-1}}, \tag{7.14}$$

defines an invariant set of (7.13), see (6.21) and (6.22). We will work in the extended space to do calculations but subsequently restrict to the space defined by (7.14) and project to $(x_{11}, \pi_1, \mu_1, \epsilon_{11})$. For simplicity, we will use the same symbols in both spaces.

The orbit γ_{21}^{10} becomes

$$\gamma_{311}^{10} = \left\{ (x_{11}, \pi_1, \mu_1, \mu_1^{-1}\mathrm{e}^{-\mu_1^{-1}}, \epsilon_{11}) \mid \pi_1 = x_{11} = \epsilon_{11} = 0,\ \mu_1 > 0 \right\},$$

in the present chart, using (7.12) and the coordinate change described by (6.23). Now, the point q_{311}^{11}, defined by $x_{11} = 0$, $\pi_1 = \mu_1 = q = \epsilon_{11} = 0$, is an equilibrium of (7.13). The linearization has $-1/\xi$ as a single non-zero eigenvalue. Therefore there exists a small neighborhood $\mathcal{U}_{311}$ of $(\pi_1, \mu_1, q, \epsilon_{11}) = 0$ in $\mathbb{R}^4$ such that there exists a local center manifold $\mathcal{M}_{311}$ of q_{311}^{11} as a graph

$$x_{11} = \xi\epsilon_{11}\mu_1^2 q H_{311}(\pi_1, \mu_1, q, \epsilon_{11}), \tag{7.15}$$

over $(\pi_1, \mu_1, q, \epsilon_{11}) \in \mathcal{U}_{311}$. Here

$$H_{311}(\pi_1, \mu_1, q, \epsilon_{11}) = -\pi_1\xi(1-\mu_1 q) + q(\xi + \alpha\pi_1) + \epsilon_{11}\mu_1^2 q h_{311}(\pi_1, \mu_1, q, \epsilon_{11}), \tag{7.16}$$

with h_{311} smooth. On this center manifold, we obtain the following reduced problem

$$\begin{aligned}
\dot{\mu}_1 &= -\mu_1^2 H_{311}(\pi_1, \mu_1, q, \epsilon_{11}), \\
\dot{q} &= -q H_{311}(\pi_1, \mu_1, q, \epsilon_{11})(1-\mu_1), \\
\dot{\pi}_1 &= \pi_1\mu_1\left(\pi_1^2(1-\mu_1 q) + H_{311}(\pi_1, \mu_1, q, \epsilon_{11})\right), \\
\dot{\epsilon}_{11} &= -\pi_1^2\mu_1\epsilon_{11}(1-\mu_1 q),
\end{aligned} \tag{7.17}$$

after division on the right hand side by $\epsilon_{11}\mu_1^2 q$. For this system, $q_{311}^{11} : \mu_1 = q = \pi_1 = \epsilon_{11} = 0$ is fully nonhyperbolic. In fact, $\mathcal{P}_{311}$ defined by $\pi_1 = q = 0$ is a set of degenerate equilibria (containing q_{311}^{11}). We therefore apply a subsequent blowup transformation of points in $\mathcal{P}_{311}$, setting

$$\pi_1 = q\pi_{11}. \tag{7.18}$$

This gives

$$H_{311}(q\pi_{11}, \mu_1, q, \epsilon_{11}) = q\tilde{H}_{311}(\pi_{11}, \mu_1, q, \epsilon_{11}),$$

with

$$\tilde{H}_{311}(\pi_{11}, \mu_1, q, \epsilon_{11}) = -\pi_{11}\xi(1-\mu_1 q) + \xi + \alpha q\pi_{11} + \epsilon_{11}\mu_1^2 h_{311}(q\pi_{11}, \mu_1, q, \epsilon_{11}).$$

See (7.16). Therefore

$$
\begin{aligned}
\dot{\mu}_1 &= -\mu_1^2 \tilde{H}_{311}(\pi_{11}, \mu_1, q, \epsilon_{111}), \\
\dot{q} &= -q\tilde{H}_{311}(\pi_{11}, \mu_1, q, \epsilon_{111})(1-\mu_1), \\
\dot{\pi}_{11} &= \pi_{11}\left(\tilde{H}_{311}(\pi_{11}, \mu_1, q, \epsilon_{11}) + \pi_1^2 q\mu_1(1-\mu_1 q)\right), \\
\dot{\epsilon}_{11} &= -\pi_{11}^2 \mu_1 q\epsilon_{11}(1-\mu_1 q),
\end{aligned}
\tag{7.19}
$$

after division of the right hand side by q. Now, we have gained hyperbolicity. In particular, $q_{311}^{11} : \pi_{11} = \mu_1 = q = \epsilon_{11} = 0$ (misusing notation slightly) is partially hyperbolic, the linearization having a single non-zero eigenvalue $\xi > 0$ with corresponding unstable eigenspace along the invariant π_{11}-axis. Also, the point q_{311}^{12} on $\mathcal{M}_{311}$, defined by $\mu_1 = q = \epsilon_{11} = 0, \pi_{11} = 1$, is a partially hyperbolic equilibrium and therefore we have the following by standard center manifold theory.

Lemma 7.6.   *There exists a local center manifold* $\mathcal{K}_{311}$ *as a graph*

$$
\pi_{11} = G_{311}(\mu_1, q, \epsilon_{11}),
\tag{7.20}
$$

over $(\mu_1, q, \epsilon_{11}) \in \mathcal{V}_{311}$, *where* $\mathcal{V}_{311}$ *is a small neighborhood of* $(0, 0, 0)$ *in* $\mathbb{R}^3$. *Here*

$$
G_{311}(\mu_1, q, \epsilon_{11}) = 1 + \epsilon_{11}\mu_1^2 h_{311}(0, \mu_1, 0, \epsilon_{11}) + q\left(\frac{\alpha}{\xi} + \frac{\xi+1}{\xi}\mu_1 + \mathcal{O}(\mu_1^2 \epsilon_{11}, \mu_1^2, q)\right),
$$

is smooth. The function h_{311} *is defined by (7.16).*

   The submanifold of $\mathcal{K}_{311}$ *within the invariant subset* $\{\epsilon_{11} = 0, q = \mu_1^{-1}e^{-\mu_1^{-1}}\}$, *recall (7.14), is a unique center manifold* W_{311}^{cu}. *In particular, its image under the coordinate transformation* $(\mu_{11}, \pi_1) \mapsto (y, z)$ *defined by (7.18), (6.22), (6.5) and (1.22) produce* $W^{cu}(Q^6)$ *with the asymptotics in lemma 1.2 for* $y \gg 1$.

See figure 29.
   Notice that the invariant graph (7.20) passes through the set of equilibria given as the graph $\pi_{11} = 1 + \epsilon_{11}\mu_1^2 h_{311}(0, \mu_1, 0, \epsilon_{11})$ over (μ_1, ϵ_{11}) within $q = 0$. On the center manifold (7.20), we have

$$
\tilde{H}_{311}(\pi_{11}, \mu_1, q, \epsilon_{11}) = -q\left(\mu_1 + \mathcal{O}(\mu_1^2 \epsilon_{11}, \mu_1^2, q)\right).
$$

Therefore, upon returning to the variables $(\pi_{11}, \mu_1, \epsilon_{11})$ and the set defined by $q = \mu_1^{-1}e^{-\mu_1^{-1}}$, recall (7.14), we have

$$
\tilde{H}_{311}(\pi_{11}, \mu_1, q(\mu_1), \epsilon_{11}) = -\mu_1 q(\mu_1)\left(1 + \mathcal{O}(\mu_1)\right),
$$

and hence obtain the following reduced problem on the center manifold

$$
\begin{aligned}
\dot{\mu}_1 &= \mu_1^2\left(1 + \mathcal{O}(\mu_1)\right), \\
\dot{\epsilon}_{11} &= -\epsilon_{11}\left(1 + \mathcal{O}(\epsilon_{11}, \mu_1)\right),
\end{aligned}
\tag{7.21}
$$

after division by $\mu_1 q$ on the right hand side.
   Consider the following sections

$$
\Sigma_{311}^{11,\text{in}} = \{(x_{11}, \pi_{11}, \mu_1, \epsilon_{11}) \,|\, \mu_1 = \nu,\, x_{11} \in [-\beta_1, \beta_1],\, \pi_{11} \in [0, \beta_2],\, \epsilon_{11} \in [0, \beta_3]\},
$$
$$
\Sigma_{311}^0 = \{(x_{11}, \pi_{11}, \mu_1, \epsilon_{11}) \,|\, \mu_1 = \delta,\, x_{11} \in [-\beta_1, \beta_1],\, \pi_{11} - 1 \in [-\beta_4, \beta_4],\, \epsilon_{11} \in [0, \beta_3]\},
$$
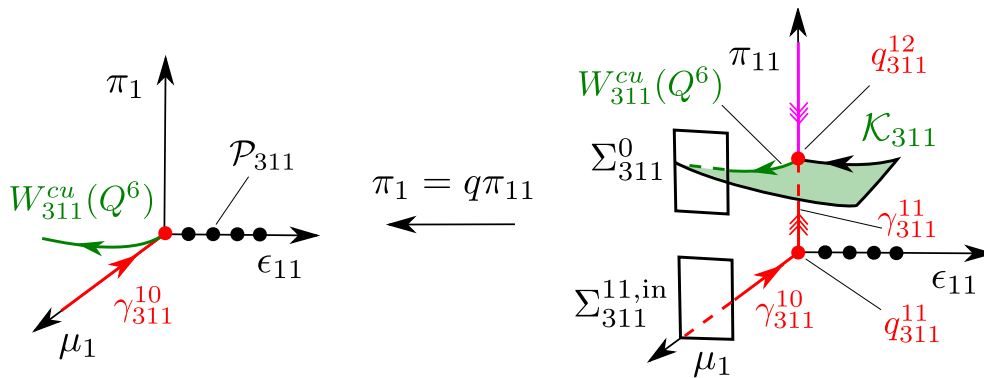
Figure 29. Illustration of the result in lemma 7.6 and the reduced problem on $\mathcal{M}_{311}$. Our view is from $\pi_1 > 0$, the π_1-axis 'coming out' of the page. On the left, we illustrate the singular dynamics in the $(\mu_1, \pi_1, \epsilon_{11})$-space obtained upon center manifold reduction to $\mathcal{M}_{311}$. To obtain this picture we use that $q = q(\mu_1)$, see (7.14). The point $\mu_1 = \epsilon_{11} = \pi_1 = 0$ projects to Q^6. Using the blowup (7.18) of the set of degenerate points $\mathcal{P}_{311}$, we gain hyperbolicity and obtain an attracting center manifold $\mathcal{K}_{311}$ (shown in green) of the partially hyperbolic equilibrium q^{12}_{311}, its intersection with $\epsilon_{11} = 0$ being the unique center manifold $W^{cu}(Q^6)$ in lemma 1.2. The purple orbit is relevant for $\alpha > 1$.

and consider the associated mapping $\Pi^{11}_{311} : \Sigma^0_{311} \to \Sigma^{11,\text{out}}_{311}$. Notice that $\mu_1 = \delta$ in Σ^0_{311} becomes $y = 1/\delta$ in the original variables using (6.22) and (1.22), in agreement with Σ^0, see (2.2). Setting

$$\gamma^{11}_{311} = \{(x_{11}, \pi_{11}, \mu_1, \epsilon_{11}) \,|\, x_{11} = 0, \ \pi_{11} \in [0, 1), \ \mu_1 = 0, \epsilon_{11} = 0\},$$

we can then describe Π^{11}_{311} by following γ^{10}_{311}, γ^{11}_{311} and $W^{cu}_{311}(Q^6)$.

Lemma 7.7. Π^{11}_{311} *is well-defined for appropriately small* $\delta > 0$, $\nu > 0$ *and* $\beta_i > 0$, $i = 1, \ldots, 4$. *In particular;*

$$\Pi^{11}_{311}(x_{11}, \pi_{11}, \nu, \epsilon_{11}) = (x_{11+}(x_{11}, \pi_{11}, \epsilon_{11}), \pi_{11+}(x_{11}, \pi_{11}, \epsilon_{11}), \delta, \epsilon_{11+}(x_{11}, \pi_{11}, \epsilon_{11})),$$

with each coordinate function being C^1. *In particular, these functions satisfy the following equalities*

$$x_{11+}(x_{11}, \pi_{11}, \epsilon_{11}) = \xi \epsilon_{11+}(x_{11}, \pi_{11}, \epsilon_{11}) \delta e^{-\delta^{-1}} H_{311}(\pi_{11+}(x_{11}, \pi_{11}, \epsilon_{11}), \delta, \delta^{-1} e^{-\delta^{-1}}, \epsilon_{11+})$$
$$+ \mathcal{O}(e^{-c\epsilon_{11}^{-1} e^{c/\log \pi_{11}^{-1}}}),$$

$$\pi_{11+}(x_{11}, \pi_{11}, \epsilon_{11}) = G_{311}(\epsilon_{11+}(x_{11}, \pi_{11}, \epsilon_{11}), \delta, \delta^{-1} e^{-\delta^{-1}}) + \mathcal{O}(e^{-c e^{c/\log \pi_{10}^{-1}}}),$$

$$\epsilon_{11+}(x_{11}, \pi_{11}, \epsilon_{11}) = e^{\delta^{-1} - \nu^{-1}} \pi_{11} \epsilon_{11}(1 + \mathcal{O}(\epsilon_{11}, \delta e - \delta^{-1}))$$

for $c > 0$ *sufficiently small.*

Proof. We consider the following system

$$\dot{x}_{11} = -x_{11}/\xi + \epsilon_{11}\mu_1^2 q \left(-\xi\pi_1(1 - \mu_1 q) - q(-\xi + \pi_1\mu_1 x_{11} - \alpha\pi_1)\right),$$
$$\dot{\pi}_{11} = \pi_{11}\left(\pi_{11}^2\epsilon_{11}\mu_1^3 q^2(1 - \mu_1 q) + x_{11}/\xi\right),$$
$$\dot{\mu}_1 = -\mu_1^2 x_{11}/\xi,$$
$$\dot{\epsilon}_{11} = -\pi_{11}^2\mu_1^3 q^3 \epsilon_{11}^2(1 - \mu_1 q),$$

with $q(\mu_1) = \mu_1^{-1}e^{-\mu_1^{-1}}$, obtained by substituting (7.18) into (7.13). First, we straighten out the stable fibers of the center manifold (7.15) through a transformation of the form $(x_{11}, \pi_{11}, \mu_1, \epsilon_{11}) \mapsto (\tilde{\pi}_{11}, \tilde{\mu}_1) = (\pi_{11}(1 + \mathcal{O}(x_{11})), \mu_1(1 + \mathcal{O}(\mu_1 x_{11})))$. Dropping the tildes we then obtain (7.19) after division by $\epsilon_{11}\mu_1^2 q(\mu_1)^2 = \epsilon_{11}e^{-2\mu_1^{-1}}$ on the right hand side. We further divide the right hand side by

$$\tilde{H}_{311}(\pi_{11}, \mu_1, q, \epsilon_{11}) + \pi_1^2 q\mu_1(1 - \mu_1 q) \approx \xi,$$

such that

$$\dot{\mu}_1 = -\mu_1^2 \frac{\tilde{H}_{311}(\pi_{11}, \mu_1, q, \epsilon_{111})}{\tilde{H}_{311}(\pi_{11}, \mu_1, q, \epsilon_{11}) + \pi_1^2 q\mu_1(1 - \mu_1 q)},$$
$$\dot{\pi}_{11} = \pi_{11},$$
$$\dot{\epsilon}_{11} = -\frac{\pi_{11}^2\mu_1 q\epsilon_{11}(1 - \mu_1 q)}{\tilde{H}_{311}(\pi_{11}, \mu_1, q, \epsilon_{11}) + \pi_1^2 q\mu_1(1 - \mu_1 q)}.$$

We then straighten out the unstable fibers of the local invariant manifold $\pi_{11} = 0$ by a transformation fixing π_{11} and taking $(\pi_{11}, \mu_1, \epsilon_{11}) \mapsto (\tilde{\mu}_1, \tilde{\epsilon}_{11}) = (\mu_1(1 + \mathcal{O}(\mu_1\pi_{11})), \epsilon_{11}(1 + \mathcal{O}(e^{-\mu_1^{-1}}\pi_{11}^2)))$ such that

$$\dot{\pi}_{11} = \pi_{11},$$
$$\dot{\mu}_1 = -\mu_1^2,$$
$$\dot{\epsilon}_{11} = 0,$$

upon dropping the tildes. Now, we integrate these equations from $\mu_1(0) = \nu$ to $\pi_{11}(T) = \delta$ using $\pi_{11}(0) \leqslant \beta_2 \ll \delta$. This gives

$$\mu_1(T) = \frac{\nu}{1 + \nu T},$$

for $T = \log(\pi_{11}(0)^{-1}\delta)$. Working our way backwards, we realise that the contraction along the stable fibers of the center manifold (7.15), during this transition, is at least $\mathcal{O}(e^{-c/(\epsilon_{11}(0)\pi_{11}(0))})$ for some $c > 0$ sufficiently small.

Subsequently, from (7.19), we then apply a finite time flow map up close to $\pi_{11} = 1 - \nu$. From here, we then straighten out the center manifold by a transformation of the form

$$\pi_{11} = 1 + \epsilon_{11}\mu_1^2 h_{311}(0, \mu_1, 0, \epsilon_{11}) + q\left(\frac{\alpha}{\xi} + \frac{\xi + 1}{\xi}\mu_1 + \mathcal{O}(\mu_1^2\epsilon_{11}, \mu_1^2 + q)\right) + \tilde{\pi}_{11}.$$

This gives

$$\dot{\pi}_{11} = -\xi\pi_{11},$$
$$\dot{\mu}_1 = \mu_1^2\left(\mu_1 q + \mathcal{O}(\pi_{11}, \mu_1^2 q)\right),$$
$$\dot{\epsilon}_{11} = -(1 + \mathcal{O}(\epsilon_{11}\mu_1^2, q\mathcal{O}\pi_{11}))\mu_1 q\epsilon_{11}$$

after a transformation of time and dropping the tilde. Now, we straighten out the stable fibers by a transformation of the form $(\pi_{11}, \mu_1, \epsilon_{11}) \mapsto (\tilde{\mu}_1, \tilde{\epsilon}_{11}) = (\mu_1(1 + \mathcal{O}(\mu_1\pi_{11})), \epsilon_{11}(1 + \mathcal{O}(e^{-\mu_1^{-1}}\pi_{11})))$. This gives

$$\dot{\pi}_{11} = -\xi\pi_{11},$$
$$\dot{\mu}_1 = \mu_1^3 q\left(1 + \mathcal{O}(\mu_1)\right),$$
$$\dot{\epsilon}_{11} = -(1 + \mathcal{O}(\mu_1))\mu_1 q\epsilon_{11},$$

upon dropping the tildes. π_{11} decouples from this system. We therefore consider the (μ_1, ϵ_{11}) system. Dividing the right hand side by $\mu_1 q(1 + \mathcal{O}(\mu_1^2))$, and applying a transformation of the form $(\epsilon_{11}, \mu_1) \mapsto \tilde{\mu}_1 = \mu_1(1 + \mathcal{O}(\mu_1))$ gives

$$\dot{\mu}_1 = \mu_1^2,$$
$$\dot{\epsilon}_{11} = -\epsilon_{11}$$

upon dropping the tildes. We then integrate this system from $\mu_1(0) = \nu_{10}$ to $\mu_1(T) = \delta$ taking $\nu_{10} \ll \delta$. This gives

$$\epsilon_{11}(T) = e^{-T}\epsilon_{11}(0),$$

with $T = \frac{1}{\nu_{10}}\left(1 - \nu_{10}/\delta\right)$. Therefore

$$\epsilon_{11}(T) = e^{-\nu_{10}^{-1}(1-\nu_{10}/\delta)}\epsilon_{11}(0).$$

Working our way backwards, we realise that the contracting along the stable fibers of the center manifold (7.20) under this transition is at least $\mathcal{O}(e^{-ce^{1/(2\nu_{10})}})$. Similarly, the contraction along the stable fibers of the center manifold $\mathcal{K}_{311}$, see (7.15), is at least $\mathcal{O}(e^{-c\epsilon_{10}^{-1}e^{2\nu_{10}^{-1}}})$. Both constants c here are sufficiently small. Now, we combine these estimates to obtain the desired result. In particular, the expression for ϵ_{11+} follows from the conservation of $\epsilon = e^{-\mu_1}\pi_{11}\epsilon_{11}$. Therefore

$$\epsilon_{11+} = e^{\delta^{-1}-\nu^{-1}}\pi_{11+}^{-1}\pi_{11}\epsilon_{11}.$$

Here $\pi_{11+} = 1 + \mathcal{O}(\epsilon_{11+}\mu_1^2, \mu_1 e^{-\mu_1})$. We therefore solve this equation for ϵ_{11+} using the implicit function theorem. $\qquad\square$

8. The transition map $\Pi^{70} : \Sigma^7 \to \Sigma^0$

We now combine the findings in ϕ_1 into a result on the transition map Π^{70}. For this, let

$$\Sigma_1^7 = \left\{(x, z, w) \,|\, z = \frac{\xi}{2\alpha(1+\nu)}, x + \frac{(1+\alpha)\xi}{2\alpha} \in [-\beta_3, \beta_3], w \in [0, \beta_4], \epsilon_1 \in [0, \beta_5]\right\},$$
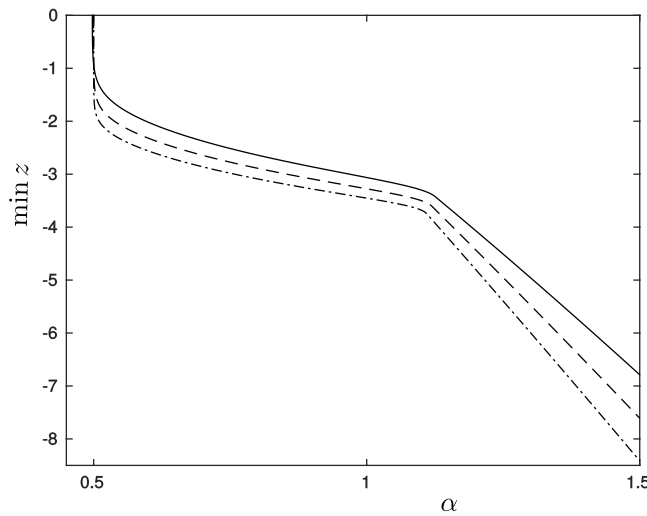
Figure 30. Bifurcation diagram of limit cycles for $\xi = 0.5$ and three different values of ϵ: $\epsilon = 0.01$ (full line), $\epsilon = 0.001$ (dashed line), $\epsilon = 0.0001$ (dash-dotted line), using $\min z$ as a measure of the amplitude. Around $\alpha \approx 1$, we see a dramatic change in $\min z$. This transition is captured by the method of the paper.

recall (5.2) and (1.22), and

$$\Sigma^0 = \{(x, z, w) \mid w = \delta, (\delta x, \delta z) \in N^0\}. \tag{8.1}$$

Here N^0 is the small neighborhood of (x^0, z^0) in (2.2). Notice also that $q^0 = (\delta x^0, \delta z^0, \delta)$ in our present $(x, z, w) = (x_1, z_1, w_1)$-coordinates, see (2.1) and (1.22). We then define the mapping $\Pi^{70} : \Sigma_1^7 \to \Sigma^0$ as the first intersection by the forward flow. Then we have

Lemma 8.1. *The mapping Π^{70} is well-defined for appropriately small $\delta > 0$, $\nu > 0$ and $\beta_i > 0$, $i = 1, \ldots, 5$ and all $0 < \epsilon \ll 1$. In particular,*

$$\Pi^{70}(x, w, \delta, \epsilon_1) = (x_+(x, w, \epsilon_1), z_+(x, w, \epsilon_1), \delta),$$

where x_+ and z_+ are C^1-functions in x and w, satisfying

$$x_+(x, w, \epsilon_1) = \delta x^0 + \mathcal{O}(\epsilon_1, w),$$
$$z_+(x, w, \epsilon_1) = \delta z^0 + \mathcal{O}(\epsilon_1, w).$$

Proof.   The result follows from the series of lemmas: lemmas 7.1, 7.3, 7.5 and 7.7, describing the relevant local transition maps in the local charts described in section 6 using standard hyperbolic methods to follow the segments γ^{7-11}, $W^{cu}(Q^6)$. Notice that the mappings between the different local sections are diffeomorphism that do not change the order.   □

We are now ready to prove lemma 2.2.

Proof of lemma 2.2.   To prove lemma 2.2 we first write

$$\Pi^1 = \Pi^{70} \circ \Pi^{17} : D(\Pi^1) \subset \Sigma^1 \to \Sigma^0, \tag{8.2}$$

in the local charts ϕ_1 and ϕ_3. In particular, Σ^1 in (8.2) is defined in ϕ_3, see (5.1), while Σ^0 is defined in ϕ_1, see (8.1). Then by lemmas 5.1 and 8.1

$$\Pi^1(x, y, \delta) = \left(\delta x^0 + \mathcal{O}(\log^{-1} \epsilon^{-1} \log \log \epsilon^{-1}), \delta z^0 + \mathcal{O}(\log^{-1} \epsilon^{-1} \log \log \epsilon^{-1}), \delta \right),$$

for all $0 < \epsilon \ll 1$, the estimates being C^1-small with respect to x and y. Transforming the result back to the original variables (x, y, z) completes the proof of lemma 2.2. $\qquad\square$

9. Discussion

In this paper, we proved existence of a new type of relaxation oscillations in a ODE system (1.3), being a caricature model of an earthquake fault, with exponential nonlinearities. The details were presented in theorem 1.5. Our approach was to use GSPT, specifically applying the adapted version of the blowup method in [22]—developed by the present author—to gain hyperbolicity where this was lost due to exponential 'flat' terms. In this way, we 'derived' an (improved) singular cycle, consisting of 12 'hyperbolic segments', from which we obtained our desired limit cycle as a perturbation for all $0 < \epsilon \ll 1$. The singular cycle was described in several figures, see e.g. figures 7, 15, 25 and 26. In [22], the adapted blowup method was mainly used on toy examples and the present analysis therefore provides the most important application of this new method to obtain rigorous results in singular perturbed systems where hyperbolicity is lost in this special way. In [19], the method is used on some planar oscillators with exponential nonlinearities.

From the results in the present paper, we deduce the following interesting consequences: firstly, in [10] chaos is observed in numerical computations of (1.3) through a period doubling cascade of the relaxation oscillation for $\alpha > \xi$ studied in the present manuscript. A corollary of our results, is that this chaos is not persistent within any fixed compact interval $I \subset (\xi, \infty)$ of α-values as $\epsilon \to 0$. Indeed, the limit cycles in theorem 1.5 do not bifurcate for any $\alpha > \xi$ and all $0 < \epsilon \ll 1$. In this sense, the period doubling cascade is an $\epsilon = O(1)$ phenomenon.

Secondly: let $(x(t), y(t), z(t)) \in \Gamma_\epsilon$. Then for $\alpha \leqslant 1$, $z(t)$ attains its minimum close to $W^{cu}(Q^6)$, see (1.14) with $y \gg 1$. On the other hand, for $\alpha > 1$, the minimum of $z(t)$ occurs at a smaller value, near the line $z = \frac{\xi(\alpha-1)}{2\alpha} y$ on C with $y \gg 1$. This follows from (1.27) and the statements proceeding it, see also appendix. There is therefore a transition in how the minimum of $z(t)$ depends upon ϵ (and α) when α crosses $\alpha = 1$. We illustrate this further in the bifurcation diagram in figure 30 using $\min z$ as a measure of the amplitude for $\xi = 0.5$ and three different values of ϵ: $\epsilon = 0.01$ (full line), $\epsilon = 0.001$ (dashed line), $\epsilon = 0.0001$ (dash-dotted line). This diagram was computed using AUTO. It shows that the limit cycles are born in Hopf bifurcations near $\alpha = 0.5$. The amplitudes increase rapidly due to the underlying Hamiltonian structure, recall (1.10), see also [3]. Subsequently they flatten out. This is where the connection to the relaxation oscillations, described in theorem 1.5, occurs. Between $\alpha \approx 0.5$–1.1 the increase in amplitude is more moderate, like $\min z \sim \log \alpha$. Examples of limit cycles are shown in figure 3. Beyond this interval of α-values, the amplitudes increase linearly in α: $\min z \sim \alpha$.

In [3] it was conjectured that the relaxation oscillations and the local limit cycles near the Hopf bifurcation belong to the same family of stable limit cycles for all $0 < \epsilon \ll 1$, as exemplified in figure 30 for particular values of ϵ. I believe that this result can be proven using the methods in the present paper, but it requires a detailed description near Q^3 where the transition from small to big oscillations occur. I have not yet pursued such an analysis. On a related matter, we highlight that, as a consequence of our approach, Γ_ϵ attracts a large set of initial

conditions. In fact, Γ_ϵ attracts all initial conditions in $K\backslash U$ where U is a small neighborhood of $K \cap W^{cs}(Q^3)$, recall theorem 1.5. I expect that a detailed analysis near Q^3 would reveal that Γ_ϵ attracts all points in $K\backslash\{0\}$.

As highlighted in [3], the physical realistic values of ϵ belong to the interval $[10^{-24}, 10^{-8}]$. Long time numerical computations are not feasible in this interval and I therefore believe that theoretical progress is fundamental for the advancement of mathematical modelling in this area. In ongoing work, I use methods from the present paper to show a similar result to theorem 1.5 for the spring-block model with the Dietrich friction law:

$$\dot{x} = (1 + \alpha)(e^{-x/(1+\alpha)} - e^z),$$
$$\dot{y} = e^z - 1,$$
$$\epsilon \dot{z} = -e^{-z}\left(y + \frac{x + z}{\xi}\right).$$

See also [1]. The set defined by L_∞ also plays an important role for this system. In fact, the analysis is completely analogous, suggesting something fundamental about this line in rate-and-state friction models.

However, there are known limitations of the Dieterich and Ruina laws. Basically, experiments suggest that friction should be an N-shaped graph of velocity (when the states are in 'quasi-steady states'). Dieterich and Ruina only capture parts of this shape, see e.g. [33, figure 1]. The more recently developed *spinodal rate-and-state friction law*, see [33] and references therein, has been developed to capture the missing pieces of the N-profile, producing a potentially widely applicable, yet complicated, friction law. In [34], travelling wave solutions of a simple model for a thin sliding slab with this friction law were analyzed numerically. The results showed a rich bifurcation structure and demonstrated that the spinodal law captures the most essential physical phenomena known from friction experiments, also those not produced by the Ruina or the Dieterich law. Ideally, in the future, we hope that our insight into the two simpler models, Ruina and Dieterich, eventually will allow for a detailed analysis of the spinodal law and increase our understanding of the numerical findings in [34]. Central to our analysis in the present paper, is the existence of reduced models on C and L_∞ (or in practice L, recall (1.29)). It is reasonable to assume, that by obtaining similar objects for the spinodal law we will enhance our understanding of system parameters and in general facilitate the process of translating data to parameter estimation.

Appendix. Case $\alpha \geqslant 1$

First, we describe $\alpha > 1$. Since the details in chart ϕ_3, in particular the proof of lemma 5.1 is unchanged, we will work in the chart ϕ_1 only. We then consider the chart $(\bar{w} = 1, \bar{q} = 1)_{11}$, recall (6.10). This gives the following equations:

$$\dot{x} = -\epsilon_1 \theta_1 w_1 \left(\theta_1 w_1 x F(w_1^{-1}) + (x + (1 + \alpha)\theta_1)\right),$$
$$\dot{\theta}_1 = -\theta_1 w_1 \left(\epsilon_1 \theta_1^2 w_1 F(w_1^{-1}) + \left(1 + \frac{x + \theta_1}{\xi}\right)\right),$$
$$\dot{w}_1 = w_1^2 \left(1 + \frac{x + \theta_1}{\xi}\right),$$
$$\dot{\epsilon}_1 = -2\epsilon_1 \left(1 + \frac{x + \theta_1}{\xi}\right)$$
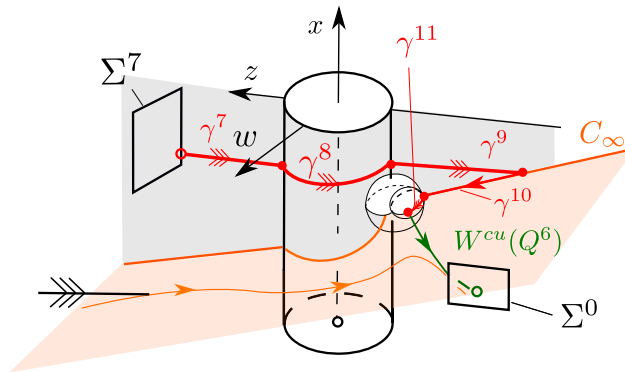
Figure A1. Improved singular orbit segments of the blowup in ϕ_1 for $\alpha > 1$. We show a view from the the positive w-axis ('coming out' of the page). The directions of the two remaining axes x and z are indicated by the arrows. The spheres are blowup of points, involving the two remaining dimensions: q and ϵ.

r_1 decouples as usual and shall therefore be ignored. In this chart γ^7 becomes

$$\gamma_{11}^7 = \left\{ (x, \theta_1, w_1, \epsilon_1) \,|\, x = -\frac{\xi}{2\alpha}(1 + \alpha),\, \theta_1 \in \left(0, \frac{\xi}{2\alpha}\right],\, w_1 = \epsilon_1 = 0 \right\},$$

for $\alpha > 1$, see e.g. (4.21). It is contained within the invariant manifold $\epsilon_1 = 0$. By desingularization through division by w_1 within this set, we obtain

$$\dot{x} = 0,$$

$$\dot{\theta}_1 = -\theta_1 \left(\epsilon_1 \theta_1^2 w_1 F(w_1^{-1}) + \left(1 + \frac{x + \theta_1}{\xi}\right) \right),$$

$$\dot{w}_1 = w_1 \left(1 + \frac{x + \theta_1}{\xi}\right).$$

The x-axis is therefore a line of equilibria. γ_{11}^7 is asymptotic to $(x, \theta_1, w_1) = (-\xi(1 + \alpha)/(2\alpha), 0, 0)$ within this set, following the associated stable manifold. Notice here that

$$\left(1 + \frac{x + \theta_1}{\xi}\right) = \frac{\alpha - 1}{2\alpha} > 0, \tag{A.1}$$

for $x = -\xi(1 + \alpha)/(2\alpha)$ and $\theta_1 = 0$, by assumption. As usual, we can track a small neighborhood of γ_{11}^7 near $\theta_1 = \text{const.} > 0$ up to $w_1 = \text{const.} > 0$ in a C^1-fashion by following the unstable manifold

$$\gamma_{11}^8 = \left\{ (x, \theta_1, w_1, \epsilon_1) \,|\, x = -\frac{\xi}{2\alpha}(1 + \alpha),\, \theta_1 = 0,\, w_1 \geqslant 0,\, \epsilon_1 = 0 \right\}.$$

In fact, the result is almost identical to lemma 7.1. We therefore skip the details.

Next, recall that $\epsilon = e^{-2w_1^{-1}} \epsilon_1$, see (6.6), so at $w_1 = \text{const.}$ we have $\epsilon_1 \sim \epsilon$. We can therefore transform the result in $(\bar{z} = 1, \bar{q} = 1)_{11}$ into the chart $(\bar{w} = 1)_2$, see (6.17), using that

$z_2 = -w_1^{-1}$. The system is a regular perturbation problem in this $(\bar{w} = 1)_2$-chart. In particular, along

$$\gamma_2^8 = \left\{ (x, \theta_2, z_2, \epsilon) \,|\, x = -\frac{\xi}{2\alpha}(1 + \alpha),\, \theta_2 = 0,\, z_2 \in \mathbb{R},\, \epsilon = 0 \right\},$$

z_2 is decreasing. This brings us into the chart $(\bar{z} = -1)_3$ using the coordinate transformation $w_3 = z_2^{-1}$. The equations in this chart are given in (6.20). The x-axis is again a line of equilibria for this system and γ_3^8 is asymptotic to the point $(x, \theta_3, w_3, \epsilon) = (-\xi(1 + \alpha)/(2\alpha), 0, 0, 0)$ within this line by following the associated stable manifold. We can (again) track a small neighborhood of γ_3^8 near $w_3 = \text{const.} > 0$ up to $\theta_3 = \text{const.} > 0$ in a C^1-fashion by following the unstable manifold

$$\gamma_3^9 = \left\{ (x, \theta_3, w_3, \epsilon) \,|\, x = -\frac{\xi}{2\alpha}(1 + \alpha),\, \theta_3 = \left[0, \frac{\xi(\alpha - 1)}{2\alpha}\right),\, w_3 = 0,\, \epsilon = 0 \right\}.$$

The result is almost identical to lemma 7.1. We skip the details again. Here γ_3^9 is asymptotic to a point $(x, \theta_3, w_3) = (-\xi(1 + \alpha)/(2\alpha), \xi(\alpha - 1)/(2\alpha), 0)$ on $C_\infty : x = -\xi - \theta_3,\, w_3 = 0$, which is normally hyperbolic in this chart. Following lemma 1.2, see also [3] and figure 6(c), we obtain an orbit γ_3^{10} of the slow flow on C_∞

$$\gamma_3^{10} = \left\{ (x, \theta_3, w_3, \epsilon) \,|\, x = -\xi + \theta_3,\, \theta_3 \in \left(0, \frac{\xi(\alpha - 1)}{2\alpha}\right],\, w_3 = 0,\, \epsilon = 0 \right\},$$

along which θ_3 is decreasing. Notice in particular, that for $\alpha > 1$ the point $(x, \theta_3, w_3) = (-\xi(1 + \alpha)/(2\alpha), \xi/2\alpha(\alpha - 1), 0)$ is always contained between Q^6 and the unstable node Q^7, the latter having coordinates $x = 0$, $\theta_3 = \xi$, $w_3 = 0$ in this chart. γ_3^{10} therefore brings us into the chart $(\bar{z} = -1, \bar{\theta} = 1, \overline{w}_3 = 1)_{311}$ where the analysis in section 7.5 is valid. See figure 29 where γ_3^{10} is shown in purple. This completes the (sketch of) proof for $\alpha > 1$. We illustrate the singular segments in figure A1.

Up until now our approach is not uniform in α. For $\alpha > 1$ for example, the approach breaks down at $\alpha = 1$ since the condition in (A.1) is violated (the bracket vanishes). To capture this, we may follow the approach in section 7.1, see figure 27. Here both $\alpha < 1$ and $\alpha > 1$ are visible (red and purple in figure 27). However, the w_{11}-axis in figure 27 is degenerate. To obtain results uniform in α we therefore blowup this axis by introducing polar coordinates in the (ρ_1, θ_1)-plane. The details are pretty standard so we also leave these out of the manuscript for simplicity.

ORCID iDs

K Uldall Kristiansen ⓘ https://orcid.org/0000-0001-6090-7649

References

[1] Bossolini E 2017 Geometric singular perturbation analysis of systems with friction *PhD Thesis* Technical University of Denmark

[2] Bossolini E, Brøns M and Kristiansen K U 2017 Canards in stiction: on solutions of a friction oscillator by regularization *SIAM J. Appl. Dyn. Syst.* **16** 2233–58

[3] Bossolini E, Brøns M and Kristiansen K U 2017 Singular limit analysis of a model for earthquake faulting *Nonlinearity* **30** 2805

[4] Carr J 1981 *Applications of Centre Manifold Theory* vol 35 (New York: Springer)

[5] De Maesschalck P and Schecter S 2016 The entry-exit function and geometric singular perturbation theory *J. Differ. Equ.* **260** 6697–715

[6] Dieterich J 1978 Time-dependent friction and mechanics of stick-slip *Pure Appl. Geophys.* **116** 790–806

[7] Dieterich J 1979 Modeling of rock friction. 1. Experimental results and constitutive equations *J. Geophys. Res.* **84** 2161–8

[8] Dumortier F and Roussarie R 1996 Canard cycles and center manifolds *Mem. Am. Math. Soc.* **121** 1–96

[9] Dumortier F, Llibre J and Arts J C 2006 *Qualitative Theory of Planar Differential Systems* (Berlin: Springer)

[10] Erickson B, Birnir B and Lavallee D 2008 A model for aperiodicity in earthquakes *Nonlinear Process. Geophys.* **15** 1–12

[11] Feeny B, Guran A, Hinrichs N and Popp K 1998 A historical review on dry friction and stick-slip phenomena *Appl. Mech. Rev.* **51** 321–41

[12] Fenichel N 1971 Persistence and smoothness of invariant manifolds for flows *Indiana Univ. Math. J.* **21** 193–226

[13] Fenichel N 1974 Asymptotic stability with rate conditions *Indiana Univ. Math. J.* **23** 1109–37

[14] Fenichel N 1979 Geometric singular perturbation theory for ordinary differential equations *J. Differ. Equ.* **31** 53–98

[15] Gucwa I and Szmolyan P 2009 Geometric singular perturbation analysis of an autocatalator model *Discrete Continuous Dyn. Syst. S* **2** 783–806

[16] Hayes M G, Kaper T J, Szmolyan P and Wechselberger M 2016 Geometric desingularization of degenerate singularities in the presence of fast rotation: a new proof of known results for slow passage through hopf bifurcations *Indagationes Math.* **27** 1184–203

[17] Hsu T H 2017 On bifurcation delay: an alternative approach using geometric singular perturbation theory *J. Differ. Equ.* **262** 1617–30

[18] Jelbart S and Wechselberger M 2019 Two stroke relaxation oscillators *Nonlinearity* **33** 2364

[19] Jelbart S, Kristiansen K U, Szmolyan P and Wechselberger M 2019 Singularly perturbed oscillators with exponential nonlinearities (arXiv:1912.11769)

[20] Jones C 1995 *Geometric Singular Perturbation Theory, Lecture Notes in Mathematics, Dynamical Systems (Montecatini Terme)* (Berlin: Springer)

[21] Kosiuk I and Szmolyan P 2015 Geometric analysis of the Goldbeter minimal model for the embryonic cell cycle *J. Math. Biol.* **72** 1337–68

[22] Kristiansen K 2017 Blowup for flat slow manifolds *Nonlinearity* **30** 2138

[23] Kristiansen K U 2019 Geometric singular perturbation analysis of a dynamical target mediated drug disposition model *J. Math. Biol.* **79** 187–222

[24] Kristiansen K U and Hogan S J 2018 Resolution of the piecewise smooth visible-invisible two-fold singularity in $\mathbb{R}^3$ using regularization and blowup *J. Nonlinear Sci.* **29** 723–87

[25] Kristiansen K U and Szmolyan P 2019 Relaxation oscillations in substrate-depletion oscillators close to the nonsmooth limit (arXiv:1909.11746)

[26] Krupa M and Szmolyan P 2001 Extending geometric singular perturbation theory to nonhyperbolic points—fold and canard points in two dimensions *SIAM J. Math. Anal.* **33** 286–314

[27] Krupa M and Szmolyan P 2001 Relaxation oscillation and canard explosion *J. Differ. Equ.* **174** 312–68

[28] Kuehn C and Szmolyan P 2015 Multiscale geometry of the olsen model and non-classical relaxation oscillations *J. Nonlinear Sci.* **25** 583–629

[29] Le Corbeiller P 1960 Two-stroke oscillators *IRE Trans. Circuit Theory* **7** 387–98

[30] Lishman B, Sammonds P R and Feltham D L 2013 Critical slip and time dependence in sea ice friction *Cold Reg. Sci. Technol.* **90–1** 9–13

[31] Olsson H, Astrom K J, de Wit C C, Gafvert M and Lischinsky P 1998 Friction models and friction compensation *Eur. J. Control* **4** 176–95

[32] Olver F W J, Lozier D W, Boisvert R F and Clark C W 2011 *NIST Handbook of Mathematical Functions* (Cambridge: Cambridge University Press)

[33] Putelat T and Dawes J H P 2015 Steady and transient sliding under rate-and-state friction *J. Mech. Phys. Solids* **78** 70–93

[34] Putelat T, Dawes J H P and Champneys A R 2017 A phase-plane analysis of localized frictional waves *Proc. R. Soc.* A **473** 0606

[35] Putelat T, Willis J and Dawes J 2008 On the seismic cycle seen as a relaxation oscillation *Phil. Mag.* **88** 3219–43

[36] Rice J, Lapusta N and Ranjith K 2001 Rate and state dependent friction and the stability of sliding between elastically deformable solids *J. Mech. Phys. Solids* **49** 1865–98

[37] Ruina A 1983 Slip instability and state variable friction laws *J. Geophys. Res.* **88** 359–70

[38] Schecter S 2008 Exchange lemmas 2: general exchange lemma *J. Differ. Equ.* **245** 411–41

[39] Woodhouse J, Putelat T and McKay A 2015 Are there reliable constitutive laws for dynamic friction? *Phil. Trans. R. Soc.* A **373** 20140401